NOLTR 63-140
REACTORS-GENERAL

EXPLOSION CONTAINMENT LAWS FOR NUCLEAR REACTOR VESSELS

16 AUGUST 1965

NOL
UNITED STATES NAVAL ORDNANCE LABORATORY, WHITE OAK, MARYLAND

NOLTR 63-140

LEGAL NOTICE

NOTICE

NOLTR 63-140

EXPLOSION CONTAINMENT LAWS FOR NUCLEAR REACTOR VESSELS

Prepared by:

W. R. Wise, Jr. and J. F. Proctor

ABSTRACT: The location of power reactors in urban areas increases the need for containment of the maximum credible nuclear accident. Such an accident could possibly involve a large and rapid energy release in the core region due to a nuclear excursion. To contain the energy release (and any subsequent release of fission products), the integrity of the reactor primary vessel is very important. To investigate this integrity, extensive theoretical and experimental analyses were performed, and basic explosion containment laws for water-filled right-circular cylinders were formulated and verified for a wide range of vessel materials and sizes. These laws express explosive charge weight as a function of vessel geometry and conventional material properties. The basic containment laws were amplified to characterize the response of reactor primary vessels to a large spectrum of postulated nuclear accidents. Included in the study are experimental data on the effects upon containment of weldments, nozzles, and end constraints.

PUBLISHED OCTOBER 1965

AIR/GROUND EXPLOSIONS DIVISION
EXPLOSIONS RESEARCH DEPARTMENT
U. S. NAVAL ORDNANCE LABORATORY
WHITE OAK, MARYLAND

NOLTR 63-140 16 August 1965

Explosion Containment Laws for Nuclear Reactor Vessels

The work described in this report was performed under Tasks I - IV of NOL Task-285, NOL Reactor Vessel Containment Program, during the period 1956-1964. The primary objective of these tasks, to determine the optimum containment design of nuclear reactor vessels by utilizing the mechanism of gross plastic deformation as a means of energy absorption, was accomplished along with the successful achievement of a number of secondary objectives. This work was done under the sponsorship of the Research and Development Branch of the Atomic Energy Commission.

The mention of names of proprietary products in this report constitutes neither an endorsement nor criticism of these products by the United States Government or by the U. S. Naval Ordnance Laboratory.

J. A. DARE
Captain, USN
Commander

C. J. Aronson

C. J. ARONSON
By direction

CONTENTS

CONTENTS

CONTENTS

LIST OF TABLES

CONTENTS

LIST OF FIGURES

CONTENTS

LIST OF FIGURES (Cont'd)

CHAPTER 1

INTRODUCTION

1.1 Foreword. The Reactor Vessel Containment Program was conducted at the U. S. Naval Ordnance Laboratory, White Oak and sponsored by the Atomic Energy Commission's Research and Development Branch over a period of eight years (1956-1964). The program was a fundamental and comprehensive research effort directed to defining the magnitude of a nuclear excursion (in terms of TNT energy and flux) that a primary nuclear vessel is capable of containing. The results of the work provide relations that prescribe the design specifications of reactor vessels for containing the energy releases due to such excursions.

1.2 Reactor Accidents. In considering the safety of any reactor system, a large number of potential accidents are examined in the light of their possible consequences. That accident with the worst consequences for the public safety and which is considered credible within the bounds of a particular reactor design is often termed the maximum credible accident or MCA (as opposed to incredible, although possibly more hazardous, due to the inherent reactor characteristics or mechanisms). This report considers a type of accident that is sometimes considered credible, namely a large and rapid release of energy at the reactor core due to an uncontrolled nuclear excursion. Whether or not such an accident is the MCA depends upon the particular reactor design.

The excursion energy generated at the reactor core is frequently expressed in terms of megawatt-seconds; however, because of similarities in rate of energy release, this accident may also be expressed in pounds of TNT particularly where destructiveness and containment integrity are basic questions. Bethe and Tait in reference (a), for example, were among the first to characterize nuclear accidents in terms of TNT.

1.3 Reactor Containment. W. B. Cottrell presents a somewhat detailed containment philosophy in reference (b); only a brief treatment will be given here. Containment is a provision to control (limit) the public exposure to radiation following any reactor accident to acceptable levels. Early in nuclear development such control was often aided in the United States through locating reactors in huge and generally remote areas such as Oak Ridge and the desert regions of Washington and Idaho. In these and similar instances, the distance from each reactor to the site boundary was intended to permit adequate control in the event of an accident.

Several needs have evolved to radically change this picture. The most significant of these is that location in wilderness areas is not consistent with today's electric power requirements for our industrial complexes, since these requirements generally imply location near or even in the midst of heavily populated areas. When central power station requirements are coupled with the growing use of atomic plants for marine propulsion and for research purposes, reactor containment is brought directly to the "front door" of the general public. Consequently, containment systems consisting of combinations of structural barriers and mechanical auxiliaries must be employed to restrict the possible spread of radioactive fission products that might be released from the core by an accident. One such barrier might be considered to be the reactor primary vessel if its integrity could be guaranteed.

1.4 Scope and Significance. The Reactor Vessel Containment Program was directed to characterizing the excursion containment potential of nuclear facilities in general and reactor primary pressure vessels in particular; this was the broad purpose. The ultimate objective was to devise general laws for containment of the excursion within the reactor vessel and to express these laws in a fundamental design format that would permit immediate and fruitful use by containment engineers.

The theoretical and experimental studies of the program were extensive in spectrum and depth. Since the excursion loading and vessel response parameters were so numerous and so complex, Saint-Venant's semi-inverse method of classical mechanics was invoked to generate an embryonic functional form of the desired solution. The necessary boundary conditions were obtained from over 100 experiments employing explosives and propellants in scaled model cylinders simulating reactor vessels. What follows is an unfolding of the rationale and the broad spectrum of tools - both theoretical and experimental - that were employed to characterize the parameters of containment and to formulate excursion or EXPLOSION CONTAINMENT LAWS FOR NUCLEAR REACTOR VESSELS.

CHAPTER 2

ANCILLARY PROGRAMS

The principal mission of the Reactor Vessel Containment Program, as originally planned, was to conduct basic studies of a general character directed to containment per se. From time to time, however, problems with particular reactors arose; these problems and their solutions are recounted briefly in the following paragraphs because they have provided information basic to the development of Containment Law rationale.

2.1 Preliminary Study of Enrico Fermi Plant. In 1957, upon request of the Atomic Energy Commission, program effort was diverted temporarily to a preliminary containment study of the Enrico Fermi Atomic Power Plant. The results of this study were reported by E. M. Fisher and W. R. Wise in reference (c); they found that:

(a) An excursion releasing energy equivalent in magnitude and violence to 1000 pounds of TNT detonated at the core would not develop shock waves of sufficient strength or missiles with sufficient energy to threaten the integrity of the secondary shield.

(b) The response of the rotating shield plug to the shock would be a vertical jump not exceeding two feet.

(c) But the internal blast pressure, the quasi static pressure generated by the gases released from the explosive charge, would be the predominate mechanism that could propel the massive shield plug through the roof of the containment building.

2.2 Energy Partition Study. The Fermi plug-jump hazard reported in reference (c) raised serious questions relating to disposition of the energy during a nuclear excursion. In consequence, upon AEC request to the Naval Ordnance Laboratory in 1958, it was decided:

To determine the partition of mechanical and non-mechanical energy resulting from the detonation of water-cased and sodium-cased explosives surrounded by air and confined within a closed plug-fitted vessel.

The initial efforts made on this task, reported by Wise in reference (d) and by J. F. Proctor in detail in reference (e), were exploratory in nature and served principally to establish problem approach and the governing parameters of the problem. Parameters such as charge weight, mass-per-frontal area of the shield plug, liquid-to-air ratio, and liquid temperature were examined in an exploratory apparatus that represented a crude model of the Enrico Fermi Reactor. Three important conclusions derived from this work were:

(a) The presence and temperature of a liquid casing surrounding the charge greatly affected energy partition: increasing quantities of liquid heat sink decreased the plug-jump and increasing temperatures increased the jump.

(b) A refined experimental apparatus would be required for accurate characterization of the principal parameters.

(c) The explosion containment potential of the Fermi composite envelope (reactor vessel, graphite shield, and primary shield tank) must be established if a meaningful plug-response solution were to be achieved.

2.3 Extensive Fermi Shield Plug Study. The previously discussed energy partition studies, comprising destructive mechanisms basic to reactor excursions generally, were continued until October, 1959. At that time, Atomic Power Development Associates, Inc. (APDA) - the designers of the Fermi Plant - requested the AEC to assist in resolving the plug-jump question as quickly as possible. Specifically, APDA recommended that NOL conduct a program addressed to the

excursion motion of the Fermi shield plug per se. Accordingly, upon AEC request to NOL, the general energy partition studies were discontinued, and the entire manpower and funds of the NOL Containment Program were directed to the following particularized objective:

> To determine the response of the Fermi shield plug to a postulated nuclear excursion equivalent in energy release and rate of release, i.e., equivalent in violence and destructiveness, to the detonation at standard conditions (Temp: 77°F, Press: atmospheric) of a center-initiated, compact cylindrical charge of 1000 pounds of TNT located at the reactor core.

Preliminary results of this extensive containment study on the Fermi Reactor (1959-1962) were reported by Wise in reference (f), by Wise, Proctor, and Walker in reference (g), and by H. B. Benefiel in reference (h). The final and comprehensive results of the entire Fermi program were reported by Wise, Proctor, and Walker in reference (i); some of the major conclusions were

(a) The maximum jump of the 143-ton shield plug resulting from the 1000-lb TNT accident would be of the order of, but not exceed, 102 feet. Thus the plug could possibly be propelled through the roof of the containment building.

(b) Containment of the postulated accident within the reactor vessel would be marginal for no loss of sodium coolant. For major losses of coolant, however, containment would be conservative. In any event, the gross containment integrity of the secondary-shield wall would not be violated.

(c) Release of the postulated energy at a rate slower than the detonation rate of TNT would yield a plug jump less than that occurring from the TNT accident.

(d) The graphite shield, due to its inertia, increases the TNT explosion containment potential of the composite (reactor vessel-primary shield tank) envelope by a factor of two or greater.

(e) The sodium, blanket, thermal shield, and other reactor vessel internals possess a significantly large capacity for absorbing heat from the TNT explosion gases during the short time that would be required for the shield plug to escape the composite envelope.

The Enrico Fermi Reactor has been modified and fitted with an energy-absorption mechanism in the machinery dome (see reference (j)) to restrict any upward plug motion resulting from an accident. If the absorber possesses the potential specified in reference (j), motion of the shield plug as a result of the postulated accident studied by NOL will not constitute a serious hazard.

CHAPTER 3

THE PRINCIPAL PROGRAM

The principal containment program consisted of several related studies conducted over a span of about eight years. The basic rationale of these studies and their synthesis follow.

3.1 Long-Term Objective. The long-term technical objective of the NOL Reactor Vessel Containment Program was to achieve the optimum containment design of nuclear reactor vessels through gross plastic deformation as a means of absorbing excursion energy. The steps of the objective were:

(a) To simulate nuclear excursions occurring in full-size reactor vessels through the use of propellants and explosives in model vessels

(b) To investigate reactor vessel response in the gross plastic domain with material, size, shape, and constraint as parameters

(c) To formulate general laws for containment of explosion-type energy releases within the reactor vessel and to express these laws in a fundamental design format that will permit immediate use by containment engineers.

Progress on the long-term objective was first reported formally (1958) by Wise in reference (k): he derived the General Strain Energy Equation of Equilibrium for a Vessel Subjected to Internal Dynamic Loading, conducted basic experiments with solid propellant in model reactor vessels, and concluded that strain energy absorption was a significant containment parameter.

3.2 General Strain Energy Equation. Consider a closed right-cylindrical vessel, e.g., a reactor pressure vessel, subjected to an accidental excursion that causes the vessel wall to flow rapidly and gross-plastically. If, during the dilation,

(a) the pressure vector at every differential surface of the internal wall, and

(b) the strain vector of every differential surface of the external wall

are known, what is the strain energy correlative with containment?

Work done upon the internal wall of the vessel must be instantaneously conserved in the immediate mechanical forms of strain, kinetic, compression, and potential (position) energy. A consequence of this conservation is the General Strain Energy Equation of Dynamic Equilibrium that was derived in reference (k). Plastic straining of the vessel wall is accompanied by the generation of heat within the wall which may or may not be dissipated from the wall depending upon the temperature of its environment. The heat of elastic and plastic strain is accounted for inherently in the strain-energy function. Although the magnitudes of the surface, strain, inertia, compression, and position energies are functions of the temperature of the wall, the validity of the equation is independent of temperature and heat flux within the range for which utilization of the wall as a pressure vessel remains practicable.

The General Strain Energy Equation is greatly simplified for the case of the homogeneous and isotropic, right-circular cylinder closed with rigid, radial constraints at the ends. The conditions of circularity, cylindricality, and rightness of the vessel provide that the spatial limits of integration be constant. If the loading is rotationally symmetric, the structural response of the homogeneous, isotropic wall will be rotationally symmetric - a finding well established by experiments reported herein and in reference (k).

Since the rationale of the General Strain Energy Equation is so germane to this report and to containment generally, its complete derivation and correlative material are reproduced in Appendix A.

3.3 Strain Energy and Containment. The mathematical and physical formulation of the Strain Energy Equation is not a theory designed for experimental confirmation; but rather a principal analytic tool through which experimental work can be used to assess the effectiveness of strain-energy absorption as a means for increasing the containment potential of reactor vessels. This assessment can be expressed as the partition of mechanical (strain energy) and non-mechanical energy resulting from excursion-type energy releases in simulated reactor vessels. With the total energy input known, the General Strain Energy Equation provides the means for obtaining the desired partition without further knowledge as to the disposition of non-mechanical energy.

The model vessels subjected to simulated excursion loading in reference (k) were right-circular cylinders with length equal to two diameters, and the material was type 304 stainless steel. The propellant employed in these basic experiments produced loadings generated in milliseconds. The results indicated that the energy containable in the plastic range exceeded that in the elastic range by an "elastic-plastic" factor of about eight. From the strain energy equation, the deformation energy was found to be about one-tenth of the total energy released.

For microseconds loading mechanisms such as the TNT shock wave, it was found later that the elastic-plastic factor exceeded that for the propellant and that the deformation energy was of the order of one-half the total energy released*. Thus, the valuable containment role of plastic strain energy became manifestly clear, and it was concluded that

* The energy released by a TNT explosion varies from 1050 to 3620 calories/gm of TNT depending upon the availability of oxygen from the surrounding atmosphere. For purposes of this report, it is assumed that the amount of gas confined within the reactor primary vessel is small and is generally inert or low in oxygen content. Therefore, the energy released by a TNT explosion within a reactor vessel would be equivalent essentially to the heat of detonation - 1050 cal/gm.

Strain Energy Absorption, achieved through the medium of large plastic deformation, is a means for substantially improving the containment potential of nuclear reactor vessels, ancillary container paraphernalia, and building enclosures.

3.4 Need for Containment Laws. Philosophically, containment must be provided to reduce the consequence of a reactor accident so that the risk of reactor operation to the public can be decreased to acceptable levels. Since power reactors located in urban locales cannot provide safety through isolation, they must rely upon "mechanical" containment devices. In the Enrico Fermi Plant, for example, there are four such barriers: the reactor vessel, the primary shield tank, the massive secondary shield, and the so-called containment building. Of these, however, the reactor vessel possesses the greatest strain energy absorption potential by far - hence, it constitutes a significant containment barrier as shown in reference (1).

The reactor vessel, in general, has great mass and strength dictated by operating design requirements, and these features constitute desirable containment attributes. It should be clearly established at the outset, however, that the optimum operating design of nuclear reactors does not in general constitute optimum containment design. The operating design characteristics of a reactor inherently restrict the structure to stresses within the elastic limit of the material. Accident containment potential, however, is greatly enhanced through gross plastic deformation. Although such deformation would render the reactor inoperable, a vastly more important objective will have been achieved if the excursion is contained or attenuated and a major catastrophe averted. This is true irrespective of the overall integrity of the primary system, since energy absorbed via gross plastic deformation is unavailable for further destruction.

The reactor vessel can and should be a vital, if not paramount, containment device for all power reactors. Even without planned containment design, some reactor vessels possess a large potential for absorbing excursion energy; with planned design, the containment potential of reactors now on the drawing board could perhaps be greatly increased. In many cases, if excursions could be completely contained within the reactor vessel, the requirements for additional barriers could be reduced and the total outlay for safety sharply curtailed.

The preceding discussion on strain energy absorption and reactor containment potential is largely qualitative or semi-quantitative. But engineers require highly quantitative information for reactor vessel containment design; they must know the dimensions, shape, and constraints correlative with containing postulated excursions. In other words, they require EXPLOSION CONTAINMENT LAWS FOR REACTOR VESSELS - laws expressed in terms of conventional materials and properties.

CHAPTER 4

SIMULATION OF NUCLEAR EXCURSIONS

The magnitude and flux of excursion energy and attendant gases determine the loading at the internal wall of the vessel. The stress-strain state in the wall and the ultimate response of the structure are complex functions of the loading, functions obtainable only through experimental means and feasibly so only through experiments in scaled models. Clearly, the character of excursion loading and the means for simulating such loading had to be considered further as a first step in the formulation of Containment Laws. This was accomplished through the use of conventional explosives and through further study of previous propellant experiments.

4.1 TNT Rationale. The rationale for employing TNT (or a similar conventional explosive like pentolite) to simulate nuclear accidents can be readily expressed: Nuclear excursions cannot be micro-scaled; TNT explosions can, and, furthermore, many of their scaling properties are well known. This makes available a very important tool that is often the sine qua non for complex multi-parameter problems: experiments in small models. Although the character of the energy released during a postulated nuclear excursion may not be identical to that of the TNT explosion, the violence factors of the two mechanisms are often sufficiently alike to permit use of the TNT model as a reasonable upper-bound simulant (reference (a)).

For reactors, postulated credible accidents cover a wide spectrum in both magnitude and flux of the energy released; these range from small releases to thousands of megawatt-seconds occurring in times from a few microseconds to seconds or more. In this respect, it is singularly important to note that conventional high explosives, like TNT and pentolite, also produce

flux-rate mechanisms that cover a broad spectrum: the shock wave of the conventional explosive is a microseconds mechanism, and the quasi-static "equilibrium" pressure generated by the released gases occurs in the domain of milliseconds and seconds. Since the fundamental characteristics of both mechanisms are known, their application to basic studies is feasible. This was demonstrated in the extensive structural response investigations of the Enrico Fermi Reactor previously referred to in Chapter 2.

At the energy density of 1050 calories per gram - a nominal value for the heat of detonation of TNT - a pound of TNT would release two megawatt-seconds of energy. Since the TNT energy flux constitutes a reasonable upperbound for nuclear excursions, there exists the practice of expressing large excursion accidents in pounds of TNT for purposes of safety assessment. That this practice is profitable in containment studies is one of the principal theses of this report.

4.2 The TNT Explosion. Consistent with the theme of interest, it is assumed that the simulated excursion would be contained within the reactor vessel. It is further assumed that normal operating pressures and temperatures exist everywhere in the reactor vessel and its environs immediately prior to detonation. The TNT charge is located at the core; it has a weight density of about 1.5 gm/cm^3, it occupies a volume of the order of the core volume, and its temperature and pressure are 25°C and atmospheric.

Upon detonation, the detonation front would propagate through the charge with a velocity of about 6000 meters/sec and pressures behind the front estimated to be of the order of 200 kilobars. In consequence, the solid explosive would be transformed almost discontinuously in time to a gaseous fireball at virtually the same volume with temperatures and pressures of

the order of 3000°C and 50,000 atmospheres (see Cole, reference (1)). The energy density and gas produced per gram of TNT would be about 1050 calories and 0.033 gram mole. As a consequence of the immense energy flux, two destructive mechanisms would be produced: the shock wave and the internal blast pressure, i.e., the quasi-static (or equilibrium) pressure generated by gases released from the explosive charge.

4.3 Shock Wave. The shock wave, which initially contains approximately one-half of the energy released, would propagate through the media surrounding the core and strike the internal wall of the reactor vessel. In response to the delivered impulse, the wall would be given a virtually instantaneous velocity. This is true, since the response time of the wall would be large relative to the significant duration of the shock wave. Portions of the wall nearest the charge would be given the greatest velocity and undergo the greatest deformation. The inertia and tensile strength of the reactor vessel would resist the impulsive force during acceleration of the wall. Subsequently, the tensile constraints would bring the wall to rest.

In general, shock wave attenuation in elastic media is less than in inelastic, plastic, or relatively compressible media. Attenuation of the shock would be greater in the reactor liquid coolant than in steel, and in air or similar gases the attenuation would be considerably greater than in the liquid or steel. Thus, it is seen that if the coolant were lost from the reactor vessel, the shock attentuation potential of the system would be increased, and the shock strength at the vessel wall would be decreased with a consequent decrease in deformation. Clearly, then, the deformation volume of the reactor vessel would be a function of reactor

coolant content: the largest deformation would be associated with the case of no coolant loss and conversely for the complete loss of coolant.

4.4 Internal Blast Pressure. Following the shock wave would be the explosion gases, which initially contain the remaining one-half of the released energy, and these gases would be confined in the reactor vessel. The resultant internal blast pressure, a quasi-static pressure as opposed to the short-duration pressure of the shock wave, would be a significant function of two variables: the volume into which the explosion gases flow and the capacity (quality and quantity) of the heat sinks available to these gases. Distortion of the vessel wall from the shock wave would precede arrival of the blast pressure at the wall, so that the expansion volume available to the explosion gases would be the sum of the initial gas volume, the void volume created by coolant losses, and the deformation volume produced by the shock.

If a major portion of liquid coolant were retained in the vessel, the coolant would constitute a significant heat sink. If a major portion or all of the coolant were lost from the vessel, the complex metal structures that generally surround the core would be important heat sinks. In any event, these heat sinks would considerably reduce the internal blast pressure. Through expansion and heat losses, the blast pressure would be generally an order of magnitude or more lower than the shock pressure, and would not be sufficient to further distort the vessel wall. This is shown in reference (1) and discussed further in section 7.6.

4.5 Propellant Loading. Again it is assumed that containment occurs and that normal operating pressures and temperatures exist everywhere in the reactor and its environs immediately prior to initiation. The solid propellant is at the core; its

weight and energy densities, temperature and pressure are like those for the TNT case just discussed. Upon initiation and burning, however, the character of the loading produced would be substantially different from that of TNT, since the energy release time would be of the order of milliseconds and seconds.

No shock wave would be produced; consequently, all of the released energy would appear initially in the product gases. As the propellant continued to burn, a stable and uniform build-up of pressure would occur (see reference (k) and section 9.7). Like the internal blast pressure of TNT, the propellant loading would be a significant function of the expansion volume and the capacity of the available heat sinks - both of which would act to decrease pressure. Since the propellant does not generate a shock wave that is immediately available for vessel deformation, energy and gas release must be large enough to overcome the negating effects of the heat sinks and expansion volume before a sufficient pressure can be developed to rupture the vessel. This pressure would correspond nearly to the static rupture strength of the vessel. It is noted, therefore, that, for marginal containment, the post-accident pressure in the reactor vessel resulting from a propellant loading would exceed considerably that from a TNT explosion (internal blast pressure). For marginal containment, the deformation pattern would be similar to that for TNT, and hence, the expansion volumes would be of the same order.

4.6 TNT-Propellant Efficiency. The heat sinks in the reactor vessel would attenuate the propellant loading to a much greater degree than for the TNT case. This follows since the exposure time would be large for all of the propellant energy released, whereas for TNT, 50 per cent of the energy released is in the shock wave delivered to the vessel wall, and this is independent of the capacity of the heat sinks. Indeed, this time-dependent absorption of energy is an overriding containment phenomenon

from which the following general conclusion can be drawn: the vessel deformation efficiency of TNT is greater than that of slower energy releases; conversely, the reactor containment potential for energy fluxes less than that of TNT is greater than for the TNT flux.

The influence upon containment of D'Alembert (or inertial) constraints is another point of important difference between propellant and TNT shock loading. Very massive components like the 143-ton Fermi shield plug would be negligibly responsive to the shock, but significantly so to propellant loading. The same rationale applies to the massive graphite blocks surrounding the Fermi reactor and the large body of water surrounding Oak Ridge's High Flux Isotope Reactor: the graphite and water would enhance the reactor containment potential for shock loading but make almost no contribution to containment for the slower propellant loading.

In summary, it is seen that energy flux constitutes an extremely significant excursion containment parameter. Energy release mechanisms of microseconds and milliseconds duration have markedly different complexions and present greatly different containment problems. And with respect to "efficiency":

(a) the deformation efficiency of TNT (the capacity for doing work on constraints that are largely non-inertial) is <u>greater</u> than that for slower energy releases

(b) the D'Alembert efficiency of TNT (the capacity for doing work on constraints that are largely inertial) is <u>less</u> than that for slower energy releases.

4.7 <u>50/50 Pentolite</u>. Mixtures of PETN ($C_5H_8O_{12}N_4$) and TNT ($C_7H_5O_6N_3$) are called pentolites, the most common being a 50/50 mixture. All of the previous discussions on the behavior of TNT applies to pentolite, and pentolite possesses additional advantages as well. In view of the ease with which it is detonated and its established replicability in small-scale tests,

50/50 pentolite was chosen as the most satisfactory explosive charge to employ in the containment program. The pentolite/TNT ratios of energy density and release of gas products per unit of reactant are 1.02 and 1.17, respectively; hence the use of pentolite in containment studies is consistent with reasonable upper-bound criteria.

CHAPTER 5

METHOD OF SOLUTION

The solution to the multi-faceted containment problem required, first of all, that a judicious choice of the principal parameters be identified and, at least, partially characterized.

5.1 Principal Containment Parameters. In review of the loading mechanisms discussed in Chapter 4, it is seen for the reactor vessel per se that the principal containment parameters can be taken as:

(a) the reactor vessel material, size, shape, and constraints

(b) the magnitude and duration of the shock wave striking the vessel wall

(c) the inertia and dynamic tensile strength of the vessel wall

(d) the heat-sink capacity of the internals of the reactor vessel, including the liquid coolant.

These basic quantities are innate to excursion containment. They are not all true parameters, however; some are pseudo parameters, consisting of a fixed element and an element that varies:

(a) The shock wave strength is a function of the density of the media surrounding the core; the density of the steel internals stays fixed, but that of the remainder varies with coolant content.

(b) The inertia of the vessel wall is a function of the wall mass and acceleration; the mass remains fixed, but the acceleration varies with the strength of the shock wave and the dynamic tensile strength of the reactor vessel.

(c) The dynamic tensile strength of the vessel wall depends upon the static strength of the wall, gross strain, and the rate of strain; the static strength is fixed, but the strain and rate of strain vary with the strength of the shock wave.

(d) The total heat-sink capacity of the reactor vessel internals consists of the combined sinks afforded by the reactor coolant and the metal structures that generally surround the core; the capacity remains constant with respect to the metal, but varies with coolant content.

5.2 Fundamental Questions. Attempts to quantify and synthesize the above parameters raised some interesting questions.

(a) What are the shock attenuation properties of the metal-coolant-gas medium that surrounds the core?; how are these properties affected by the temperature of the medium and the loss of coolant from the system?

(b) The shock strength and, hence, the acceleration of the wall is unknown; how does the inertial constraint influence the deformation volume of the reactor vessel?

(c) The dynamic tensile strength of the vessel wall varies significantly with gross plastic strain and the rate of strain. The shock loading and inertial constraints are unknown; what are the strain and strain-rate functions?

(d) The explosion gases mix with the metal-coolant-gas medium surrounding the core. The character of the interface between the explosion fireball and the surrounding medium is unknown; what are the millisecond chemical and thermodynamic mechanisms that govern the heat-sink capacity of the medium?

(e) The TNT internal blast pressure and propellant-type gas pressures depend upon the heat-sink capacity of the reactor internals and the volume into which the equilibrium gases expand. But the heat-sink and gas-expansion quantities are unknown functions of unknown functions, etc., with coolant content appearing as a significant variable in all.

5.3 State of the Art. Upon consideration of the above questions and some reflection, it was not difficult to perceive the extremely complex functional form of the pseudo parameters that characterize containment. The governing chemical, thermodynamic, and physical phenomena were, for the most part, micro or milliseconds mechanisms that did not lie in the realm of classical knowledge. In short, when the program was started, the state of the art would not permit a quantitative characterization of the pseudo-parameters via available theory and empiricism. This meant that one and only one method of solution could be employed: Saint-Venant's semi-inverse method of classical mechanics.

5.4 Saint-Venant's Semi-Inverse Method. Since teleological solutions (those directed to a specific purpose) do not require that everything be known about all of the parameters, bound and/or lumped parameter solutions frequently provide important general information in a restricted domain of interest. One of the most useful algorisms for obtaining such solutions is Saint-Venant's semi-inverse method of classical mechanics. Here, upon identifying and characterizing the principal parameters to the extent in which they are known (both empirically and theoretically), a synthesis of these parameters is used to construct an incomplete functional form of the desired solution.

This embryonic functional form constitutes certain necessary conditions that the complete solution must satisfy. In general, however, the necessary conditions expressed in the embryonic function are not sufficient to guarantee the complete solution; this must be achieved through the judicious imposition of boundary conditions. Depending upon the nature of the problem, the boundary conditions may be determined from further theoretical considerations, experimental data, or, very often, a combination of the two.

Of course, it may be correctly inferred that the semi-inverse method will not yield a solution if the embryonic form cannot be adequately determined. If the character of the multi-parameter problem is extremely complex, the state of the art will frequently not yield a solution without numerous experimental data. This was the case with containment: it meant that the necessary boundary conditions could be established only through fundamental and extensive experiments in scaled models of reactor vessels.

5.5 Hopkinson Scaling. There exist many schemes for predicting the behavior of a prototype from experiments in scaled models; see, e.g., H. G. Snay's specific treatment relating to underwater explosion phenomena in reference (m) and H. L. Langhaar's more general treatment in reference (n). A study of the various methods showed Hopkinson scaling (also known as iso-velocity or cube-root scaling) to be the most appropriate for the containment problem.

Briefly, in Hopkinson scaling, linear dimensions of the prototype and model are related by a constant scale factor λ, but velocity and the acceleration due to gravity do not scale. This fundamental choice determines the character of all other Hopkinson quantities. Classical model/prototype ratios of quantities basic to containment are listed below:

Velocity, pressure, stress, strain	unity
length, time, displacement, specific impulse . . .	λ
area, surface force, inertia	λ^2
mass, weight, volume, momentum, impulse	λ^3
acceleration, time rate of strain	λ^{-1}

A fundamental requirement of all scaling methods is that phenomena of interest in the prototype be predictable from experiments conducted in the model, and such will be the case if the scaling character of each phenomenon is known. Upon

relating this requirement to the containment problem, the difficulty in obtaining a solution became more evident: for example, not only was the quantitative chemical and thermodynamic character of the close-in TNT-coolant reaction generally unknown, its scaling properties were unknown as well. Specifically, this scaling question was whether the TNT-coolant mechanism in the prototype and model would vary time wise with λ as in Hopkinson scaling, or be time dependent in another way. More generally, there existed the question: What are the scaling properties of excursion loading, considering that the reactor vessel deforms dynamically and gross-plastically?

5.6 Conceptual Design of Models. Power reactor vessels and many others are complex welded structures that are basically cylindrical in shape with length $\geq$ two diameters. The end closures are of various types, and the vessel wall, including the closures, is interrupted by numerous nozzles to accommodate pipes, control devices, etc. Aside from housing the core, blanket, and control mechanisms, the reactor vessel is filled or partially filled with a circulating coolant. Now as discussed previously, the spectrum of excursion accidents is quite large in both magnitude and flux of the energy released: it ranges from small accidents to thousands of megawatt-seconds occurring in times from a few microseconds to seconds or more. Furthermore, the accidents of this spectrum can take place anywhere in the coolant loss domain from no loss to a complete loss.

The range of excursions, the conditions under which they may occur, and the multiplicity and complexity of the principal parameters made it clear that the general containment problem was one of inordinate scope and difficulty. Rather than attempt an immediate solution to the general problem, it seemed prudent to seek first a basic upper-bound solution - a solution for

containing a postulated excursion under the most adverse conditions in a vessel of elementary shape. A priori, the "most adverse conditions" for an excursion of given magnitude are:

(a) that the excursion occur at the greatest energy flux, i.e., that the energy be released in the shortest time and

(b) that the reactor vessel be filled with liquid coolant or suffer no loss of coolant.

For obvious reasons the right circular cylinder was chosen as the most convenient and useful shape for the reactor vessel models. Early experiments with TNT in water and air showed that the near-rupture deformation pattern (see Figure 6.1) is always restricted to about two diameters; hence the majority of the models possessed length equal to two diameters. Since the density and compressibility of water are only slightly different from those of other known liquid reactor coolants and since, in the containment domain, TNT shock attenuation is believed to be negligibly sensitive to these differences, water was employed as the model reactor coolant.

The basic upper-bound containment solution, then, was for the case of the TNT explosion occurring in a right cylindrical vessel with length equal to two diameters and filled with liquid coolant. Once the basic upper-bound solution was in hand, the rationale was that it could be modified to provide safe and reasonable solutions for less adverse accident conditions and for vessels fitted with weldments, nozzles, and other discontinuities.

5.7 Summary. The principal parameters of containment, both classical and pseudo, were set forth, and some fundamental questions were raised to indicate the difficulty of quantitative parametric characterization. An upper-bound, lumped-parameter solution via Saint-Venant's semi-inverse method was postulated as the only path that would yield the desired Containment Laws.

The semi-inverse method, Hopkinson scaling, and conceptual models were discussed, and case conditions for the basic upper-bound containment solution were specified.

The semi-inverse method is pursued in subsequent chapters via the following steps:

(a) formulation of the semi-inverse embryonic solution (i.e., an embryonic Containment Law format)

(b) conduct of an extensive experimental program employing explosives and propellants to simulate nuclear excursions in Hopkinson models of reactor vessels

(c) reduction of experimental data to satisfy boundary condition requirements of the embryonic solution

(d) modification of the basic upper-bound solution to provide safe and reasonable solutions for the less adverse conditions of the accident spectrum and for vessels fitted with weldments, nozzles, and other discontinuities.

CHAPTER 6

EMBRYONIC FORMAT

The first step in the Semi-Inverse Method of solution is to synthesize everything that is known (or seems reasonable) about the problem and to construct an embryonic or trial solution from the synthesis.

6.1 Preliminary Experiments. An examination of available containment information showed that even an adequate trial format of a basic containment law could not be written down without some preliminary experiments. Among the first of these were tests employing pentolite in right-cylindrical model vessels filled with water or air at atmospheric pressure. The principal results were the "localization factors" shown in Figure 6.1. (Figures and tables appear at the end of each chapter.) Here it is seen that the character of the shock is such that near-rupture deformation is localized to about two radii for air and four radii for water. Hence, for vessels with inside length L and inside radius R_1 such that $L \geq 4R_1$, it was indicated that the explosion containment potential is not an appreciable function of vessel length. A priori, this would be true irrespective of the loss of reactor coolant in any degree.

In other preliminary experiments employing pentolite in water-filled models, dilations were photographed with a Beckman-Whitley Dynafax camera operating at 25,000 frames per second. Typical vessel data, test conditions, and sequential frames are shown in Figure 6.2. The total dilation time was about 600 microseconds; at 40 microseconds per frame, the motion was recorded in 15 frames. Radial deformation and strain of the external wall at the mid-meridian is plotted versus time in Figure 6.3. From these data, radial velocity and strain rate versus time are plotted in Figure 6.4; radial velocity and strain rate versus radial strain are plotted in Figure 6.5.

The geometries of the curves in Figures 6.3, 6.4, and 6.5 are singularly significant. The deformation-time plot can be interpreted as parabolic. If this is done, it follows that the velocity-strain plot is parabolic and that the velocity-time plot is linear. From D'Alembert's Principle, this means that the force acting to bring the mid-meridian wall to rest was constant throughout the entire deformation. Several important consequences of these findings were:

(a) Specifically, the data provided important parametric information for the embryonic containment law

(b) More generally, new insight was provided into the response of pressure vessels to explosion loading in the containment domain (the response domain in which containment occurs), and

(c) New insight and new corroborative data were added to the meager information available on the effects of very rapid strain rates upon the strength of ductile steels. These data were obtained for a mid-meridian ring that deformed gross-plastically under the action of an apparently constant retarding force. Only this force, a function of the dynamic strength of the material, and the D'Alembert term determined the motion. Hence, these rate-of-strain data are inherently free of the end, inertial, and short loading time effects so common to dynamic-tensile and impact experiments.

The results of the preliminary experiments together with available explosions phenomenology motivated and permitted formulation of the embryonic solution, first for the general case and then for a specific case.

6.2 General Case. A closed vessel is subjected to internal explosion loading. The vessel wall is a strain-hardening steel that flows gross-plastically. It is assumed that the wall material is of uniform constant mass density and that the wall remains a continuum.

We frame the vessel in an orthogonal coordinate system for which the Lagrangian spatial coordinates

$$x_{io} , \quad i = 1,2,3$$

denote the original position (i.e., the position at event time $t = 0$) of all points in the vessel wall including the surface. Since the Eulerian coordinates

$$x_i = x_i(x_{io}, t)$$

are at least of class C^1 and the Jacobian

$$\frac{\partial (x_1, x_2, x_3)}{\partial (x_{10}, x_{20}, x_{30})} = J$$

is everywhere positive in the wall, the Eulerian and Lagrangian integrals are related in the usual way by

$$\int f(x_i)\, \hat{dx_i} = \int f(x_i)\, J\, \hat{dx_{io}}$$

where the $\hat{dx_i}$ and $\hat{dx_{io}}$ are products, respectively, of the dx_i and dx_{io}.

Upon detonation of the explosive, the shock wave propagates through the media surrounding the charge and strikes the internal wall; whereupon the wall, it is hypothesized here, responds with a virtually instantaneous initial velocity

$$\vec{v}_o = \vec{v}_o(x_{io})$$

The instantaneous-velocity hypothesis is reasonable since the effective shock loading time is an order of magnitude less than the gross deformation time. Velocity-time and velocity-strain integrations of the second law of motion, respectively, yield

$$\int_t \int_A [\, \vec{p}\,(x_{io},\, t) \cdot d\vec{A}\,]\, \vec{\eta}\, dt = \frac{w}{g} \int_V \vec{v}_o(x_{io}) \hat{dx}_{io} \qquad (6.1)$$

$$\int_V D(x_{io})\, \hat{dx}_{io} = \frac{w}{2g} \int_V \vec{v}_o^{\,2}(x_{io})\, \hat{dx}_{io} \qquad (6.2)$$

where the symbology is

$\vec{v}_o$ . . . . initial velocity of vessel wall, ft/sec
t . . . . duration of shock interval, sec
$\vec{\eta}$ . . . . unit vector in direction of $d\vec{A}$
$\vec{p}$ . . . . vector shock pressure, psfg
w . . . . wall mass density, lb/ft^3
g . . . . acceleration due to gravity, ft/sec^2
A, V . . . wall internal area and volume, ft^2, ft^3
D . . . . wall deformation energy density, $ft\text{-}lb/ft^3$

Equation (6.1) states that the total impulse delivered to the vessel wall is equal to the total initial momentum of the wall; (6.2) states that the total work done in deforming the wall is equal to the total initial kinetic energy of the wall. Neither the momentum nor the kinetic energy is conserved, but the conservation of mechanical energy inherent in (6.2) is valid.

6.3 Specific Case. While the general relations expressed in equations (6.1) and (6.2) possess a conceptually desirable form, they will not yield a quantitative containment solution in terms of currently available information. We turn then to a less general solution: one that is further restricted to a water-filled right-cylindrical vessel for which

(a) the initial values of the internal and external radii, R_1 and R_e, the internal length L, and the wall thickness h_o are related by

$$L \geq 4R_1, \qquad 10 \leq R_1/h_o \leq 40 \qquad h_o = R_e - R_1$$

(b) R_1 and the explosive-charge radius R_c are related by

$$R_1 \geq 3R_c$$

(c) the water is in a liquid state attendant normal operating conditions*

* It should be noted that the analysis and experimental work to follow assumes the water to be at room temperature and atmospheric pressure rather than at elevated values. This, however, does not constitute a significant restriction. The elevated temperatures and pressures normally associated with sodium or water reactors should not affect appreciably the shock impulse delivered to the vessel wall. Any elevated pressure would alter only the elastic strain energy of the vessel, but this is considered negligible in the gross-plastic deformation domain.

(d) the vessel wall is homogeneous and isotropic

(e) no constraints other than the tensile and shearing constraints in the wall act to retard gross plastic deformation of the vessel

(f) the explosive charge is compact (length ≈ diameter) and is detonated at the centroid of the vessel

(g) there are no nozzles, welds, or other wall discontinuities.

The above restrictions contain three inequalities. The first of these, $L \geq 4R_i$, is motivated by the "localization factor" for water illustrated in Figure 6.1. It is mentioned again that the character of the shock is such that deformation is localized to not more than four radii for either water or air surrounding the charge. Hence, for $L \geq 4R_i$, the explosion containment potential of the reactor vessel simulant is not an appreciable function of its length. The lower limit of the second inequality, $R_i/h_o \geq 10$, is an accepted value for thin-wall theory; the upper limit, $R_i/h_o \leq 40$, is the maximum value selected for this study. The third inequality, $R_i \geq 3R_c$, is invoked because of the extent to which hydrodynamic phenomenology for the subject problem is unknown closer to the charge. It is important to note that since specifications of the large majority of reactors can be interpreted to satisfy the above restrictions on configuration, no loss in generality accrues in this respect.

Consistent with the cylindrical coordinate system, we put

$$x_{10} = r_o, \qquad x_{20} = \theta_o, \qquad x_{30} = z_o$$

and if we place the system origin at the centroid of the cylinder with major and z axes colinear, it follows from symmetry that equations (6.1) and (6.2) reduce, respectively, to

$$2\pi R_1 \int_t \int_{-L/2}^{L/2} [\, \vec{p}(z_o,t) \cdot \vec{r}\,]\, \vec{r}\, dz_o dt = \frac{wV_u}{g} \int_{-L/2}^{L/2} \vec{v}_o(z_o) dz_o \qquad (6.3)$$

$$V_u \int_{-L/2}^{L/2} D_h(z_o)\, dz_o = \frac{wV_u}{2g} \int_{-L/2}^{L/2} \vec{v}_o^{\,2}(z_o)\, dz_o \qquad (6.4)$$

where $\vec{r}$ is the unit vector in the radial direction,

$$V_u = \pi (R_e^2 - R_i^2) \qquad (6.5)$$

is the volume per unit length of cylinder, and

$$D_h = D_h(z_o)$$

is the average value of $D(z_o)$ across the wall thickness h.

6.4 Unit-Length Ring. We elect at this point to consider the response of a single unit-length ring located at the mid-meridian of the cylinder in the (r, θ, o) plane with radii R_i and R_e. Upon detonation of the explosive charge, this ring

being closest to the charge centroid, receives the greatest impulse, undergoes the largest deformation, and is subjected to the highest stress. In fact, the hoop stress in the mid-meridian ring constitutes an excellent containment index, since experimental evidence indicates, as shown in Figure 6.6, that marginal rupture for ductile cylinders always results from the propagation of a fissure that originates at the mid-meridian. Invoking this rationale, we find that, for the mid-meridian ring of length unity, the variable z_o becomes the parameter $z_o = 0$, and equations (6.3) and (6.4) take the forms

$$2\pi R_1 \int_t \hat{p}(0,t)\, dt = \frac{w}{g} V_u \hat{v}_o(0) \tag{6.6}$$

$$D_h(0) = \frac{w}{2g} \hat{v}_o^2(0) \tag{6.7}$$

The simultaneous solution of equations (6.5), (6.6), and (6.7) yields

$$I^2 = \left(\int_t \hat{p}(0,t)\, dt \right)^2 = \frac{w(R_e^2 - R_i^2)^2}{2g R_i^2} D_h(0) \tag{6.8}$$

where I is the specific impulse (lb sec/ft^2). Thus the functions of interest at this stage of the embryonic solution are I, the specific impulse, and D_h, the deformation energy density.

6.5 Specific Impulse. An established power law relating charge weight W and charge distance R_1 to specific impulse for explosions in free water is given by Cole in reference (1) as

$$I_f = KW^{1/3} (W^{1/3}/R_1)^{\beta} \tag{6.9}$$

where the nomenclature is

I_f . . . . specific incident impulse in free water, lb sec/in^2
W . . . . explosive charge weight, lb
R_1 . . . . distance from charge center, ft
K, β . . . . constants

The quantities K and β are treated as constants in the free-water domain for a given explosive. For pentolite, $\beta = 1.05$ in the broad spectrum of conventional underwater applications; for the narrow containment domain, however, it was found that the classical acoustic law ($\beta = 1$) can be assumed with no loss in generality. Thus equation (6.9) reduces to

$$I_f = KW^{2/3}/R_1 \tag{6.10}$$

Of course, the total impulse of (6.10) will not be absorbed by the vessel wall; a portion will be lost due to reflection and the complex phenomena attendant to all such highly transient high-pressure interfaces. To account for these losses, as well as a difference in units, we hypothesize that I (lb sec/ft^2), the impulse absorbed by the vessel wall, is related to the free-water impulse I_f (lb sec/in^2) by an "efficiency factor" function ξ such that

$$I = 144\ I_f/\xi \tag{6.11}$$

It seems reasonable to expect that ξ is a function of the wall distance from the charge and the D'Alembert and tensile constraints in the wall. More specifically, we know that the classical hoop stress is a function of R_1/h_o. Consistent with the semi-inverse method and the teleological character of the desired solution, we incorporate this rationale into the trial format and write

$$\xi = \xi\ (R_1/h_o) \tag{6.12}$$

whereupon the impulse absorbed by the vessel wall becomes

$$I = 144\ KW^{2/3}/R_1\xi \tag{6.13}$$

6.6 Deformation Energy. The true stress-classical strain diagram is quite linear for the case of a ductile steel deformed statically in the gross plastic domain. With sufficient accuracy for our semi-inverse rationale, we can write that

$$\sigma_t = \sigma_y + \left[\frac{\sigma_u(1 + \epsilon_u) - \sigma_y}{\epsilon_u} \right] \epsilon \tag{6.14}$$

where the nomenclature is

σ_t . . . . true stress, psi
σ_y . . . . conventional yield stress, psi
σ_u . . . . conventional ultimate stress, psi
ϵ . . . . conventional instantaneous strain, in/in
ϵ_u . . . . conventional ultimate strain (elongation), in/in

For the case of gross plastic deformation occurring at rapid rates of loading, the stress σ in a strain-hardening steel like 304 stainless is at least a function of the strain ϵ and the strain rate $\dot{\epsilon}$. The stress may also be a function of $\ddot{\epsilon}$ and higher derivatives of ϵ with respect to time: but since little or nothing is known about these higher order effects, it will be assumed here in the usual way that the stress function is

$$\sigma = \sigma (\epsilon, \dot{\epsilon}) \qquad (6.15)$$

i.e., the stress is a function of the strain-hardening and strain-rate mechanisms alone. For deformations that occur at continuously decreasing rates of strain, the strength of the material decreases continuously with strain as a function of the strain-rate mechanism and increases continuously with strain as a function of the strain hardening mechanism.

It is interesting to entertain the net influence of the strain-hardening and strain-rate mechanisms implied in Figures 6.3, 6.4, and 6.5. In reference (o), Tardif and Erickson report the work of a number of investigators on the strain-rate enhancement of the yield point in mild steel. The data are presented graphically with the ratio

$$R = \frac{\text{dynamic yield stress}}{\text{static yield stress}}$$

on the ordinate and strain rate on the abscissa. Among the results are those of M. J. Manjoine who found that a strain rate of 1300 per second produces the ratio R ≈ 3. Manjoine also found that the ratio R is quite stable, varying exponentially from 2-1/2 to 3 for strain rates between 200 and 1300 per second. For the stainless steel and loading conditions of Figures 6.2, his results imply an increase in the yield point from 30,000 psi to 90,000 psi, a value that is equal to the true static stress at 37 per cent elongation.

If Manjoine's results are accepted for the moment, this means that when the vessel started to deform at a strain rate of 1300 per second and when it came to rest with a 37 per cent elongation, the hoop stress at the mid-meridian was the same value: 90,000 psi. This coincidence and the stability of the strain-hardening and strain-rate effects are consistent with the finding in section 6.1 that the force acting to bring the mid-meridian wall to rest was constant during the deformation of this particular vessel. It is interesting to entertain a hypothetical hoop stress-strain diagram that might be generated from such loading conditions. This is done in Figure 6.7, and a comparison is made with statically generated diagrams. From a general point of view, however, it must be noted that strain rate, for the conditions under discussion, varies inversely with the scale factor, λ. This means that in larger vessels the strain-rate enhancement of tensile strength would be diminished and that, of course, the mid-meridian force would no longer be a constant.

Manjoine also presented strain-rate data for mild steel in reference (p). Bodner and Symonds, in reference (q), fitted a curve to these data and found that

$$\sigma_d = \sigma_y \left[\left(\frac{\dot{\epsilon}}{40.4} \right)^{0.2} + 1 \right] \qquad (6.16)$$

where the nomenclature is

σ_d . . . . dynamic yield stress, psi
σ_y . . . . static yield stress, psi
$\dot{\epsilon}$ . . . . strain rate, per second

Johnson in reference (r) reported results of explosion tests with small unconstrained rings of various materials. The experimental techniques that he employed eliminated longitudinal and shear stresses and ensured a virtually instantaneous wall velocity with no further loading once the ring began gross motion. From D'Alembert's Principle he determined the true dynamic hoop stress in the ring as a function of strain, and for several ductile materials he found that this stress, aside from being elevated with strain rate, was linear with strain. Of course, there exist other strain-rate data that could be listed here, but the above examples and discussion are sufficient to indicate the rationale attendant the development of a deformation energy function for strain that is dynamic and gross plastic.

A priori and specifically from the relations (6.14) and (6.15), we try the embryonic form

$$D_h(0) = 144\, \sigma_t\, \epsilon\, \Upsilon_1\, (\dot{\epsilon}_o) \tag{6.17}$$

where $\dot{\epsilon}_o$ is the initial strain rate corresponding to the initial wall velocity $\vec{v}_o$. The simultaneous solution of equations (6.8), (6.13), and (6.17) yields

$$W = [\, \Upsilon_1\, \Upsilon_2\, w\, \sigma_t\, \epsilon\, (R_e^2 - R_i^2)^2\,]^{3/4} \tag{6.18}$$

where

$$\Psi_1 = \Psi_1(\dot{\epsilon}_o), \quad \Psi_2 = \frac{\xi^2}{288 g K^2} = \Psi_2(R_i/h_o) \tag{6.19}$$

Equation (6.18) constitutes the embryonic containment law format where an extensive experimental program is required to establish the deformation energy function Ψ_1 and the efficiency factor function Ψ_2.

R_i WAS INTERNAL RADIUS PRIOR TO DEFORMATION

ALL CHARGES WERE DETONATED AT THE CENTROID

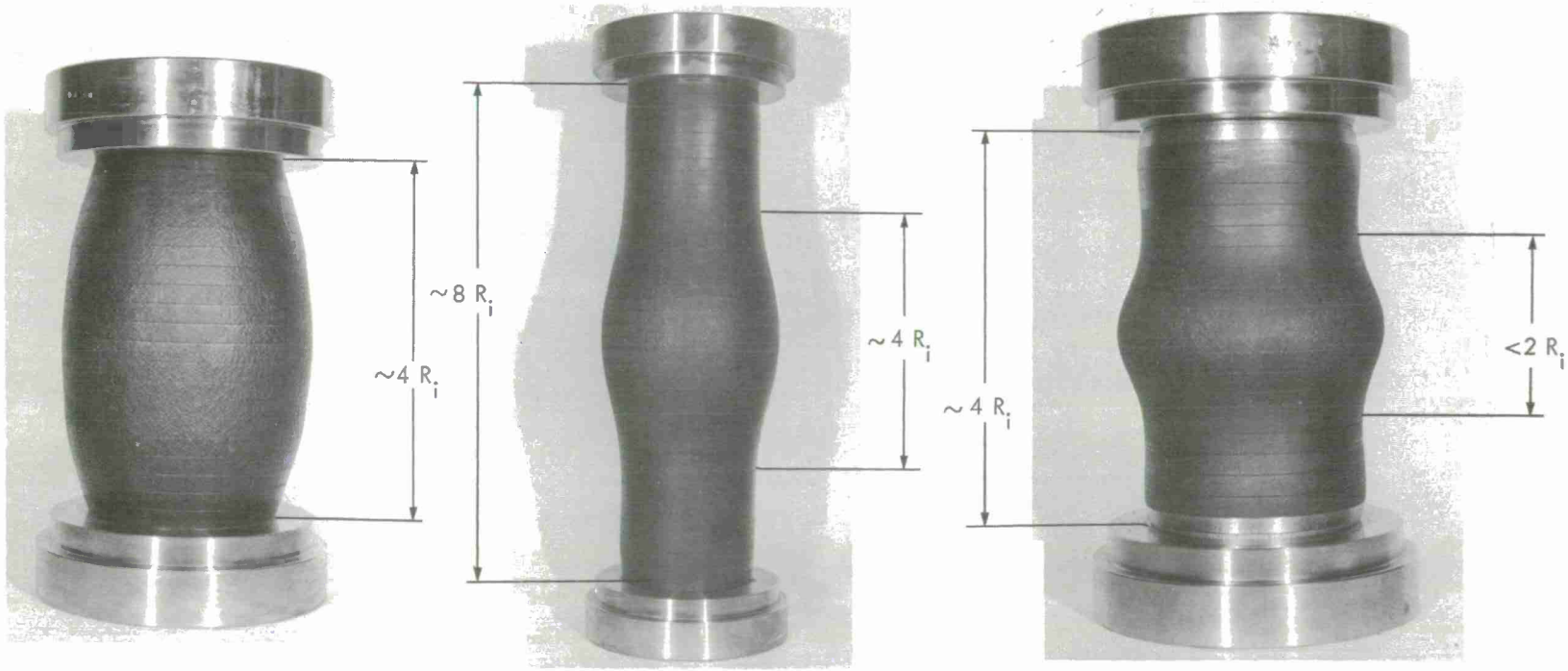

18 GRAMS IN WATER

19 GRAMS IN WATER

50 GRAMS IN AIR

VESSELS WERE ORIGINALLY RIGHT-CIRCULAR CYLINDERS, 5" ID, and 1/8" WALL. INTERNAL LENGTH OF LEFT AND RIGHT VESSELS WAS 10"; THAT OF CENTER VESSEL WAS 20". ALL WERE CENTRIFUGALLY CAST FROM 304 STAINLESS STEEL.

FIG. 6.1 LOCALIZATION FACTORS OF VESSELS DILATED WITH PENTOLITE IN AIR AND WATER

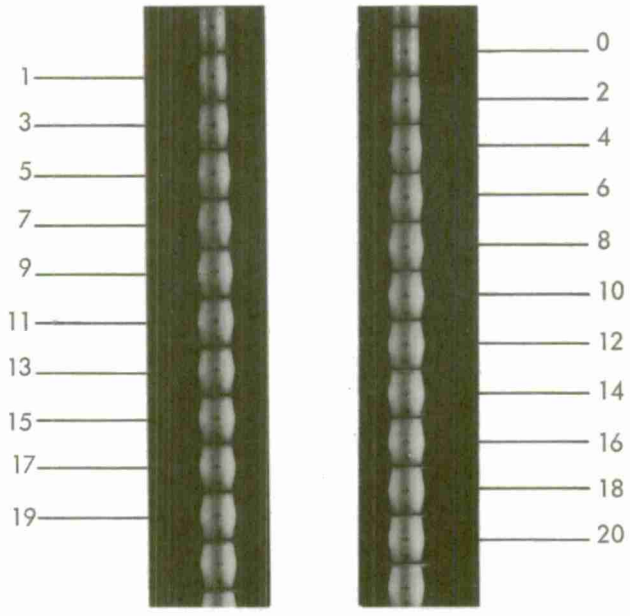

NOTES:

VESSEL MATERIAL AND SHAPE: 10" ID, 20" LENGTH, 1/4" WALL, ROLLED FROM 304 STAINLESS STEEL PLATE, WELDED ALONG LONGITUDINAL SEAM.

TEST CONDITIONS: VESSEL FILLED WITH WATER AT 70°F AND ATMOSPHERIC PRESSURE, 200 GRAMS PENTOLITE DETONATED AT CENTROID.

PHOTOGRAPHY: VESSEL DILATION RECORDED BY BECKMAN-WHITLEY DYNAFAX CAMERA OPERATING AT 25,000 FPS. FRAMES SHOWN ABOVE TAKEN AT 40-MICROSECOND INTERVALS, TOTAL DILATION TIME-600 MICROSECONDS (15 FRAMES).

FIG. 6.2 EXPLOSIVE DILATION OF MODEL VESSEL

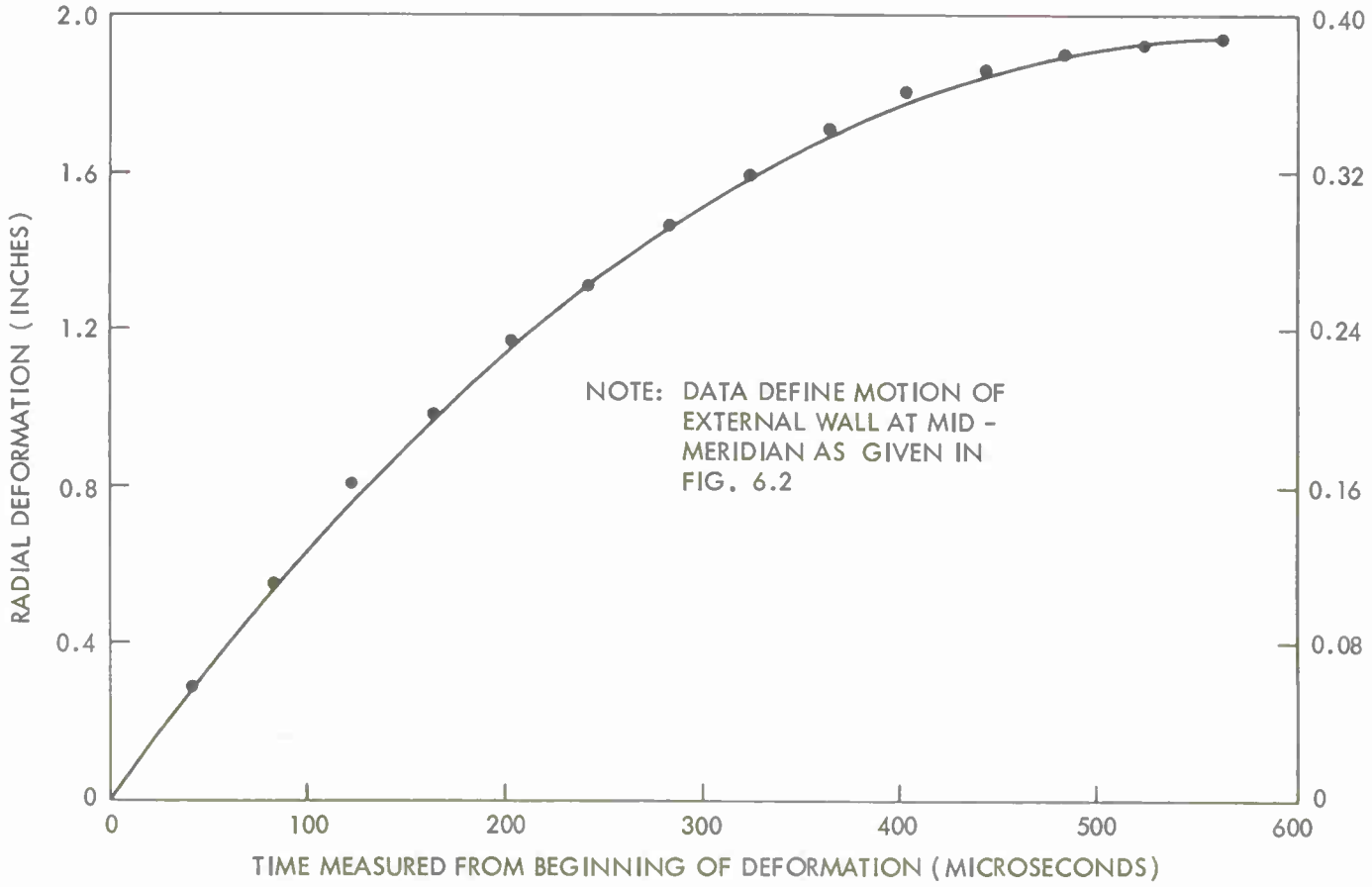

FIG. 6.3 DEFORMATION-STRAIN-TIME PLOT OF EXPLOSIVELY DILATED VESSEL

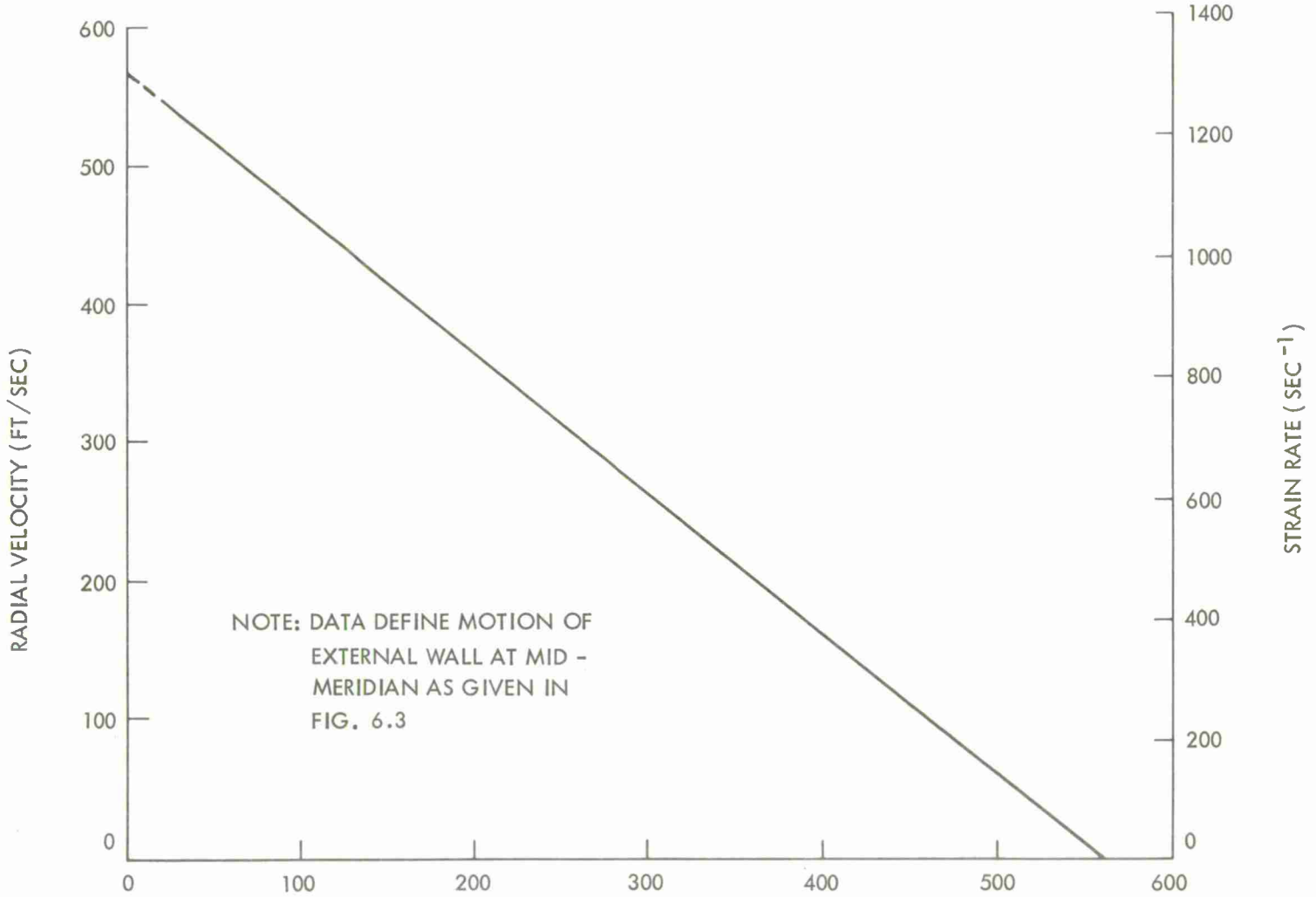

FIG. 6.4 VELOCITY-STRAIN RATE-TIME PLOT OF EXPLOSIVELY DILATED VESSEL

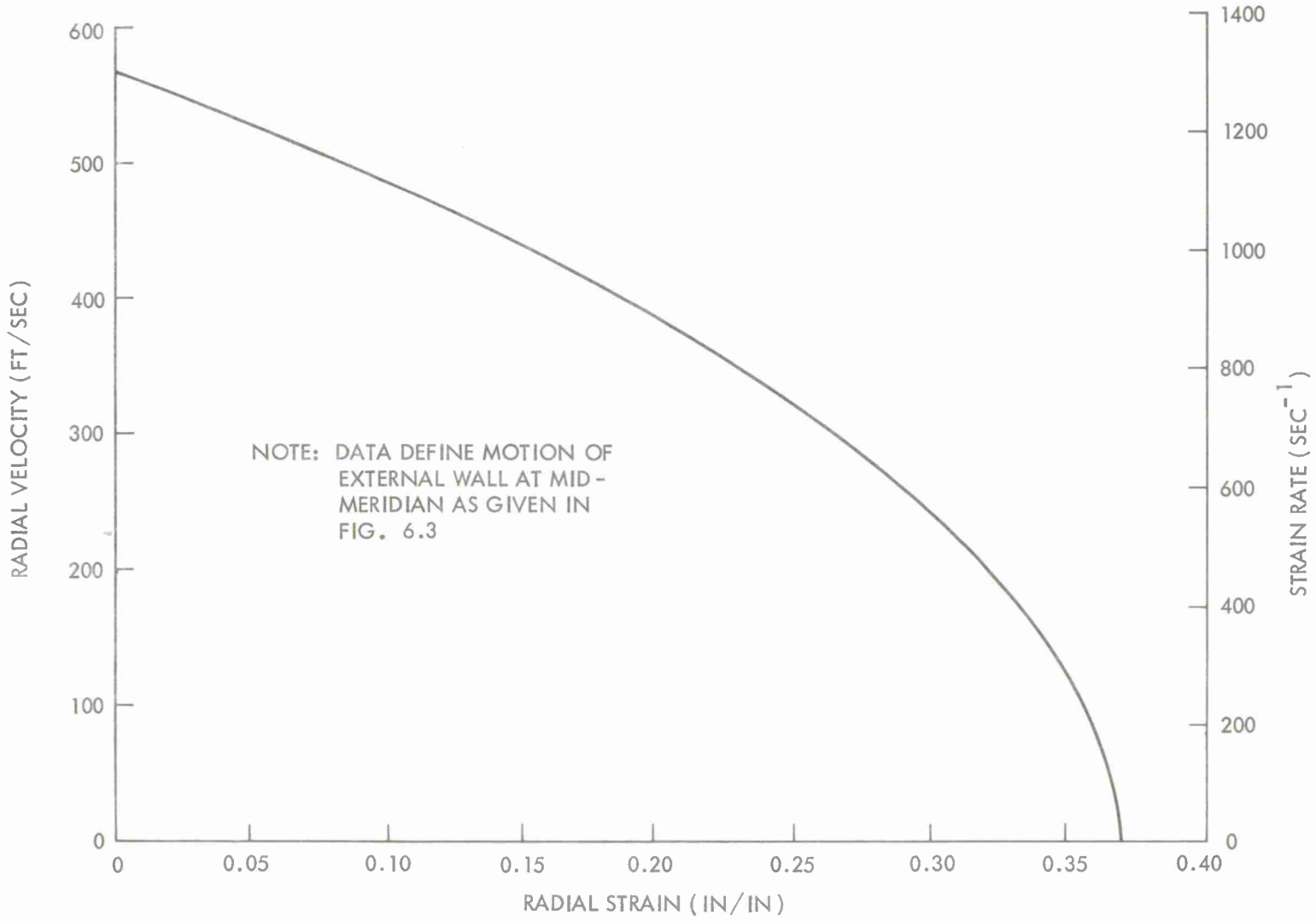

FIG. 6.5 VELOCITY - STRAIN RATE - STRAIN PLOT OF EXPLOSIVELY DILATED VESSEL

19 GRAMS OF PENTOLITE IN WATER
PRODUCED THIS MARGINAL RUPTURE

TYPICAL MARGINALLY RUPTURED VESSEL SHOWS THAT FISSURES ORIGINATE AT THE MID-MERIDIAN AS EXPECTED. WALL MATERIAL WAS CENTRIFUGALLY CAST 304 STAINLESS STEEL. ORIGINAL DIMENSIONS WERE 5" ID, 10" INTERNAL LENGTH, 1/8" WALL THICKNESS.

FIG. 6.6 DEFORMED VESSEL SHOWING ORIGIN OF RUPTURE

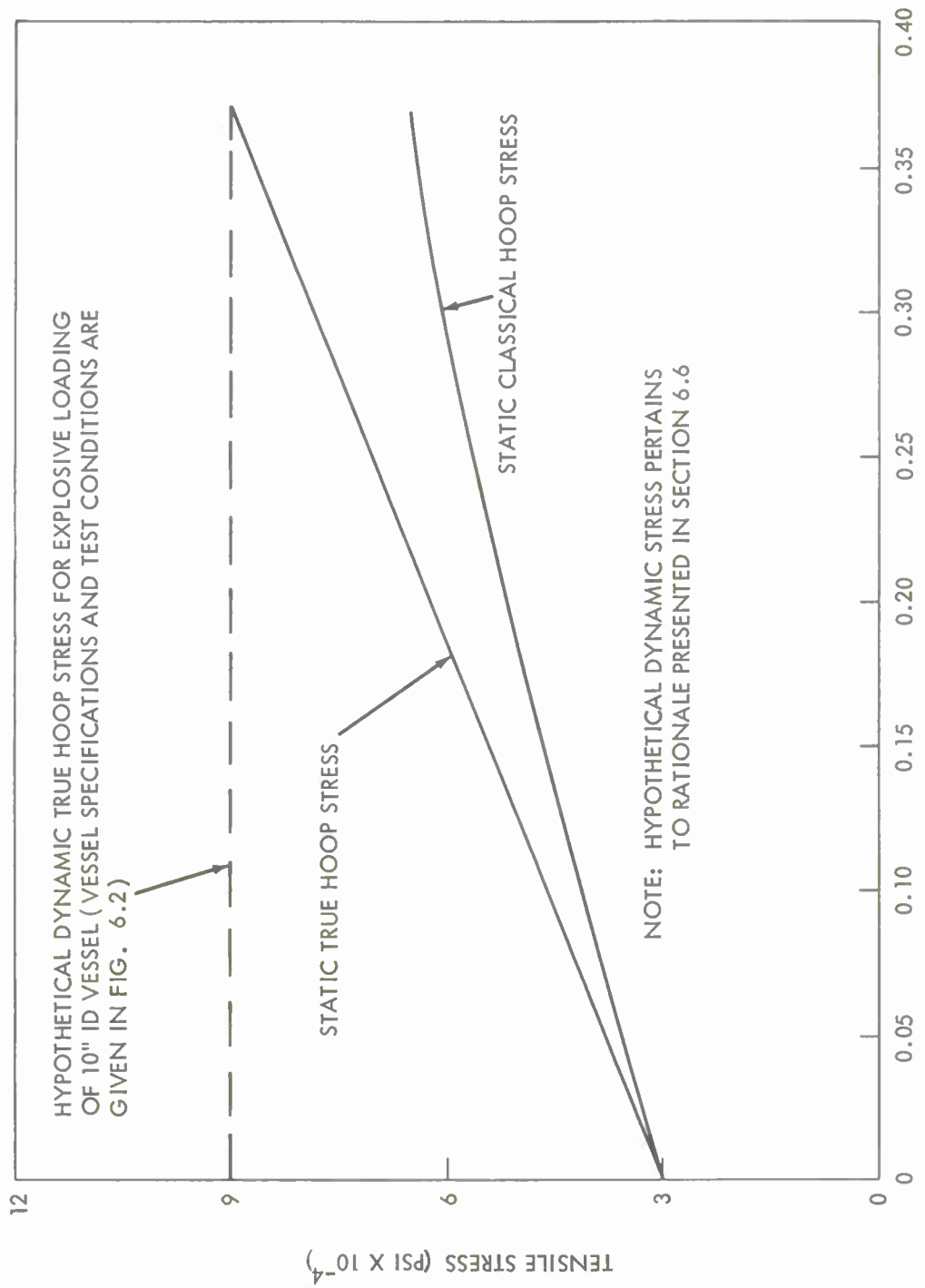

FIG. 6.7 COMPARISON OF DYNAMIC AND STATIC STRESS - STRAIN DIAGRAMS

CHAPTER 7

EXPERIMENTAL PROGRAM AND RESULTS

The following experimental program provided necessary boundary conditions for evaluating the deformation energy and efficiency factor functions of the embryonic containment law format.

7.1 Idealized Models. The major effort of the experimental program was directed to explosively dilating model reactor vessels without nozzles or significantly restrictive end constraints. In each of these experiments:

(a) the model vessel was provided with a weak water-tight closure at the lower end (the upper end was open)

(b) the vessel was filled with water at atmospheric pressure and 70°F

(c) a compact (length ~ diameter) pentolite charge was detonated at the centroid of the vessel.

Although the models were limited to convenient sizes for laboratory testing, an ample spectrum of sizes and wall thicknesses was investigated, as listed in the following table:

ID (in)	Length (in)	Wall Thickness (in)
5	10	1/16, 1/8, 1/4
5	20	1/8
10	20	1/8, 1/4, 1/2
15	30	1/2
20	40	1/4, 1/2, 1
20	60	1

To provide containment law knowledge for a wide range of ductile materials, model vessels were fabricated from 1020 mild

steel, 212 flange steel, several types of stainless steel, and one type of aluminum. These materials and their mechanical properties are given in the table below:

Material	Yield Stress (psi)	Ultimate Stress (psi)	Ultimate Strain (in/in)
304 Stainless Steel	30,000	65,100	0.60
304 Stainless Steel*	43,000	83,800	0.60
410 Stainless Steel	66,000	94,300	0.26
410 Stainless Steel	151,500	197,900	0.08
212 Flange Steel*	46,500	76,200	0.27
1020 Mild Steel*	42,000	66,900	0.30
6061-T6 Aluminum	40,000	45,000	0.15

The stress and strain values are averages obtained from numerous tensile test specimens of each material. Vessels made of materials denoted by an asterisk (*) were constructed of rolled plate with one or two longitudinal welded seams. In general, the light-wall vessels were made with a single weld; the heavy-wall vessels were made with two welds. Welds represented a departure from the idealized vessel concept, but special precautions were taken to ensure that the welds were capable of withstanding the same stress and deformation as the parent metal; thus the welded vessels could be considered as idealized models. The precautions were:

(a) the welds were continuous and full penetration

(b) the weld material possessed essentially the same mechanical properties as the parent metal

(c) the vessels were annealed to relieve any residual and thermal stresses resulting from the rolling and welding processes.

By virtue of these precautions, welds of equal or perhaps better quality than those expected in actual reactor vessels were ensured. The remaining stainless steels in the above table were in the form of centrifugally cast tubing (seamless), and the sole aluminum was in the form of extruded seamless tubing. Figure 7.1 shows typical test vessels of the seamless and welded varieties.

The test procedure followed throughout the program consisted of explosively dilating a minimum of four vessels for each given material and size. In this manner it was possible to approach and determine the condition of marginal containment. (Marginal containment is consistent with the maximum charge weight that can be detonated in a vessel without causing rupture.) In terms of experimental procedure, three vessels were employed to yield intermediate values of terminal radial strain (the at-rest mid-meridian strain) correlative with charge weight. The fourth yielded the maximum radial strain correlative with marginal containment, and a 25,000-frame/second Beckman-Whitley Dynafax camera recorded the deformation-time history during dilation. Treatment of these photographic data in the manner described in section 6.1 resulted in the determination of initial strain rates for the various vessels.

Table 7.1 gives the following data for 104 experiments in water-filled, idealized model vessels.

(a) charge weight

(b) terminal radial strain at the mid-meridian

(c) mode of vessel containment or failure

(d) initial strain rate as determined from the high-speed photographs.

Figure 7.2 shows two 10" ID, 20" length, 1/4" wall, 304 stainless steel cylinders that typify deformation patterns of marginal containment. Several observations can be made from the data of Table 7.1; they are:

(a) For a given vessel size and material, a high degree of uniformity in the terminal radial strain data is noted as charge weight increases toward the marginal containment weight. This is demonstrated in Figure 7.3, which shows four 304 stainless-steel cylinders in stages of increasing deformation.

(b) In nearly all cases of marginal containment, the maximum radial strain was slightly less than the correlative average ultimate strain given in the materials table earlier in this section. The two exceptions were the

10" ID, 20" length, 1/4" wall, 410 annealed stainless steel vessels, and the

20" ID, 40" length, 1/2" wall, 212 flange steel vessels.

Not only did the strains of these materials exceed the listed average values, they exceeded the maximum ultimate strains given by any of the respective certified tensile test specimens.

7.2 Effects of Welds. It is recalled from section 7.1 that fabrication of the rolled-plate vessels was such as to ensure welds of containment potential equivalent to that of the parent material. The success of this effort was evidenced in vessel responses such as those shown in Figures 7.2 and 7.3. It is noted that the deformation capacity of the welded-plate vessels was not less than that of their seamless counterparts. Although the majority of the welded vessels demonstrated excellent deformation properties, there were cases of premature rupture due to weld failures either in the weld material itself or in the heat-affected zone adjacent to the weld. However, it is seen from Table 7.1 that in all cases the vessels were capable of deforming without rupture to strains greater than 1/3 ϵ_u and, with only several exceptions, to strains greater than 1/2 ϵ_u. From these data it was postulated that the maximum strain of welded reactor vessels should be restricted to

$$\varepsilon \leq \varepsilon_u/3$$

7.3 Effects of End Closures. Of the 104 experiments reported in Table 7.1, nine were conducted in vessels fitted with rigid radial end constraints of the type shown in Figure 7.4. These vessels were 5" ID, 10" length, 1/8" and 1/4" wall, 304 stainless steel (cast) cylinders and are denoted in Table 7.1 by ***. It is seen immediately from the experimental results that the end closures decreased substantially the strain at which rupture occurred: from approximately 0.50 to 0.38 in/in. From these data it was postulated that the permissible strain for a vessel with rigid end closures should be restricted to

$$\varepsilon \leq \varepsilon_u/2$$

It can be expected that, for the vessels fitted with hemispherical or dished end closures, the permissible strain would exceed that for the case of rigid ends.

7.4 Effects of Nozzles. To index the limiting effects of nozzles on containment, experiments were conducted under the following four conditions:

(a) vessel fitted with single circular aperture at mid-meridian; aperture diameter 1/5 that of vessel diameter

(b) vessel fitted with single closed-end tube inserted at mid-meridian in aperture of same diameter as in (a); tube secured to vessel wall by continuous fillet welds around circumference of insert

(c) vessel same as in (a) except that three apertures were equally spaced around circumference at mid-meridian

(d) vessel same as in (c) except that three closed-end tubes were inserted in apertures and secured to vessel wall by continuous fillet welds around circumference of inserts.

Types (a) and (b) are shown undeformed in Figure 7.5; post-test deformations are shown in Figure 7.6. Experimental results from 12 tests are given in Table 7.2. Although these experiments do not represent a comprehensive study of nozzles, they permitted the following upper-bound observations.

(a) For a single mid-meridian aperture of diameter ~ 1/5 the diameter of the vessel, the maximum permissible strain for 304 stainless steel was about 0.10 in/in or 1/6 ε_u.

(b) For a nozzle welded on both sides of the vessel wall, the maximum permissible strain for 304 stainless steel was 0.33 in/in or about 1/2 ε_u.

(c) The presence of multiple apertures or nozzles at the mid-meridian did not affect appreciably the respective containable charge weights for the cases of one aperture or one nozzle, although the average circumferential strain was less. However, the local deformation and thickness of the vessel wall at points equidistant from the discontinuities appeared to have the same characteristics as the uninhibited deformation of idealized models for equivalent charge weights.

On the basis of these experiments, it was postulated that the maximum permissible strain for vessels with nozzles (no constraints external to vessel) should be

$$\varepsilon \leq \varepsilon_u/2$$

There is additional reason to believe that this strain restriction is conservative; the integrity of the welded nozzles of the models is not considered as sound as the flanged or forged nozzles found in typical reactor vessel construction. Appendix B gives additional data concerning the strain pattern around an aperture and nozzle for the two vessels shown in Figure 7.6. These data should be useful to those concerned with the detail design of nozzle connections for reactor vessels and ancillary piping.

7.5 Loss-of-Coolant Experiments. To determine the enhancement in explosion containment potential resulting from the complete loss of liquid coolant, a limited number of experiments were conducted in 5" ID, 10" length, 1/16" and 1/8" wall, 304 stainless steel (cast) vessels of the type shown in Figure 7.4. In each test the vessel was filled with air at atmospheric pressure and ambient temperature, and the explosive charge was detonated at the centroid of the vessel. Charge weight - terminal strain results are given in Table 7.3, and the uniform increase in deformation with charge weight for 1/8" wall models is shown in Figure 7.7. The localized deformation pattern and a comparison with that of water-filled vessels were shown previously in Figure 6.1.

7.6 Applicability of Free-Water Explosion Relations. In the development of the embryonic format (Chapter 6), it was assumed that conventional free-water explosion relations could be employed in characterizing the wall loading. However, Cole in reference (1) states that the use of these relations is questionable for distances closer to the charge than 7 to 10 charge radii. In some of the water-filled vessel experiments, the distance to the vessel wall was as small as 3 charge radii. Therefore, to indicate the adequacy of the free-water relations for this close-in domain, pressure-time records were obtained from two experiments conducted in a closed, rigid-wall, cylindrical control vessel shown in Figure 7.8. In each test:

(a) a 1/4" diameter tourmaline piezoelectric gage was located at the mid-meridian approximately 1/4" from the internal wall surface

(b) the vessel was filled completely with water at atmospheric pressure and 70°F

(c) a compact 18-gm pentolite charge was detonated at the vessel centroid.

A pressure-time trace obtained from one of these tests is shown in Figure 7.9. The peak shock pressure of ~ 52,000 psi was a combination of the incident and reflected waves. After the shock decayed, two steps of pressure were noted. The first step, ~ 25,000 psi, is believed to be the maximum internal-blast pressure; it should have remained at this level for the duration of the 1/2-msec trace*. However, due to a partial top-closure failure and subsequent movement, the pressure suddenly dropped to 19,000 psi. The piezoelectric gages employed in this study were calibrated via the method and rationale reported by R. L. Davis in reference (s).

From a reactor containment point of view, the most important portion of the plot shown in Figure 7.9 is the shock wave. Conventional free-water equations for the pentolite shock wave are given by Cole in reference (1) and by the Naval Ordnance Laboratory in reference (t) as

$$P = P_m \, e^{-t/\theta} \tag{7.1}$$

where

$$P_m = 2.25 \times 10^4 \, (W^{1/3}/R_1)^{1.13} \tag{7.2}$$

$$\theta = 0.06 \, W^{1/3} \, (W^{1/3}/R_1)^{-0.18} \tag{7.3}$$

* It is to be expected that the internal blast pressure in the rigid wall vessel would exceed significantly that correlative with gross plastic deformation. For example, if the product gases in this rigid wall vessel were allowed to expand isothermally 100 fold, as in the case of gross plastic deformation, the blast pressure would be reduced to about 250 psi - several orders of magnitude below the shock pressure.

and the nomenclature and units are

P . . . . incident wave pressure, psig
P_m . . . . peak pressure of incident wave, psig
t . . . . time, msec
θ . . . . time constant of incident wave decay, msec
W . . . . charge weight, lb
R_i . . . . distance from charge, ft

If the shock is assumed to be a plane acoustic wave reflected from a normal rigid surface with a velocity of about 5000 ft/sec, then, for W = 18 gm ≈ 0.04 lb, the calculated pressure felt by a gage 1/4" from a 2.5" radius cylinder wall would be that given by the dashed-line curve shown in Figure 7.10.

The frequency response of the recording instrumentation was about 50,000 cycles/second. Modification of the calculated curve was made to account for this recording deficiency (this was more feasible than correcting the experimental data), and the solid-line curve in Figure 7.10 resulted. A comparison of this hypothesized solid-line curve with the shock portion of the actual pressure-time trace (Figure 7.9) is significant: good agreement exists in the sense that the parameter of importance to containment is the impulse or the area under the incident pressure-time curve. These experiments provided important additional evidence that conventional free-water shock relations can be employed fruitfully in characterizing the shock loading function correlative with containment.

The application of equations (7.1), (7.2), and (7.3) to the vessel and test conditions specified in Figure 6.2 yields the pressure-time plot shown in Figure 7.11. Superposed on this curve are the deformation- and velocity-time plots given by Figures 6.3 and 6.4. It is noted that the displacement and

pressure curves are shown with the same origin, although it is known that, time-wise, the shock wave preceded the plastic deformation. Since the framing rate of the high-speed camera could not define time zero closer than 40 microseconds, common origins were chosen for convenience. It is seen that 90 per cent of the incident impulse occurred within 100 microseconds as compared to the total deformation time of 600 microseconds. The fact that the loading time was short relative to the deformation time is consistent with the instantaneous velocity hypothesis of section 6.2: when the shock wave strikes the internal wall of the confining vessel, the wall responds with a virtually instantaneous initial velocity.

SEAMLESS WELDED PLATE

FIG. 7.1 TYPICAL TEST VESSELS OF SEAMLESS AND WELDED CONSTRUCTIONS

10" ID - 20" LENGTH - 1/4" WALL
304 STAINLESS STEEL
WATER - FILLED
CHARGE AT CENTROID
CHARGE WEIGHT = 189.8 GM
MAX. RADIAL STRAIN = 0.463 IN/IN

SEAMLESS

10" ID - 20" LENGTH - 1/4" WALL
304 STAINLESS STEEL
WATER - FILLED
CHARGE AT CENTROID
CHARGE WEIGHT = 275.5 GM
MAX. RADIAL STRAIN = 0.487 IN/IN

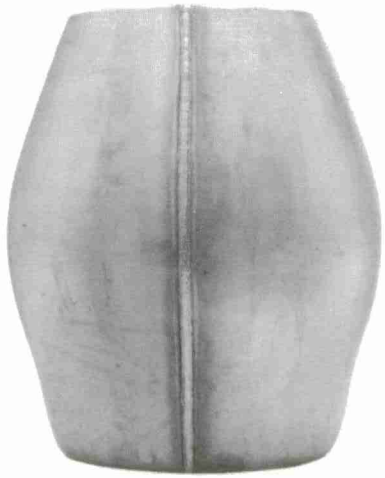

WELDED PLATE

FIG. 7.2 MARGINAL CONTAINMENT IN SEAMLESS AND WELDED VESSELS

10" ID - 20" LENGTH - 1/8" WALL
304 STAINLESS STEEL, WELDED PLATE
WATER-FILLED, CHARGE AT CENTROID

PENTOLITE CHARGE WEIGHT:	80.2 GM	100.8 GM	120.1 GM	140.0 GM
RADIAL STRAIN AT MID-MERIDIAN:	0.366 IN/IN	0.434 IN/IN	0.506 IN/IN	0.568 IN/IN

FIG. 7.3 UNIFORM DEFORMATION INCREASE WITH CHARGE WEIGHT FOR WATER-FILLED VESSELS

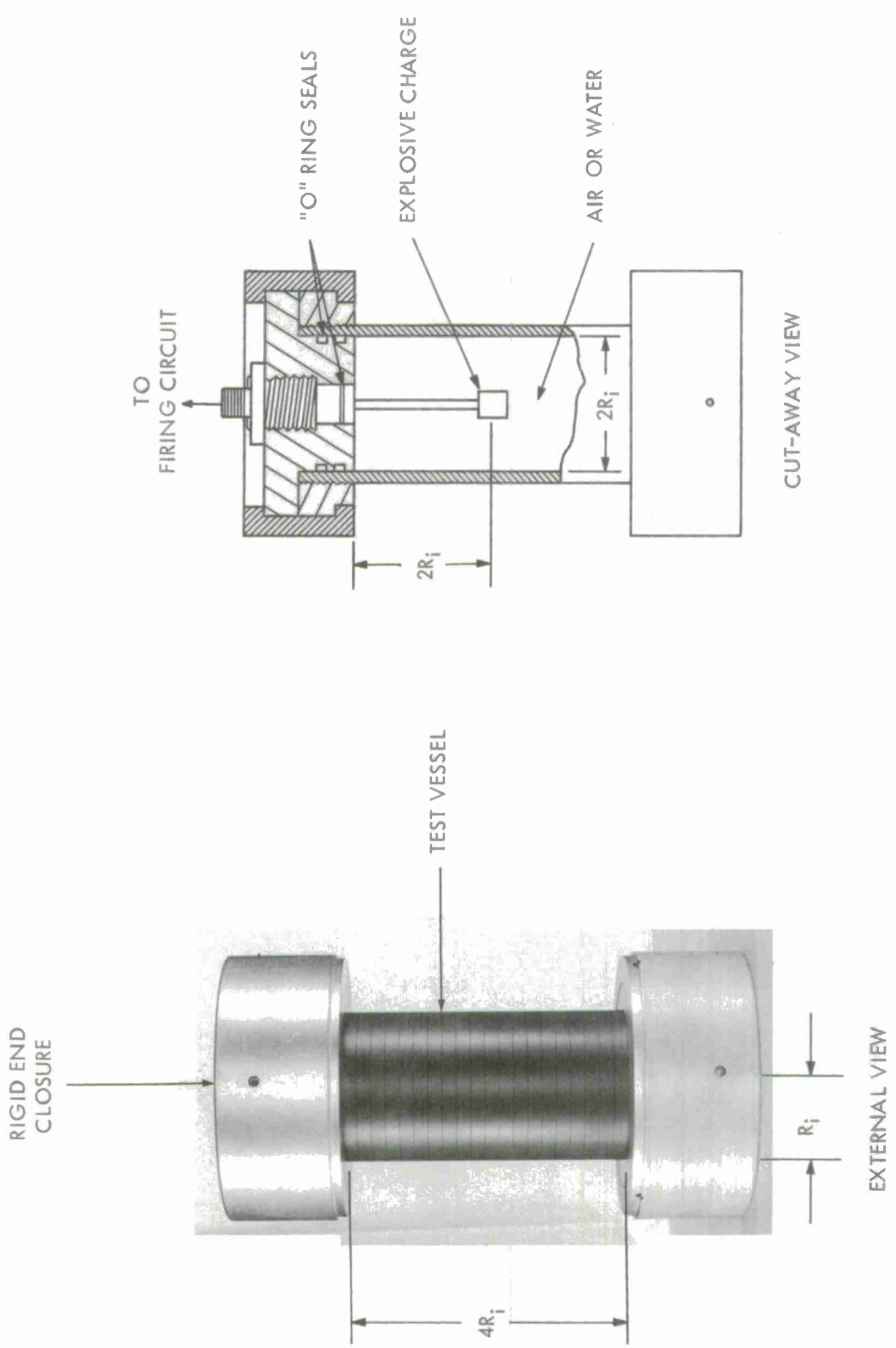

FIG. 7.4 TEST VESSEL FITTED WITH RIGID END CLOSURES

NOTE: NOZZLE WALL THICKNESS
EQUAL TO THAT OF VESSEL

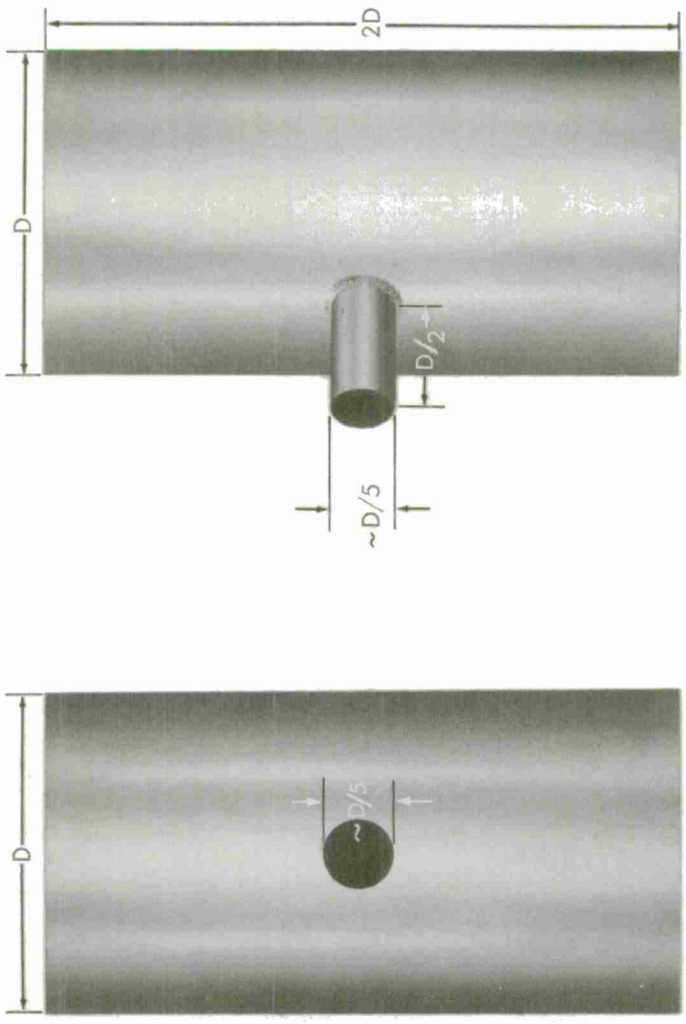

FIG. 7.5 VESSELS FITTED WITH APERTURE AND NOZZLE

10" ID - 20" LENGTH - 1/4" WALL
304 STAINLESS STEEL, CAST
WATER-FILLED; CHARGE AT CENTROID

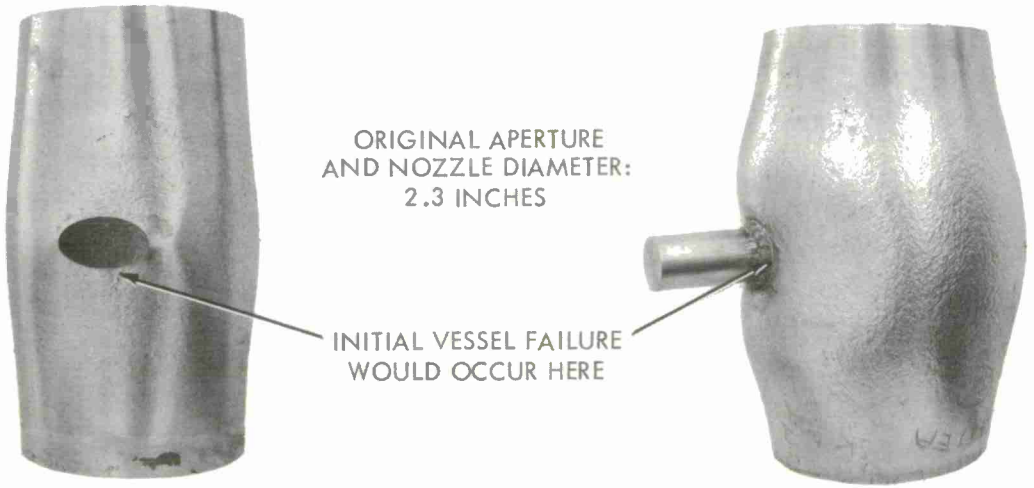

FIG. 7.6 EFFECTS OF APERTURE AND NOZZLE ON DEFORMATION

VESSELS SIZE: 5" ID - 10" LENGTH - 1/8" WALL
MATERIAL: 304 STAINLESS STEEL, CAST
CHARGE LOCATION: CENTROID OF VESSEL

PENTOLITE CHARGE WEIGHT:	17.9 GM	38.0 GM	50.2 GM
RADIAL STRAIN AT MID-MERIDIAN:	0.059 IN/IN	0.171 IN/IN	0.280 IN/IN

FIG. 7.7 UNIFORM DEFORMATION INCREASE WITH CHARGE WEIGHT FOR AIR-FILLED VESSELS

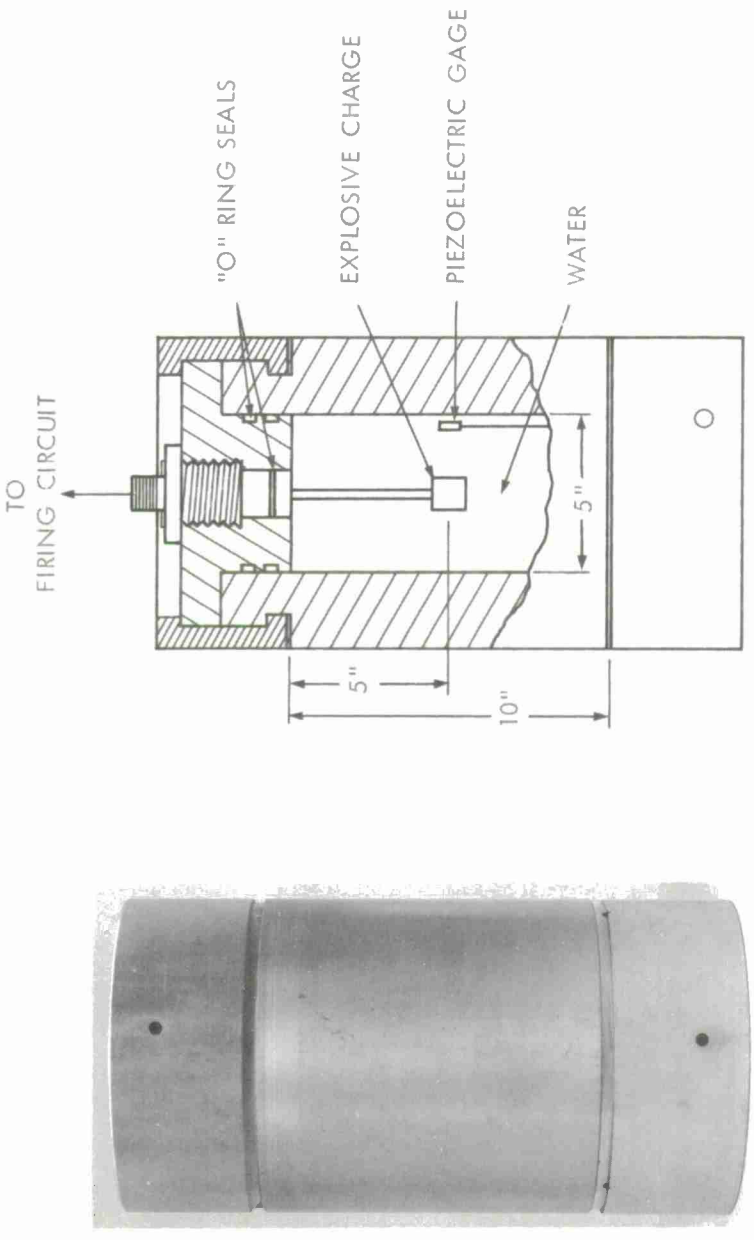

FIG. 7.8 RIGID WALL, CYLINDRICAL CONTROL VESSEL

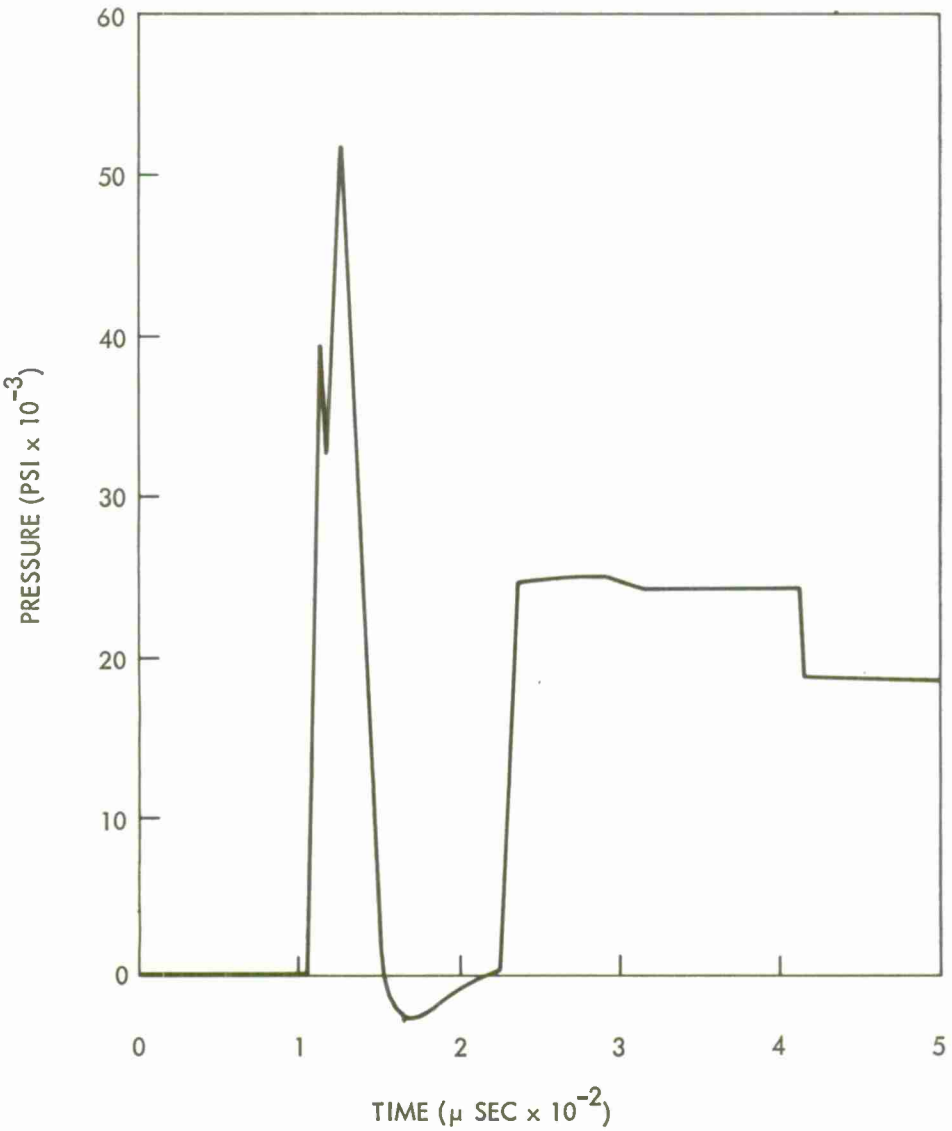

FIG. 7.9 RECORDED PRESSURE-TIME TRACE FROM 18-Gm EXPLOSION IN CONTROL VESSEL

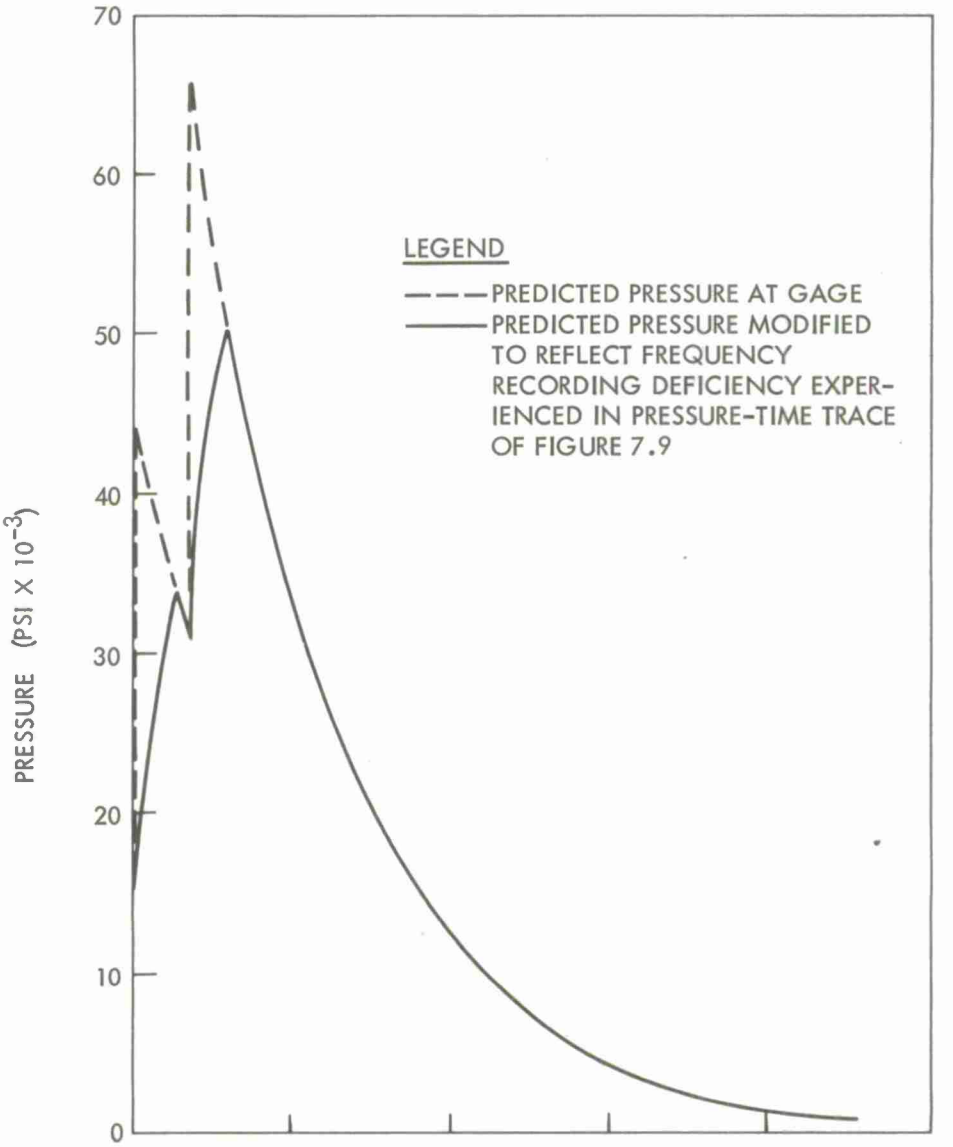

FIG. 7.10 PREDICTED PRESSURE-TIME CURVES FOR 18-Gm EXPLOSION IN CONTROL VESSEL

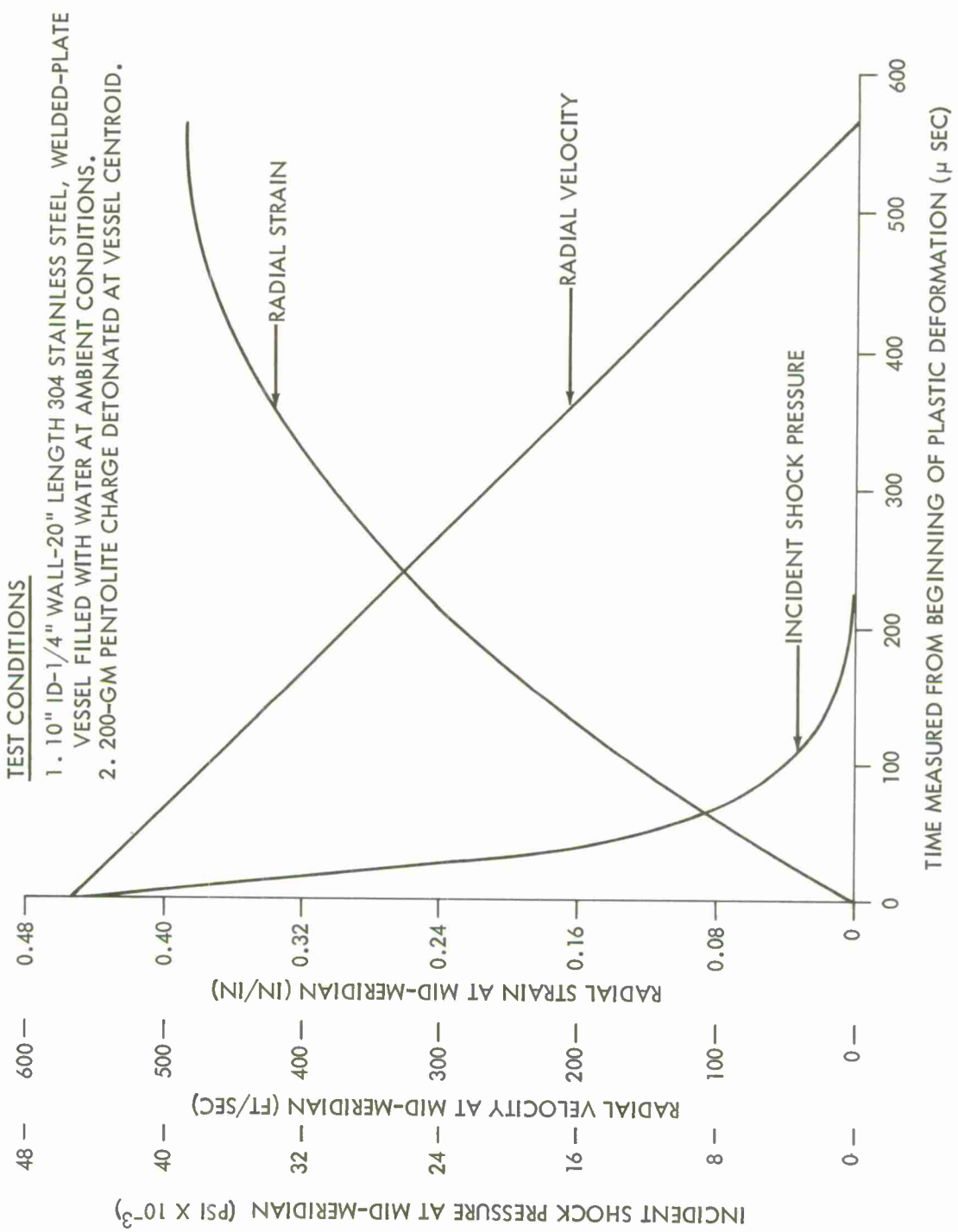

FIG. 7.11 COMPARISON OF SHOCK DURATION WITH VESSEL RESPONSE TIME

TABLE 7.1

RESULTS OF EXPERIMENTS IN EXPLOSION-LOADED, WATER-FILLED IDEALIZED VESSELS

304 STAINLESS STEEL, WELDED-PLATE CYLINDERS

INTERNAL DIAMETER (INCHES)	LENGTH (INCHES)	WALL THICKNESS (INCHES)	PENTOLITE CHARGE WEIGHT (GRAMS)	TERMINAL[+] RADIAL STRAIN (IN/IN)	FAILURE[++] OR CONTAINMENT MODE	INITIAL STRAIN RATE (SEC^{-1})	TEST NO.
5	10	0.060	8.0	0.289	5	-	1
			9.0	0.316	1,3	2070	2
			10.0	0.343	1,4	-	3
			11.0	0.366	1,4	-	4
		0.118	12.0 **	0.195	6	-	5
			18.0 **	0.271	6	-	6
			22.0 **	0.331	6	-	7
			22.0	0.349	6	-	8
			23.0	0.357	5	2850	9
			24.0	0.304	1,3	-	10
			25.0	0.349	1,4	-	11
		0.253	50.1	0.295	6	-	12
			56.1	0.338	5	2900	13
			60.1	0.295	1,4	-	14
			64.1	0.338	1,4	-	15
10	20	0.118	80.2	0.366	6	-	16
			100.8	0.434	6	-	17
			120.1	0.506	6	1570	18
			140.0	0.568	5	-	19
		0.253	160.0 **	0.280	6	-	20
			180.0 **	0.315	6	-	21
			200.0 **	0.348	6	1300	22
			210.2	0.383	6	-	23
			229.3	0.425	6	-	24
			275.5	0.487	5	1570	25
			325.4 *	0.387	2,4	1870	26
			325.7 *	0.546	2,4	-	27
			359.8	0.569	2,4	1940	28
		0.515	669.3 *	0.512	5	1640	29
			725.7 *	0.468	3	-	30
			775.5 *	0.490	4	1970	31
20	40	0.253	280.8	0.180	6	-	32
			477.8	0.231	2,3	568	33
			960.0	-	2,4	790	34
			960.8	0.297	2,4	805	35
		0.515	1702.6 *	0.412	6	-	36
			2103.1	0.523	5	-	37
			2242.0 *	0.516	3	-	38
			2248.5	0.529	5	-	39
			2501.0	0.561	4	-	40
		1.030	1000.0	0.110	6	-	41
			2501.0	0.265	5	-	42
			3492.0	0.288	2,3	-	43
			5011.0	0.342	2,4	-	44
	60	1.030	2496.0	0.236	1,3	-	45

TABLE 7.1 (Continued)

RESULTS OF EXPERIMENTS IN EXPLOSION-LOADED, WATER-FILLED IDEALIZED VESSELS

INTERNAL DIAMETER (INCHES)	LENGTH (INCHES)	WALL THICKNESS (INCHES)	PENTOLITE CHARGE WEIGHT (GRAMS)	TERMINAL+ RADIAL STRAIN (IN/IN)	FAILURE++ OR CONTAINMENT MODE	INITIAL STRAIN RATE (SEC^{-1})	TEST NO.
304 STAINLESS STEEL, CENTRIFUGALLY-CAST CYLINDERS							
5	10	0.125	16.0 ***	0.295	6	-	46
			18.0 ***	0.352	5	-	47
			19.0 ***	0.381	3	-	48
			21.0 ***	-	4	-	49
		0.250	50.1 ***	0.375	5	-	50
			50.5 ***	0.354	5	-	51
			50.5 ***	0.385	3	-	52
			58.1	0.425	6	-	53
			70.2	0.461	6	-	54
			75.3	0.497	5	-	55
			85.0	0.483	3	-	56
			100.0 ***	-	4	-	57
	20	0.125	19.0 ***	0.370	5	-	58
10	20	0.250	189.8	0.463	5	1450	59
			189.9	0.440	3	1490	60
			200.2	0.413	4	-	61
			250.1	-	4	-	62
		0.500	461.0	0.421	6	-	63
			481.2	0.447	5	1810	64
			497.7	0.436	3	-	65
			569.2	0.440	4	-	66
410 STAINLESS STEEL, CENTRIFUGALLY-CAST CYLINDERS							
ANNEALED							
5	10	0.250	25.3	0.118	6	-	67
			28.0	0.131	6	-	68
			28.0	0.132	6	1860	69
			28.0	0.141	5	-	70
			29.0	-	3	-	71
			30.3	-	4	-	72
10	20	0.250	110.2	0.173	6	-	73
			130.1	0.220	6	-	74
			160.6	0.258	6	310	75
			180.4	0.292	6	-	76
			199.6	0.341	6	-	77
			220.5	0.364	5	-	78
			239.8	0.379	3	-	79
		0.500	210.0	0.125	6	-	80
			230.4	0.147	5	950	81
			249.7	-	4	-	82
			320.5	-	4	-	83
HARDENED							
5	10	0.250	22.0	0.045	5	-	84
			26.0	0.050	3	-	85

TABLE 7.1 (Continued)

RESULTS OF EXPERIMENTS IN EXPLOSION-LOADED, WATER-FILLED IDEALIZED VESSELS

INTERNAL DIAMETER (INCHES)	LENGTH (INCHES)	WALL THICKNESS (INCHES)	PENTOLITE CHARGE WEIGHT (GRAMS)	TERMINAL+ RADIAL STRAIN (IN/IN)	FAILURE++ OR CONTAINMENT MODE	INITIAL STRAIN RATE (SEC^{-1})	TEST NO.
212 FLANGE STEEL, WELDED PLATE CYLINDERS							
10	20	0.515	200.0 *	0.154	6	-	86
			229.3 *	0.183	5	867	87
			275.0 *	0.118	1,3	-	88
			324.4 *	0.128	1,4	-	89
20	40	0.515	902.7	0.242	6	-	90
			1103.0	0.300	6	-	91
			1200.3	0.328	5	670	92
			1351.5	0.357	3	650	93
		1.030	2002.6	-	1,4	-	94
			2251.0	0.230	5	-	95
			2497.0	0.226	1,3	-	96
			2498.0	0.185	2,3	-	97
MILD STEEL, WELDED PLATE CYLINDERS							
10	20	0.253	140.0 **	0.271	1,3	1010	98
			145.0 **	-	1,4	-	99
			145.0 **	-	1,4	-	100
6061 - T6 ALUMINUM, EXTRUDED CYLINDERS							
15	30	0.500	60.0 **	0.0553	6	-	101
			85.2 **	0.0855	5	-	102
			90.0 **	0.0875	3	-	103
			99.9 **	0.0929	4	-	104

NOTES

* Cylinders were of double-weld construction (two longitudinol seoms, 180° opart).

** No certified mechanicol properties were avoiloble for this materiol.

*** Cylinders were fitted with rigid, radiol end closures.

\+ The terminol strain is the ot-rest mid-meridian strain.

++ The following code describes mode of cylinder failure or contoinment.

1 --- failure occurred in heat offected zone adjocent to weld
2 --- foilure occurred in weld material
3 --- marginol rupture
4 --- non-morginol rupture
5 --- marginol contoinment
6 --- non-marginol contoinment

TABLE 7.2

RESULTS OF EXPERIMENTS IN EXPLOSION-LOADED, WATER-FILLED VESSELS FITTED WITH APERTURES OR NOZZLES

TEST NO.	ID (in)	LENGTH (in)	WALL THICK. (in)	MATERIAL	TYPE OF DISCONTINUITY	CHARGE WEIGHT (gm)	AVERAGE CIRCUMFERENTIAL STRAIN (in/in)	MODE OF FAILURE
105	10	20	0.250	304 S.S. CAST	THREE 2.3" DIA. APERTURES	42.5	0.036	SMALL FISSURES (~1/2" LONG) AT TWO OF THREE APERTURES
106	10	20	0.250	304 S.S. CAST	ONE 2.3" DIA. APERTURE	42.5	0.104	SMALL FISSURE (~ 1/4" LONG) AT APERTURE
107	10	20	0.250	304 S.S. CAST	ONE 2.3" DIA. APERTURE	50.1	0.116	MEDIUM FISSURE (~1 1/4" LONG) AT APERTURE
108	10	20	0.250	304 S.S. CAST	ONE 2.75" DIA. APERTURE	58.0	0.133	MEDIUM FISSURE (~1 5/8" LONG) AT APERTURE
109	10	20	0.250	304 S.S. CAST	ONE 2.3" DIA. APERTURE	100.3	0.199	VESSEL FAILED WITH FISSURE ORIGINATING AT APERTURE
110	10	20	0.250	304 S.S. CAST	ONE NOZZLE	100.5	0.231	WELD FAILURE AROUND NOZZLE; NOZZLE WELDED TO OUTSIDE SURFACE OF VESSEL ONLY.
111	10	20	0.250	304 S.S. CAST	ONE NOZZLE	130.0	0.328	NO FAILURE
112	10	20	0.250	304 S.S. CAST	ONE NOZZLE	130.8	0.336	NO FAILURE
113	10	20	0.250	304 S.S. CAST	THREE NOZZLES	128.8	0.330	VESSEL FAILED; FAILURE ORIGINATED IN THE HEAT AFFECTED ZONE AROUND ONE NOZZLE
114	10	20	0.515	304 S.S. PLATE	ONE NOZZLE	383.0	0.194	VESSEL FAILED; WELD FAILURE AROUND NOZZLE; WELD ON INSIDE SURFACE WAS INCOMPLETE DUE TO END PLATE ON VESSEL
115	20	40	0.515	304 S.S. PLATE	ONE NOZZLE	1300.7	0.148	VESSEL FAILED; FAILURE ORIGINATED IN THE HEAT AFFECTED ZONE AROUND NOZZLE
116	20	60	1.030	304 S.S. PLATE	ONE NOZZLE	2004.4	-	VESSEL FAILED; WELD FAILURE AROUND NOZZLE

NOTE

1. Descriptions of the vessels used in these experiments are given in Section 7.4 and Figure 7.5.

2. All charges were pressed pentalite.

TABLE 7.3

RESULTS OF EXPERIMENTS IN EXPLOSION-LOADED, AIR-FILLED VESSELS

TEST NO.	ID (in)	LENGTH (in)	WALL THICK. (in)	CHARGE WEIGHT (gm)	TERMINAL RADIAL STRAIN (in/in)	FAILURE MODE
117	5	10	0.062	16.1	0.126	NO FAILURE
118	5	10	0.062	20.0	0.168	NO FAILURE
119	5	10	0.062	23.1	0.226	NO FAILURE
120	5	10	0.062	25.0	-	MARGINAL RUPTURE
121	5	10	0.125	17.9	0.059	NO FAILURE
122	5	10	0.125	38.0	0.171	NO FAILURE
123	5	10	0.125	50.2	0.280	NO FAILURE
124	5	10	0.125	52.0	-	MARGINAL RUPTURE
125	5	10	0.125	60.0	-	NON-MARGINAL RUPTURE

NOTES

1. Vessel material was 304 stainless steel, cast.
2. These experiments were conducted in vessels of the type shown in Figure 7.4.
3. All charges were pressed pentolite.

CHAPTER 8

EVALUATION OF EMBRYONIC FUNCTIONS

The extensive experimental results of Chapter 7 provide the necessary and sufficient boundary conditions for evaluating the embryonic functions, ψ_1 and ψ_2, generated via Saint-Venant's semi-inverse method in Chapter 6.

8.1 Efficiency Factor Function ψ_2. It proves convenient to evaluate the embryonic functions in the reverse order of their derivation. We start by rewriting equation (6.18) in the form

$$\psi_1\psi_2 = \frac{W^{4/3}}{w\sigma_t\, \epsilon(R_e^2 - R_i^2)^2} \tag{8.1}$$

where the true stress function σ_t, as previously defined, is

$$\sigma_t = \sigma_y + \left[\frac{\sigma_u (1 + \epsilon_u) - \sigma_y}{\epsilon_u} \right] \epsilon \tag{6.14}$$

All parametric values on the right-hand side of equation (8.1) are known from Table 7.1 for the case of containment, and the calculated products $\psi_1\psi_2$ for these cases are given in Table C-1 of Appendix C.

It was hypothesized in equation (6.19) that ψ_2 is a function of R_i/h_o. Figure 8.1 shows this significant dependence, from which the best straight line through averaged values of the groupings is taken to be

$$\psi_2 = 10^{-5} (3.41 + 0.117\, R_i/h_o) \tag{8.2}$$

8.2 Deformation Energy Function ψ_1. For cylinders, we define the radial strain ϵ as

$$\epsilon = \frac{R - R_1}{R_1} \tag{8.3}$$

where R and R_1 are the instantaneous and initial internal radii, respectively. Then the strain rate $\dot{\epsilon}$ is

$$\dot{\epsilon} = \frac{1}{R_1}\frac{dR}{dt} = \frac{v}{R_1}$$

where v is the scalar quantity, $v = |\vec{v}|$. Since the initial strain rate of the wall at the mid-meridian was hypothesized to index the density of the deformation energy, we put

$$\dot{\epsilon}_o = v_o(0)/R_1 \quad , \quad v_o = |\vec{v}_o| \tag{8.4}$$

Combining equations (6.7), (6.8), (6.13), and (8.4), taking K = 2.18 for pentolite from reference (1), and accounting for units, we obtain

$$\xi = \frac{20216\ w^{2/3}}{\dot{\epsilon}_o w\ R_1(R_e^2 - R_1^2)} \tag{8.5}$$

Table C-2 in Appendix C gives ξ for 23 experiments in which the strain rate was monitored. The trial format assumed $\xi = \xi\,(R_i/h_o)$. This functional relation is plotted in Figure 8.2; the best straight line through the averaged values of the groupings yields

$$\xi = 1.47 + 0.0373\, R_i/h_o \tag{8.6}$$

and upon combination with (8.5), we find

$$\dot{\epsilon}_o = \frac{20216\, w^{2/3}}{(1.47 + 0.0373\, R_i/h_o)\, w\, R_i(R_e^2 - R_i^2)} \tag{8.7}$$

The strain rate based on (8.7) appears in Table C-1 for all contained experiments. Table C-2 gives the deviation of these (8.7) results from the experimental values, and it is noted that the deviations are as high as 15 per cent. A plot of $\dot{\epsilon}_o$ and ψ_1, both from Table C-1, is given in Figure 8.3; motivation for the log-log scales was provided by the fractional-power strain rate function given in equation (6.16). The best straight line through these data yields

$$\psi_1 = 0.318\, \dot{\epsilon}_o^{0.15} \tag{8.8}$$

which, when incorporated into (8.1), reduces the effect of the maximum strain rate deviation of (8.7) from 15 per cent to less than 3 per cent.

The simultaneous solution of (8.7) and (8.8) yields

$$\Psi_1 = 0.318 \left[\frac{20216\ W^{2/3}\ (R_e^2 - R_i^2)^{-1}}{w\ R_i (1.47 + 0.0373\ R_i/h_o)} \right]^{0.15} \qquad (8.9)$$

and we now have Ψ_1 and Ψ_2 completely defined in terms of charge weight and simple properties of the confining vessel.

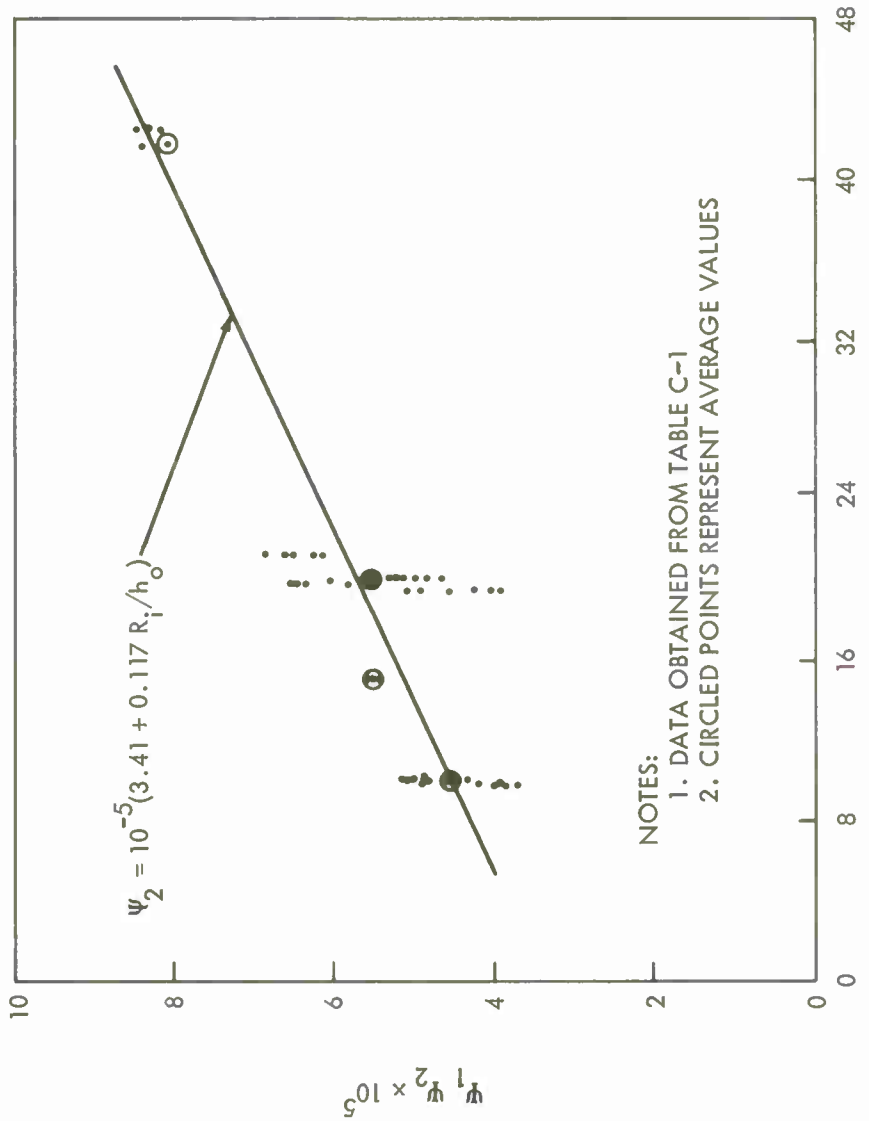

FIG. 8.1 VARIATION OF $\Psi_1\ \Psi_2$ WITH R_i/h_o

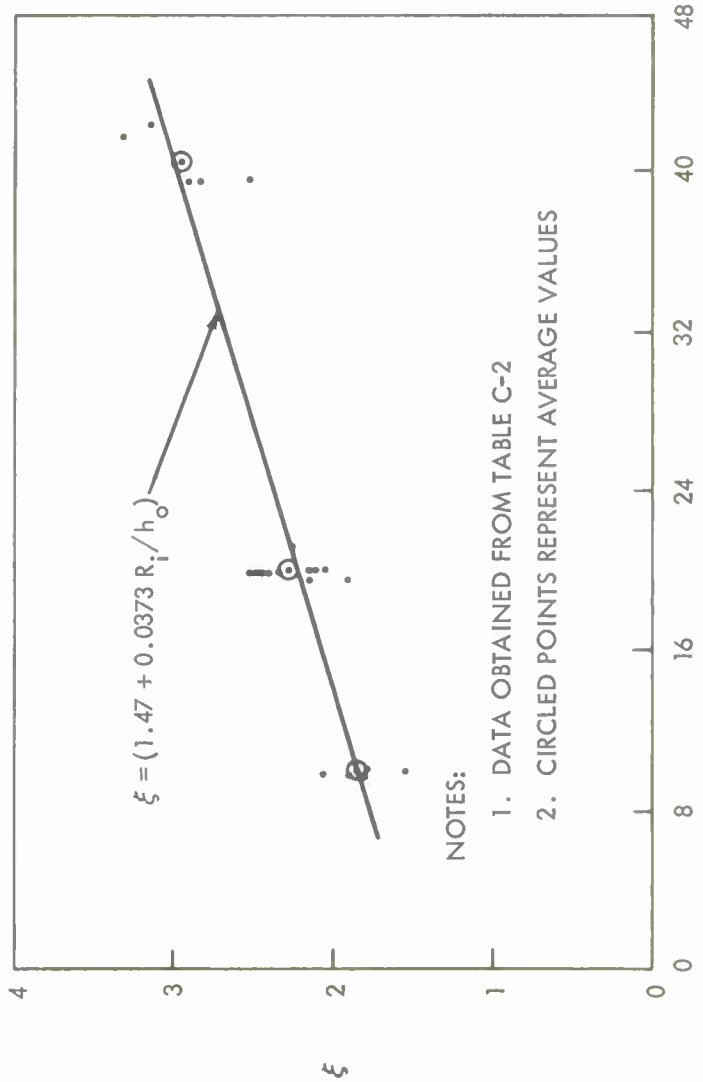

FIG. 8.2 VARIATION OF ξ WITH R_i/h_o

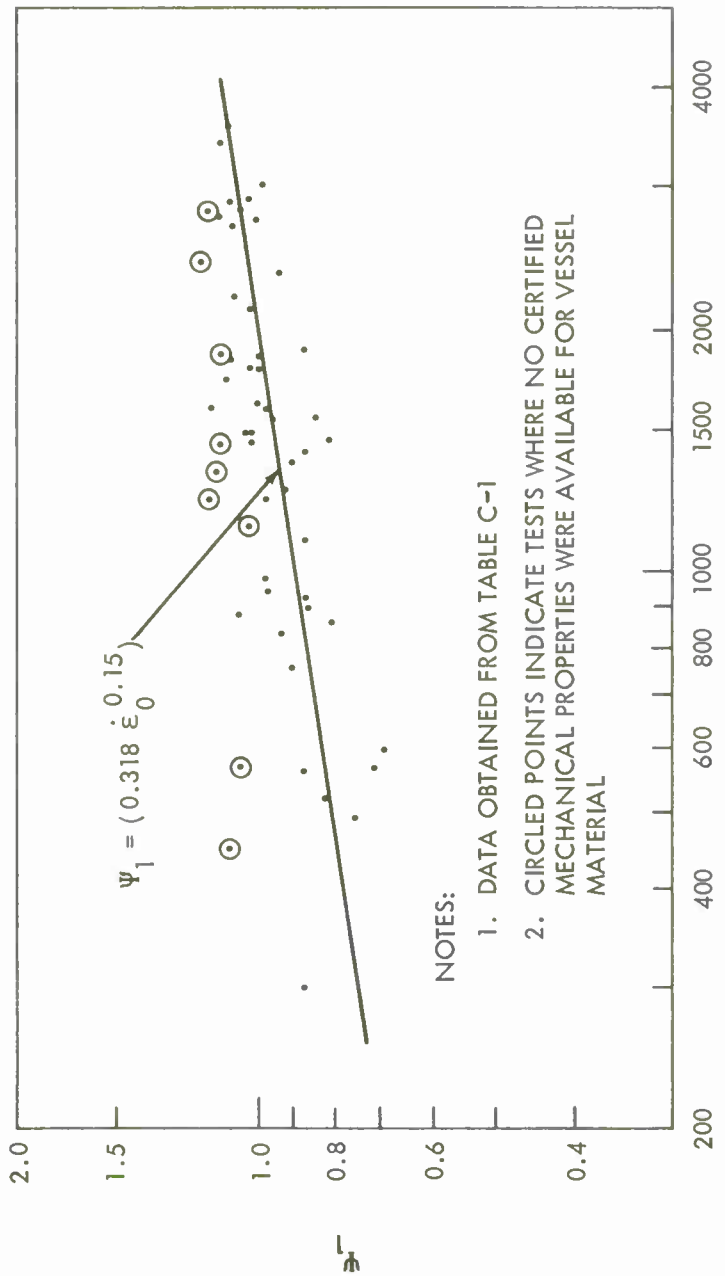

FIG. 8.3 VARIATION OF Ψ_1 WITH INITIAL STRAIN RATE $\dot{\varepsilon}_0$

CHAPTER 9

CONTAINMENT LAWS

The TNT rationale, embryonic format, extensive experimental program, and evaluation of the trial functions now culminate in final Containment Law formulations.

9.1 TNT Containment Law for Ideal Vessels. The embryonic form of the Containment Law

$$W = \left[\psi_1 \psi_2 \, w \, \sigma_t \, \epsilon \, (R_e^2 - R_i^2)^2 \right]^{3/4} \qquad (6.18)$$

constitutes certain necessary conditions; further necessary conditions are provided by

$$\psi_1 = 0.318 \left[\frac{20216 \, W^{2/3} (R_e^2 - R_i^2)^{-1}}{w R_i (1.47 + 0.0373 \, R_i/h_o)} \right]^{0.15} \qquad (8.9)$$

$$\psi_2 = 10^{-5} (3.41 + 0.117 \, R_i/h_o) \qquad (8.2)$$

The simultaneous solution of equations (6.18), (8.2), and (8.9) yields the TNT Containment Law for ideal vessels (no nozzles, weldments, or rigid end constraints):

$$\bar{W}_I = \left[\frac{1.407 \, \sigma_t \, \epsilon \, (3.41 + 0.117 \, R_i/h_o)(R_e^2 - R_i^2)^{1.85}}{10^5 \, w^{-0.85} \, (1.47 + 0.0373 \, R_i/h_o)^{0.15} R_i^{0.15}} \right]^{0.811} \qquad (9.1)$$

where

$$\sigma_t = \sigma_y + \left[\frac{\sigma_u (1 + \epsilon_u) - \sigma_y}{\epsilon_u}\right] \epsilon \ , \ \epsilon \leq \epsilon_u$$

and the bar on $\bar{W}$ indexes the valid domain of the equation as set forth in (a) through (g) of section 6.3. Theoretically, the maximum value of (9.1) occurs for $\epsilon = \epsilon_u$ and is given by

$$(\bar{W}_I)_{max} = \left[\frac{1.407\ \sigma_u\ \epsilon_u\ (1 + \epsilon_u)(3.41 + 0.117\ R_i/h_o)(R_e^2 - R_i^2)^{1.85}}{10^5\ w^{-0.85}\ (1.47 + 0.0373\ R_i/h_o)^{0.15}\ R_i^{0.15}}\right]^{0.811} \qquad (9.2)$$

In practice, however, the mid-meridian strain correlative with marginal containment is usually less than ϵ_u. This is seen from comparing the conventional ultimate strain values of section 7.1 with the marginal containment strains reported in Table 7.1

9.2 TNT Containment Law for Real Vessels. For a containment law to be useful to the pressure vessel designer, it must yield safe solutions for "real" vessels, i.e., vessels fitted with nozzles, weldments, and rigid end closures. Experiments designed to evaluate specifically the limiting effects of these discontinuities on containment were reported in Chapter 7. On the basis of the results, it was found that the safe or permissible strain domains correlative with the discontinuities are

(a) welded nozzles: $\epsilon \leq 1/2\ \epsilon_u$ (section 7.4)
(b) rigid end closures: $1/3\ \epsilon_u \leq \epsilon \leq 1/2\ \epsilon_u$ (section 7.3)
(c) welded plate: $\epsilon \leq 1/3\ \epsilon_u$ (section 7.2)

From an examination of these limits, it is postulated that real vessels can be expected to withstand safely strains as large as $1/3\ \epsilon_u$. Imposing this restriction on equation (9.1), we find that the TNT Containment Law for real vessels is

$$\overline{W}_R = \overline{W}_I \tag{9.3}$$

except that

(a) $\epsilon \leq 1/3\ \epsilon_u$

(b) the valid domain indexed by the bar on $\overline{W}_R$ consists of (a) through (f) of section 6.3, and additionally

(c) the vessel wall, weldments, closures, and nozzles must possess everywhere the chemical, mechanical, and physical properties specified in the design, and

(d) these properties, as they relate to containment, must not be negated in time by flaws, NDT (nil ductility temperature) considerations, radiation effects, stress concentrations, high temperatures, cycling, etc.

The literature abounds with studies on phenomena that degrade the mechanical properties of steel. Among the more authoritative of these are G. R. Irwin's treatment of flaws in reference (u), the work of W. S. Pellini and P. P. Puzak on NDT considerations in reference (v), and G. M. Adamson's data on radiation effects in reference (w).

The maximum value of equation (9.3) occurs for $\epsilon = 1/3\ \epsilon_u$ and is given by

$$(\bar{W}_R)_{max} = \left[\frac{0.1563\ \epsilon_u\ w^{0.85}(3.41 + 0.117\ R_i/h_o)(R_e^2 - R_i^2)^{1.85}}{10^5\ (2\ \sigma_y + \sigma_u + \sigma_u \epsilon_u)^{-1}(1.47 + 0.0373\ R_i/h_o)^{0.15} R_i^{0.15}} \right]^{0.811} \qquad (9.4)$$

where, in review, the nomenclature and units for equations (9.1) through (9.4) are

W	. . . .	charge weight (TNT or pentolite), lb
w	. . . .	weight density of vessel material, lb/ft^3
R_i	. . . .	initial internal radius of vessel, ft
R_e	. . . .	initial external radius of vessel, ft
h_o	. . . .	initial wall thickness of vessel, ft
ϵ	. . . .	conventional* permissible strain of vessel material, in/in
ϵ_u	. . . .	conventional* ultimate strain of vessel material, in/in
σ_t	. . . .	true stress*, psi, see equation (9.1)
σ_y	. . . .	conventional* yield stress of vessel material, psi
σ_u	. . . .	conventional* ultimate stress of vessel material, psi

* It is noted that all ingredients of the Containment Laws are in terms of conventional materials and properties - quantities readily available to the design engineer; however, if the vessel material is subjected to temperatures that degrade its energy absorption properties - i.e., its stress-strain values - then, of course, these degraded values must be employed in equations (9.1) through (9.4).

9.3 Accuracy. Deviations between predictions based on equation (9.1) and results from the contained experiments are given in Table C-1 and plotted in Figure 9.1. If all tests are considered, the average deviation is $^{+5}_{-6}$ per cent, and the maximum deviation is $^{+14}_{-20}$ per cent. If we exclude those tests for which no certified mechanical properties were available (denoted by circles) and those tests for which the final at-rest strain exceeded the maximum certified ultimate elongation (denoted by squares), the deviation is substantially reduced to an average $\pm$ 4 per cent and a maxumum of $^{+10}_{-12}$ per cent. Irrespective of the preferred deviation, agreement between the containment law predictions and the experimental results is considered excellent in light of the following statements:

(a) The calculations made in Table C-1 of Appendix C were based on an average stress-strain equation for a given material. Frequently, individual certified tensile tests varied from the average by as much as 10 per cent and in a few cases as high as 20 per cent.

(b) Deviations in the replicability of explosion phenomena frequently exceed 5 per cent and are sometimes as high as 10 per cent.

Experimental results of vessels fitted with weldments and rigid end closures are included in Table C-1 and Figure 9.1 and, hence, in the accuracy data presented above. Experimental results of the vessels fitted with nozzles also satisfy equation (9.1) with a maximum deviation of 1 per cent. A typical example is taken from Table 7.2: 304 stainless steel (cast) vessel, 10" ID, 20" length, 1/4" wall, ϵ = 0.328 in/in, W = 130 gm. With σ_t determined from values given in Appendix C, equation (9.1) yields $\overline{W}_I$ = 129 gm, a deviation of less than 1 per cent. The strain profile of this vessel is shown in Figure 7.6; since it is asymetric, ϵ indexes the "local" or uninhibited portion of the mid-meridian (which, in this case, lies opposite the one nozzle). With two or more nozzles, the local region would be

more restricted. Because of this difference in the interpretation of ϵ, the deviation data for nozzle experiments were not included in Table C-1 and Figure 9.1

9.4 Upper-Bound Containment Law for Reactor Vessels. It is recalled that the excursion accident spectrum is large in both magnitude and flux of the energy released: it ranges from small accidents to thousands of megawatt-seconds occurring in times from a few microseconds to seconds or more, and these can take place anywhere in the coolant-loss domain from no loss to a complete loss. The range of excursions and the conditions under which they may occur, the multiplicity and complexity of the parameters, and the state of the art preclude an exact solution to the reactor containment problem at this time.

This means that only restricted solutions are possible. Of these, we can postulate, a priori, that upper-bound solutions for containing the postulated excursion under the most adverse conditions:

(a) energy flux comparable to that of TNT

(b) reactor vessel filled with liquid coolant

are the most basic and the most valuable; and that these solutions are precisely those provided by the TNT Containment Laws, (9.1) through (9.4). One further clarification is necessary:

> To avoid ambiguity in relating a postulated excursion to a TNT simulation, it is assumed that, irrespective of the compounding of nuclear or other events that may occur in the reactor, the upper bound on the resultant total accident (the energy released) is in each case relative to and occurs at the normal operating conditions of the reactor. Furthermore, it is assumed that the release of gas products per unit energy of reactant does not exceed that for TNT.

Upon some reflection, it is seen that the limitations on compounding and gas products are necessary for upper-bound containment predictions; but that since the majority of excursions can be interpreted to satisfy these conditions, no serious loss in generality accrues. It is concluded that the TNT Containment Laws (9.3) and (9.4) constitute a safe and wholly defensible upper-bound solution to the entire spectrum of postulated excursions and the conditions under which they may occur.

9.5 Less Adverse Accident Conditions. The TNT Containment Laws (9.3) and (9.4) will provide safe upper bounds for the entire spectrum of excursions and the conditions under which they may occur. If the energy flux is similar to that of TNT and the reactor vessel is full of liquid coolant, these Laws will yield upper bounds that are both safe and reasonable. If, however, the excursion conditions are less adverse - the energy is released at rates less than that of TNT and/or a loss of coolant occurs - the upper-bound solution will, of course, be safe, but its reasonableness will be decreased. Modifications of the upper-bound Laws are necessary if solutions for less adverse conditions are to be both safe and reasonable. Three cases of excursion conditions less adverse than those for the upper-bound solution are presented in the following sections.

9.6 TNT Energy Flux, Complete Loss of Coolant. The explosion experiments conducted in vessels filled with air instead of water (section 7.5) provide pertinent information for the case of TNT energy flux and a complete loss of coolant from the reactor vessel prior to the accident. A direct comparison between the water and air conditions is presented in Figure 9.2.

It is assumed here that the pressure within the reactor vessel after a complete loss of coolant, but prior to an excursion, is atmospheric. This assumption is not restrictive since only sodium reactors are subject to postulated excursions following a complete loss of coolant, in which case the pressure would be at or near atmospheric. It is seen immediately that everywhere within the specified radial strain domain for air, the containment potential is at least a factor of three greater than that for water and that up to 0.20 in/in, the factor is at least four. These values for ideal vessels, however, could not be expected to hold for real vessels.

Since the localization factor for air is half that of water (Figure 6.1), deformation at the mid-meridian would be much more violent; hence, nozzle and weld failures would occur at smaller radial strains for air than for water. This effect can be compensated for by restricting the strain for the air case to $\epsilon \leq \epsilon_u/6$. Then the permissible values for 304 stainless steel are

$$\epsilon_{air} = \epsilon_u/6 = 0.10 \text{ in/in} , \quad \epsilon_{water} = \epsilon_u/3 = 0.20 \text{ in/in}$$

and from a comparison of the correlative charge weights (Figure 9.2), it is hypothesized that the value $2\,\overline{W}_R$ constitutes a safe upper bound everywhere in the radial strain domain of equation (9.3), and, of course, this includes (9.4).

The air/water containment ratio decreases with increasing radial strain as shown in Figure 9.2, and beyond the limiting strain for air (about 0.27 in/in), the decrease becomes significant. For example, a typical limiting strain for water (in the case of no rigid end constraints) is 0.46 in/in, from which the Figure yields an air/water containment ratio of about 1.9. Such values are somewhat academic, however, since they are not consistent with admissible strains of the realistic Containment Law, (9.3).

For intermediate losses of liquid coolant, the composite-vessel experiments of reference (i) indicate that the condition of overriding importance is whether or not the coolant level in the véssel is sufficient to completely envelope the core. If the core is completely enveloped, the containment potential will follow closely that of the no coolant-loss condition with, perhaps, a slight enhancement. If the coolant loss is such that the core is not enveloped, the containment potential will be somewhat greater (say 3/2) than that for the no-loss condition, and this potential factor will converge to the value 2 $\overline{W}_R$ for increasing coolant loss.

In the containment domain, the strength of the shock is not an appreciable function of the temperature of the medium through which it propagates. In view of this, it is postulated (for TNT energy flux) that the values $\overline{W}_R$ for no coolant loss and 2 $\overline{W}_R$ for complete coolant loss are valid everywhere in the temperature range from 65°F to 850°F.

9.7 Lesser Energy Flux, No Coolant Loss. Experiments with solid propellant in water-filled, 5" ID vessels provide useful bounds for the case of energy fluxes less than that of TNT and no loss of liquid coolant from the vessel prior to the accident. The propellant employed in the experiments of reference (k) possessed an energy density similar to that of TNT; the water was 70°F. The energy flux is reflected in the pressure-time and strain-time plots of Figure 9.3. The release time of about 40 milliseconds, if scaled to a typical reactor - say one with ID of 10 feet - would correspond to about one second. More generally, for the conditions here, the release time for a reactor of radius R_i (feet) can be taken as

$$\Omega_1 = 200\ R_{in}\ \text{(milliseconds)}$$

where R_{in} is the numerical value of R_1. The propellant experiments and the TNT Containment Law for Ideal Vessels, equation (9.1), index in Figure 9.4 the significant increase in containment correlative with energy fluxes less than the TNT flux.

Although the propellant experiments were conducted in vessels with rigid end closures, the uniformity of loading over the full vessel length resulted in deformations similar to those of the open-end explosion experiments. It is seen from Figure 9.4 that everywhere within the specified radial strain domain for the propellant, the containment potential is at least a factor of five greater than that for the explosive. Much more important, however, is the restricted strain domain, $\epsilon \leq \epsilon_u/3$, of the TNT Containment Law for real vessels, equation (9.3). For 304 stainless steel, an allowable maximum is $\epsilon = 0.20$ in/in. From the use of this value in comparing the correlative weights of propellant and explosive in Figure 9.4, it is hypothesized, for water at 70°F and energy release times $\geq \Omega_1$, that the value $8 \mid \overline{W}_R \mid$ is a safe upper bound, $\mid \overline{W}_R \mid$ being the energy density of $\overline{W}_R$ without regard to energy flux.

Unlike the case for TNT energy flux, containment potential for lesser fluxes decreases significantly with increased system temperature. Liquid coolant temperatures in excess of 70°F will decrease the enhancement factor of eight in accord with the basic heat-sink rationale presented in Appendix D and reference (i). In essence this rationale hypothesizes that, for extensive metal and/or coolant heat sinks, the internal blast pressure varies directly with absolute temperature and charge weight. Thus for water at 200°F and release times $\geq \Omega_1$, it is hypothesized that $6 \mid \overline{W}_R \mid$ is a safe upper bound. For sodium at 850°F and release times $\geq \Omega_1$, it is hypothesized that a safe upper bound is $3 \mid \overline{W}_R \mid$.

It is recalled that the principal reason for considering the less adverse conditions of the accident spectrum was to generate containment law solutions for this portion of the spectrum that would be more reasonable than that given by the TNT law. In this vein, it is desirable to entertain briefly the relation

$$(\Omega_1)_c = \frac{1000}{3} R_{in} \quad \text{(milliseconds)}$$

Now $(\Omega_1)_c$ is qualitatively more conservative than Ω_1, but it is believed that the use of these values in the foregoing containment predictions would produce solutions of comparable reasonableness. This deduction expands the release time spectrum of propellant energy fluxes by 5/3 and permits the convenient tabular format employed in Table 9.1.

The heat-sink experiments of reference (1) provide a significant index to the time-heat absorption character of accidents that occur in times of the order of hundreds of milliseconds. The results of these experiments in 3.5" ID models indicate that the major portion of heat absorption from the internal blast pressure gases occurred within five milliseconds. Scaled to a full-size reactor, say one with ID of 10 feet, this time would be of the order of 170 milliseconds. More generally, the release time here for a reactor of radius R_i (feet) can be taken as

$$\Omega_2 = \frac{100}{3} R_{in} \quad \text{(milliseconds)}$$

It appears, then, that no appreciable quantity of heat is absorbed in the interim between Ω_1 and Ω_2, and it is hypothesized that $6 \mid \bar{W}_R \mid$ is also a safe upper bound for water at 200°F and release times $\geq \Omega_2$. Likewise, it seems reasonable to take $3 \mid \bar{W}_R \mid$ as a safe upper bound for sodium at 850°F and release times $\geq \Omega_2$.

At some point in the energy release time domain less than Ω_2, shock waves will be produced rather than a uniform pressure build-up. This will be true irrespective of whether the reactor liquid coolant be lost or retained in any quantity. From a consideration of the dearth of definitive information in this domain, it is postulated that $\mid \bar{W}_R \mid$ for the case of no coolant loss and $2 \mid \bar{W}_R \mid$ for the case of complete coolant loss are the highest safe upper bounds that can be adequately defended.

9.8 Lesser Energy Flux, Complete Loss of Coolant. The explosion experiments conducted in vessels filled with air instead of water (section 7.5) also provide some guide lines for the case of energy fluxes less than that of TNT and a complete loss of coolant from the reactor vessel prior to the accident. In this regard it is pertinent to note that:

(a) In the containment domain, the magnitude of the internal blast pressure is never sufficient to produce vessel deformation beyond that generated by the shock wave; this is true irrespective of whether the transmission medium be liquid or gas.

(b) Unlike the case for TNT energy flux (section 9.6), the lesser energy flux in air would not produce a highly localized deformation at the mid-meridian, but rather a pattern similar to that for TNT in water (Figure 6.1). Hence the permissible strain for the lesser energy flux in air and the TNT flux in water would be the same: $\epsilon \leq \epsilon_u/3$.

In view of (a) and (b), it is hypothesized from Figure 9.2 that $3 \mid \overline{W}_R \mid$ is a safe upper bound for air at 70°F and release times $\geq \Omega_2$. Again as in section 9.6, it is assumed that atmospheric pressure exists in the reactor vessel prior to the excursion.

If extensive metallic heat sinks are available to the released gases, as in the case with the core region of the Enrico Fermi Reactor (compare Tables 8.2 and 8.5 of reference (1)), and if it is assumed that the partition of energy with respect to the heat sink for the slow release is similar to that for TNT, the containment potential could be increased by a factor exceeding two. Under these conditions it is hypothesized that $6 \mid \overline{W}_R \mid$ is a safe upper bound for air at 70°F and release times $\geq \Omega_2$. As mentioned previously, containment potential is affected adversely for the case of slow energy fluxes (those less than that of TNT) occurring at elevated temperatures. The decrease in containment potential with increasing temperature is significant irrespective of whether the coolant be retained or lost. For air at 200°F, extensive metallic heat sinks, and release times $\geq \Omega_2$, it is hypothesized - again from the heat-sink rationale of Appendix D - that $4 \mid \overline{W}_R \mid$ is a safe upper bound. Similarly, $3 \mid \overline{W}_R \mid$ is hypothesized to be a safe upper bound for air at 850°F.

For intermediate losses of liquid coolant, the containment potential would be analogous to that for the TNT energy flux:

(a) if the quantity of coolant in the vessel is sufficient to completely submerge the core and the release times are $\geq \Omega_2$, the containment potential will converge on the values for no coolant loss - $8 \mid \overline{W}_R \mid$ for water at 70°F, $6 \mid \overline{W}_R \mid$ for water at 200°F, and $3 \mid \overline{W}_R \mid$ for sodium at 850°F - as the coolant loss decreases.

(b) if the quantity of coolant in the vessel is not sufficient to submerge the core and the release times are $\geq \Omega_2$, the containment potential will converge on the values for complete coolant loss - $6 \mid \overline{W}_R \mid$ for water at 70°F, $4 \mid \overline{W}_R \mid$ for water at 200°F, and $3 \mid \overline{W}_R \mid$ for sodium at 850°F - as the coolant loss increases.

9.9 Restrictions on Less Adverse Conditions. A summary of maximum containable energy releases for various accident conditions is presented in Table 9.1. For the case of no coolant loss and energy release times Ω (milliseconds) given by

$$\text{TNT release time} \leq \Omega < \frac{100}{3} R_{in}$$

the results in Table 9.1 are both reasonable and highly defensible; they have been verified directly by established rationale and extensive experimental results. For all other conditions

$$100 \leq 3\,\Omega / R_{in} \leq 1000$$

the results in Table 9.1 are also believed to be safe and reasonable. However, they are not postulated results; they are hypothesized results. As such, they do not constitute absolute upper bounds in the sense of the postulated quantities nor do they possess the inherent generality of the results for TNT-like energy fluxes. Nevertheless, for particular accidents and containment conditions, the rationale of the slow-release results can frequently be employed to yield highly defensible containment predictions.

9.10 Blast Shielding and Inertial Constraints. All of the results presented in Table 9.1 are addressed to reactor vessels with no external constraints, i.e., no restraining forces other than the strain-generated tensile and shearing forces in the vessel wall itself. However, in the design of many reactors, there exist neutron and blast shielding of various types surrounding the reactor vessel. In some cases, this shielding and other external constraints can enhance excursion containment potential to a marked degree. In the EBR-II reactor, for example, a crushable blast shield envelops the reactor vessel; reference (x) indexes the energy absorption potential of such a shield. Here, radial deformation of the reactor vessel would be opposed by the crushable shield, and the opposing force would increase with increasing vessel strain. This type of external constraint can greatly enhance the containment potential of reactor vessels for the entire energy flux spectrum of nuclear accidents.

Other constraint examples are the graphite neutron shielding surrounding the Enrico Fermi reactor and the large pool of water surrounding Oak Ridge's HFIR (High Flux Isotope Reactor). Experiments reported in reference (i) indicate that the graphite shielding of the Fermi reactor enhances its TNT containment potential by a factor of two or more. The same enhancement would result from the HFIR pool water. However, these masses - the graphite and pool water - constitute inertial constraints only; hence, they are effective only for TNT energy fluxes and those of like order.

No general statement can be made as to the containment enhancement factor of inertial constraints. However, information presented in this section and in reference (i) can be employed in some cases to increase the bounds presented in Table 9.1.

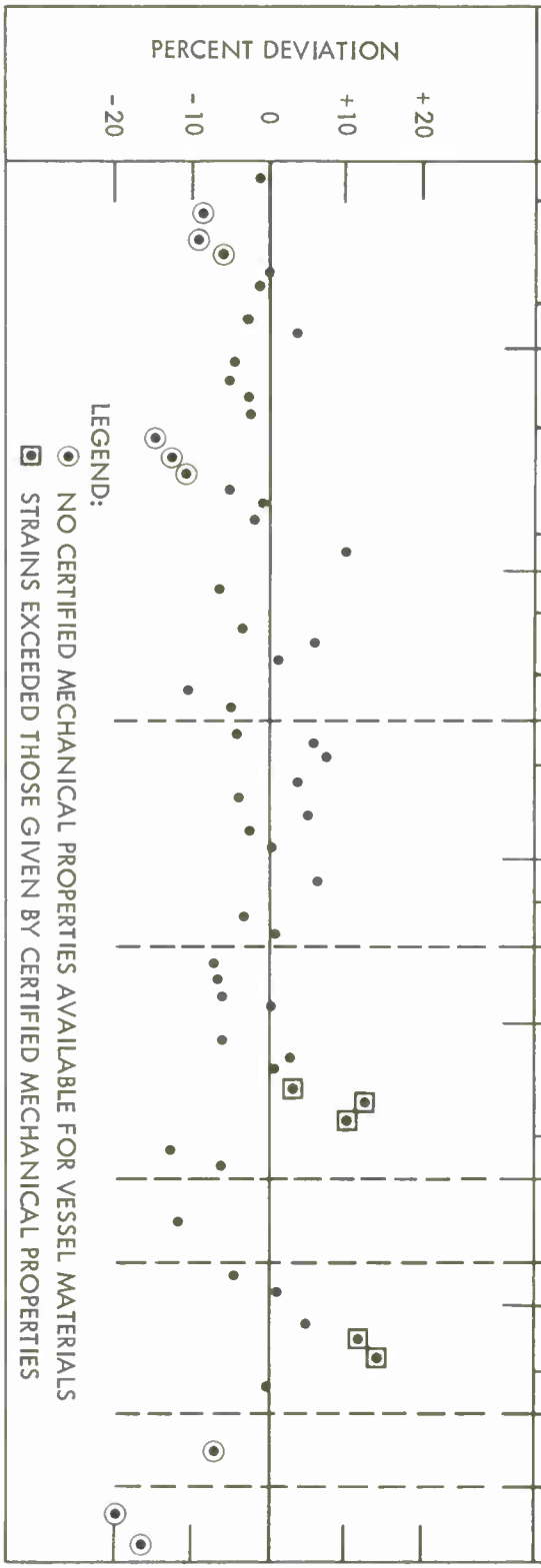

WALL THICKNESS h_o (inches)	INTERNAL RADIUS R_i (inches)	VESSEL MATERIAL
0.060	2.5	304 S.S. PLATE
0.118		
0.253		
0.118	5.0	
0.253		
0.515		
0.253	10.0	
0.515		
1.030		
0.125	2.5	304 S.S. CAST
0.250		
0.250	5.0	
0.500		
0.250	2.5	410 S.S. CAST (ANNEALED)
0.250	5.0	
0.500		
0.250	2.5	410 S.S. CAST (HARDENED)
0.515	5.0	212 FLANGE STEEL PLATE
0.515	10.0	
1.030		
0.253	5.0	MILD STEEL PLATE
0.500	7.5	6061-T6 ALUM. EXTRUDED

FIG. 9.1 DEVIATIONS OF PREDICTED CHARGE WEIGHT (EQUATION (9.1)) FROM EXPERIMENTAL RESULTS

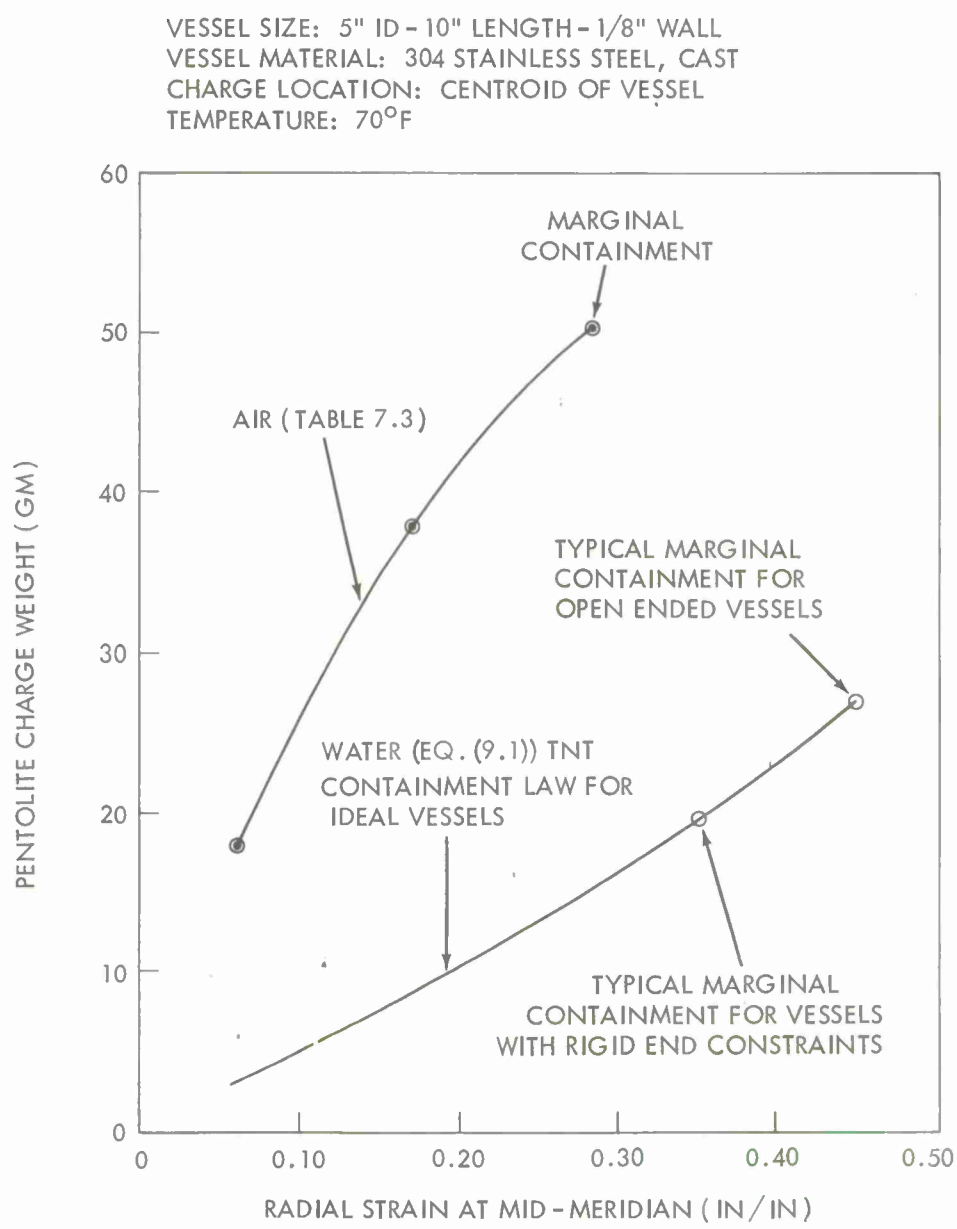

FIG. 9.2 COMPARISON OF EXPLOSION TESTS IN AIR-FILLED AND WATER-FILLED VESSELS

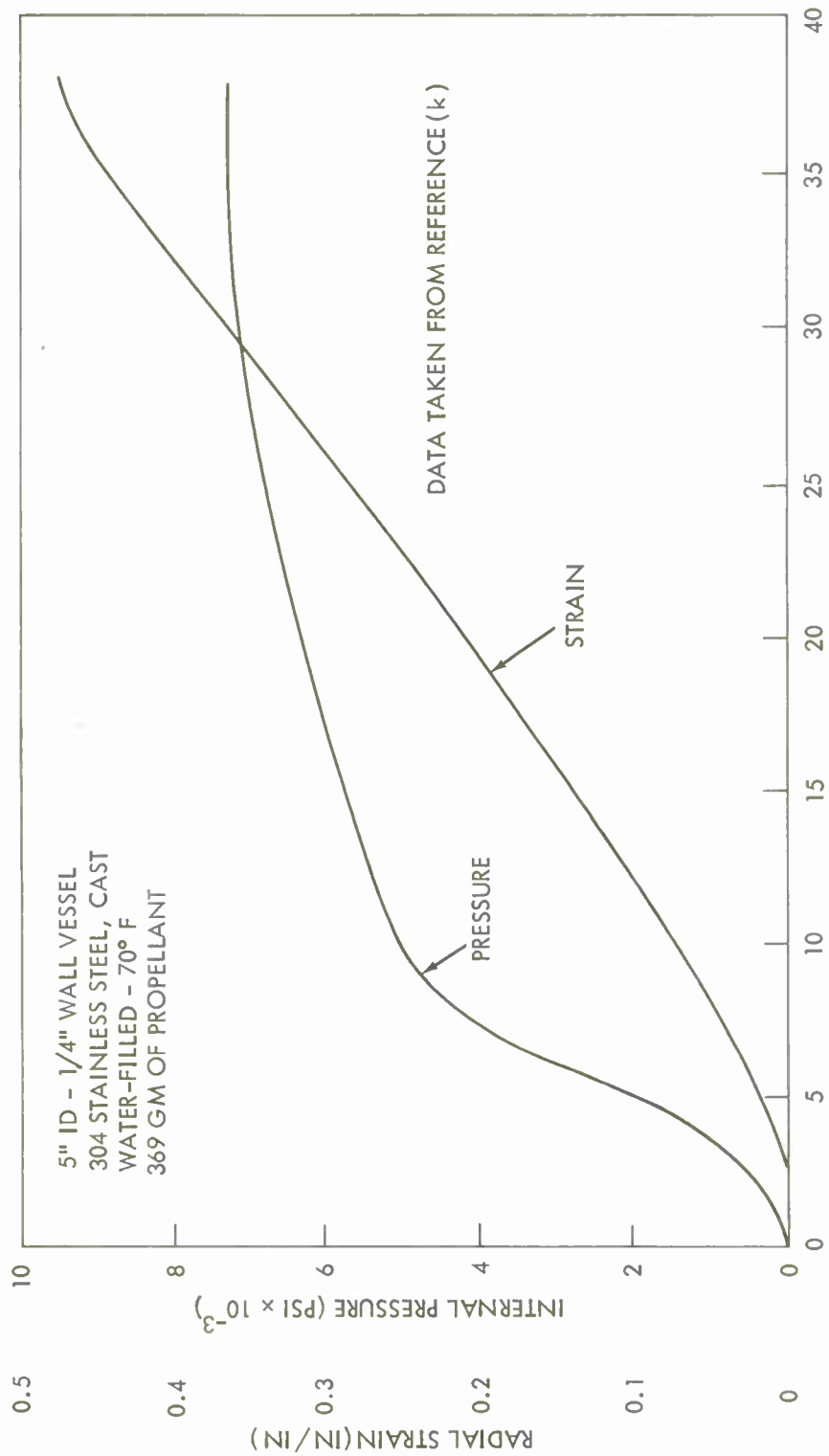

FIG. 9.3 VARIATION OF PRESSURE AND STRAIN WITH TIME FOR PROPELLANT-LOADED VESSEL

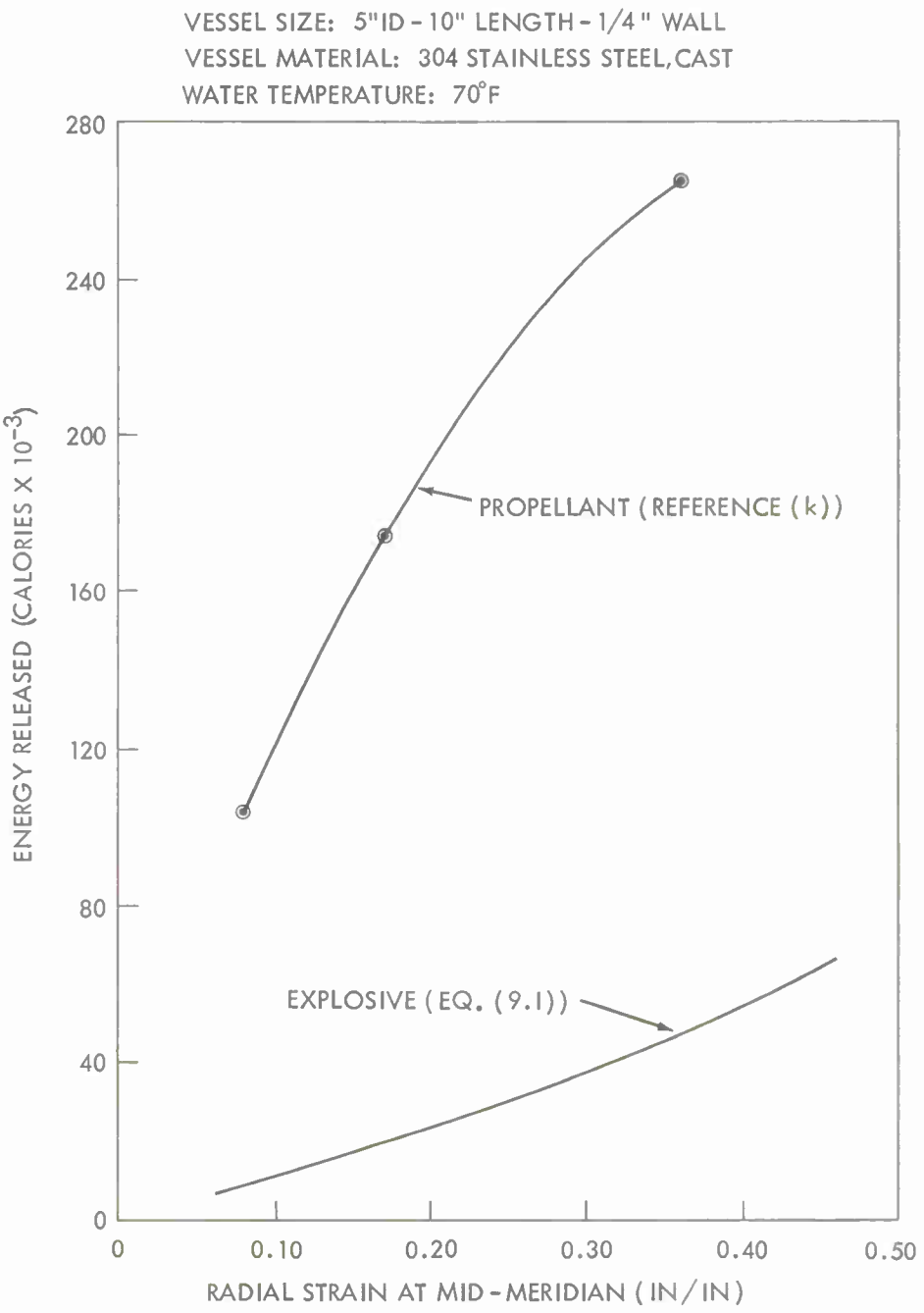

FIG. 9.4 COMPARISON OF PROPELLANT AND EXPLOSION LOADINGS IN WATER-FILLED VESSELS

TABLE 9.1

SAFE * CONTAINABLE CHARGE WEIGHTS

FOR REAL VESSELS
UNDER VARIOUS ACCIDENT CONDITIONS

SYSTEM TEMPERATURE, T (°F)		QUANTITY OF COOLANT IN VESSEL	Ω , DURATION OF ENERGY RELEASE (millisecands)	
			$(TNT)_D \leq \Omega < 100\, R_{in}/3$	$100 \leq 3\Omega/R_{in} < 1000$
T = 70		FULL	$(\overline{W}_R)_{max}$	*8 $\lvert(\overline{W}_R)_{max}\rvert$
		NONE	*2 $(\overline{W}_R)_{max}$	*6 $\lvert(\overline{W}_R)_{max}\rvert$ †
T = 200		FULL	$(\overline{W}_R)_{max}$	*6 $\lvert(\overline{W}_R)_{max}\rvert$
		NONE	*2 $(\overline{W}_R)_{max}$	*4 $\lvert(\overline{W}_R)_{max}\rvert$ †
T = 850		FULL	$(\overline{W}_R)_{max}$	*3 $\lvert(\overline{W}_R)_{max}\rvert$
		NONE	*2 $\overline{W}_R)_{max}$	*3 $\lvert(\overline{W}_R)_{max}\rvert$ †

NOTES

1. Real vessels are those fitted with weldments, nozzles, and end closures.
2. $(TNT)_D$ is time duratian af TNT energy release.
3. R_{in} is the numerical value of R_i(ft).
4. $(\overline{W}_R)_{max}$ is given by equatian (9.4).
5. $|(\overline{W}_R)_{max}|$ is the energy density (1050 calories per gram) af $(\overline{W}_R)_{max}$ without regard ta energy flux.
6. *The caefficients af these quantities are hypothesized values.
7. † These values are valid only far the case of extensive metallic heat sinks (see section 9.8).

CHAPTER 10

SUMMARY AND CONCLUSIONS

10.1 Summary. Nuclear excursions range from small accidents to thousands of megawatt-seconds occurring in times from a few microseconds to seconds or more, and these can take place anywhere in the coolant-loss domain from no loss to a complete loss. The violence and destructiveness of this spectrum of accidents were examined, and the most adverse accident (the most difficult to contain per unit energy released) was found to be that correlative with TNT energy flux for a reactor vessel completely filled with liquid coolant. The philosophy of containment and its increased need in urban areas were presented: from these, it was deduced that engineers require highly quantitative Containment Laws to effect economical reactor vessel containment design.

The principal parameters of reactor vessel containment were identified and partially characterized. Consistent with Saint-Venant's semi-inverse method of classical mechanics, a synthesis of the lumped parameters was employed to formulate an embryonic Containment Law format. Extensive experiments in Hopkinson models (some fabricated with weldments, nozzles, and rigid end closures) of reactor vessels were conducted; these provided boundary conditions for evaluating the embryonic format and resulted in the basic TNT Containment Laws presented in Chapter 9. The consideration of less adverse accident conditions - energy fluxes less than that of TNT and loss of coolant - led to hypotheses of increased and more reasonable safe upper bounds for accidents of this type (Table 9.1).

10.2 Conclusions. A priori - fundamental rationale, extensive experimental data, and comprehensive syntheses of empirical and theoretical containment knowledge - the following conclusions are drawn:

(a) The basic TNT Containment Laws, equations (9.1) through (9.4), and their attendant conditions, restrictions, and qualifications have been carefully and cautiously generated. These laws are known to be consistent with extensive experimental results; they constitute upper bounds that are wholly defensible throughout the entire spectrum of accidents set forth in section 10.1.

(b) The TNT Containment Laws for Real Vessels (those fitted with weldments, nozzles, and rigid end closures), equations (9.3) and (9.4), constitute wholly defensible upper bounds that are both safe and reasonable for TNT-like energy fluxes and the condition of no liquid coolant loss from the reactor vessel prior to the accident.

(c) The TNT Containment Laws for Real Vessels, equations (9.3) and (9.4), constitute safe upper bounds that are wholly defensible throughout the entire spectrum of accidents set forth in Table 9.1. The reasonableness of those bounds decreases, however, with decreasing energy flux and increasing loss of liquid coolant from the reactor vessel prior to the accident.

(d) TNT energy flux and no liquid coolant loss constitute the most adverse accident conditions. Accidents that occur with lesser energy fluxes and/or loss of liquid coolant are less severe and more amenable to containment. Increased containment bounds for the less adverse accident conditions are presented in Table 9.1. These bounds are hypothesized values; they are believed to be both safe and reasonable, but they are not as highly defensible as the bounds provided by the TNT Containment Laws for Real Vessels, equations (9.3) and (9.4).

(e) The Containment Laws and other bounds presented in this report are expressed in terms of conventional materials and properties - quantities readily available to the containment design engineer.

(f) Aside from reactors, the fundamental rationale and extensive experimental results presented herein contribute directly to high-strain-rate phenomenology; they will be applicable to pressure vessels generally and to a wide spectrum of dynamic structural response problems.

(g) Since the TNT (or pentolite) explosion produces shock and blast pressure mechanisms that cover a wide spectrum of energy flux, and since the fundamental characteristics of these mechanisms are known, their applications to basic excursion containment studies can be highly profitable.

(h) The reactor containment community is seriously enjoined and cautioned: In general, realistic appraisals of the excursion response and containment potential of reactor vessels should not be attempted without basic experimental evidence of the type presented herein and in reference (i).

The basic Containment Laws and correlative material presented in this report are believed to constitute the most extensive and authoritative reactor vessel, excursion containment information existing on this subject. The results and conclusions presented in this report are final, and they constitute the Laboratory's official opinion.

ACKNOWLEDGEMENTS

The authors express grateful appreciation to Dr. Donna Price and Dr. Hans Snay for their consultation and advice on some of the problems encountered in this program; and a special debt of gratitude is acknowledged to Dr. Donald T. Bonney for his consultation and careful technical review of this report. Thanks are also expressed to Mr. Lloyd Walker for his conduct of a portion of the model vessel experiments and to Mr. Leslie Roslund and other contributing members of the Explosions Research Department and the Photographic Division for their help in the experimental program.

REFERENCES

(a) H. A. Bethe and J. H. Tait, An Estimate of the Order of Magnitude of the Explosion When the Core of a Fast Reactor Collapses, RHM (56/113), Atomic Energy Research Establishment, Harwell, Berks, England, April 1956.

(b) Cottrell, Wm. B., Introduction (Chapter 1 of U. S. Reactor Containment Technology, CF 64-11-31 Draft), to be issued in 1965.

(c) Fisher, E. M. and Wise, W. R., Jr., Containment Study of the Enrico Fermi Fast Breeder Reactor Plant, NavOrd Report 5747, October 1957.

(d) Wise, W. R., Jr., NOL Reactor Vessel Containment Program, Progress Reports No. 4 through 18, 1 October 1958 through 31 December 1959.

(e) Proctor, James F., Energy Partition of Water-Cased Explosions in an Idealized Model Reactor Vessel, NOLTR 62-155, June 1960.

(f) Wise, W. R., Jr., Possible Jump of Rotating Shield Plug for Enrico Fermi Atomic Power Plant, NOL Letter Report of 15 May 1962, NOL Reactor Vessel Containment Program.

(g) Wise, W. R., Jr., Proctor, J. F., and Walker, L. P., Enrico Fermi Shield Plug Response to a 1000-lb TNT Accident, Experimental Mechanics, Vol. 3, No. 10, October 1963, presented at Society for Experimental Stress Analysis, Spring Meeting, Seattle, Washington, May 8 through 10, 1963.

(h) Benefiel, Harry B., A Method for Measuring Internal Blast Pressure-Time Histories of Confined, Sodium-Cased Explosions, NOLTR 62-45, August 1962.

(i) Wise, W. R., Jr., Proctor, J. F., and Walker, L. P., Response of Enrico Fermi Reactor to TNT Simulated Nuclear Accidents, NOLTR 62-207, November 1964.

(j) Power Reactor Development Co. Report, Technical Information and Hazards Summary Report, Section 1: Reactor and Plant Design, June 1961.

(k) Wise, W. R., Jr., An Investigation of Strain-Energy Absorption Potential as the Criterion for Determining Optimum Reactor-Vessel Containment Design, NavOrd 5748, June 1958.

(l) Cole, Robert H., Underwater Explosions, Princeton University Press, Princeton, N.J., 1948.

(m) Snay, Hans G., The Scaling of Underwater Explosion Phenomena, NOLTR 61-46, June 1961.

(n) Langhaar, Henry L., Dimensional Analysis and Theory of Models, John Wiley & Sons, Inc., New York, 1960.

(o) Tardif, H. P. and Erickson, W., The Experimental Properties of Metals Under Dynamic Loading, CARDE Technical Memorandum No. 192/58, Canadian Armament Research and Development Establishment, 1958.

(p) Manjoine, M. J., Influence of Rate of Strain and Temperature on Yield Stresses in Mild Steel, Journal of Applied Mechanics, Vol 11, 1944.

(q) Bodner, S. R. and Symonds, P. S., Plastic Deformation in Impact and Impulsive Loading of Beams, Brown University, ONR Contract Nonr-562(10).

(r) Johnson, P. C. and others, Basic Parameters of Metal Behavior Under High Rate Forming, Arthur D. Little, Inc., six interim reports, WALTR 11.2/20, WALTR 111.2/20 - 1 through 5, 1961-62.

(s) Davis, R. L., The Use of a Knock-Off Tube as a Quick Pressure-Release Mechanism, NOLTR 63-134, May 1964.

(t) U. S. Naval Ordnance Laboratory, Explosion Effects Data Sheets, NavOrd 2986, 1955, Confidential.

(u) Irwin, G. R., Fracture Mechanics, Structural Mechanics, Proceedings of the First Symposium on Naval Structural Mechanics, Pergamon Press, New York, 1960.

(v) Pellini, W. S. and Puzak, P. P., Practical Considerations in Applying Laboratory Fracture Test Criteria to the Fracture-Safe Design of Pressure Vessels, NRL Report 6030, November 1963.

(w) Adamson, G. M. and others, HRP Civilian Power Reactor Conference Held at Oak Ridge, March 21-22, 1956, TID-7524, March 1957.

(x) Wise, W. R., Jr., Calculation of the Energy Absorption Potential for the Blast Shield of the Argonne National Laboratory Nuclear Reactor, EBR-II, NavOrd Report 4470, February 1957.

APPENDIX A

GENERAL STRAIN ENERGY EQUATION FOR EXCURSION-LOADED REACTOR VESSEL

Consider a closed right-cylindrical vessel, e.g., a reactor pressure vessel, subjected to an accidental excursion that causes the vessel wall to flow rapidly and gross plastically in 3-space and time in a general way. If, during the dilation,

(a) the pressure vector at every differential surface of the internal wall, and

(b) the strain vector of every differential surface of the external wall

are known, what is the strain energy correlative with containment?

We shall derive the general strain energy equation of dynamic equilibrium for an internally-loaded, hollow, right-circular cylinder closed with rigid, radial constraints at the ends. The closures are right discs fitted concentrically with the hollow cylinder. The cylinder and closures together are defined as the cylinder unit which comprises the solid equilibrium system to be investigated. The cylinder and closures separately constitute the primary and secondary systems, respectively, and are treated as phenomenological continua for which it is assumed only that the material is incompressible and of uniform, constant mass density; the common assumptions of homogeneity and isotropy will not be invoked at this time. The dimensions and physical properties of the secondary system are such that it is not stressed

beyond the elastic limit during loading of the cylinder unit; thus all plastic deformation is restricted to the primary system. The load generating and transmission media (as yet undefined) internal to the primary and secondary systems comprise the fluid or tertiary system.

Throughout the entire loading it is postulated that all the mechanical surface-loading work done on the solid system manifests itself in the immediate mechanical forms of strain energy, the energy required to accelerate the mass of the solid system, the energy required to compress and accelerate the atmosphere external to the solid system, and the energy absorbed or expended in effecting a change in the potential energy of position of the solid system. For any time t let

E_{pp} ... be total surface shearing-force work done on solid system by motion of pressure-loading forces parallel to internal wall, ft-lb

E_{pn} ... be total surface normal-force work done on solid system by motion of pressure-loading forces normal to internal wall, ft-lb

E_p .... be total pressure-loading-force work done on solid system, ft-lb

E_i .... be total inertia-force energy generated in solid system as a consequence of mass acceleration, ft-lb

E_{po} ... be total change in potential energy of position of solid system, ft-lb

E_a .... be total compressive and inertia-force work done on atmosphere external to solid system, ft-lb

E_s .... be total strain energy absorbed by solid system as a consequence of deformation, ft-lb

External mechanical work done upon the primary and secondary systems must be instantaneously conserved in the immediate mechanical forms of strain, kinetic, compression, and potential (position) energy. It follows, a priori, that a consequence of this conservation is

$$E_p = E_{pp} + E_{pn} = E_s + E_i + E_{po} + E_a \qquad \text{(A-1)}$$

Plastic straining of the primary system is accompanied by the generation of heat within the system which may or may not be dissipated from the system depending upon the temperature of its environment. It has only to be recognized here that, with respect to equation (A-1), the heat of elastic and plastic strain is inherently accounted for in the strain energy term E_s. Although the magnitudes of the surface, strain, inertia, compression, and position energies are functions of the temperature of the solid system, the validity of equation (A-1) is independent of temperature and heat flux within the range for which utilization of the system as a pressure vessel remains practicable.

We choose r, θ, and z to be the radial, circumferential, and longitudinal coordinates, respectively, for a cylindrical coordinate system in which z is directed vertically upward. The axes of revolution of the cylinders and closures coincide with the z-axis, and the internal face of the lower closure lies in the r, θ, z = 0 plane as shown in Figure A-1. Let r_o, θ_o, and z_o be Lagrangian coordinates which denote the original position of each solid-system particle at time $t = t_o = 0$.

A-1 Normal Pressure-Force Work. We first derive an expression for the normal pressure-force work done upon the solid system. We choose

$$r_i = r_i(\theta_o, z_o, t)$$

$$\theta_i = \theta_i(\theta_o, z_o, t) \qquad \text{(A-2)}$$

$$z_i = z_i(\theta_o, z_o, t)$$

to be the radial, circumferential, and longitudinal coordinates, respectively, which define the internal surface of the vessel. These functions as well as all others defined in this appendix are assumed to be differentiable to the extent required for the work. Let

$$p_r = p_r(r_i, \theta_i, z_i, t)$$

$$p_\theta = p_\theta(r_i, \theta_i, z_i, t) \qquad \text{(A-3)}$$

$$p_z = p_z(r_i, \theta_i, z_i, t)$$

be the loading pressures generated, respectively, in the r, Θ, z directions and

$$dA_r = r_i\, d\theta_i\, dz_i$$

$$dA_\theta = dr_i\, dz_i \qquad \text{(A-4)}$$

$$dA_z = r_i\, dr_i\, d\theta_i$$

be the projected differential areas upon which

$$p_r, p_\theta, p_z$$

respectively, bear to generate the differential pressure forces

$$dP_r = p_r r_i \, d\theta_i \, dz_i$$

$$dP_\theta = p_\theta \, dr_i \, dz_i \qquad \text{(A-5)}$$

$$dP_z = p_z r_i \, dr_i \, d\theta_i$$

If

$$u_i = u_i(\theta_o, z_o, t)$$

$$v_i = v_i(\theta_o, z_o, t) \qquad \text{(A-6)}$$

$$w_i = w_i(\theta_o, z_o, t)$$

respectively, define the radial, circumferential, and longitudinal displacements of the solid system internal surface, the differential displacements through which the pressure forces

$$dP_r, \; dP_\theta, \; dP_z$$

move in time dt are

$$du_i = \frac{\partial u_i}{\partial \theta_o} d\theta_o + \frac{\partial u_i}{\partial z_o} dz_o + \frac{\partial u_i}{\partial t} dt$$

$$dv_i = \frac{\partial v_i}{\partial \theta_o} d\theta_o + \frac{\partial v_i}{\partial z_o} dz_o + \frac{\partial v_i}{\partial t} dt \qquad \text{(A-7)}$$

$$dw_i = \frac{\partial w_i}{\partial \theta_o} d\theta_o + \frac{\partial w_i}{\partial z_o} dz_o + \frac{\partial w_i}{\partial t} dt$$

We elect here to follow the path of a single particle in time so that the Lagrangian differentials

$$d\theta_o,\ dz_o$$

vanish, and we obtain

$$du_i = \frac{\partial u_i}{\partial t}\,dt, \qquad dv_i = \frac{\partial v_i}{\partial t}\,dt, \qquad dw_i = \frac{\partial w_i}{\partial t}\,dt \tag{A-8}$$

The differential work done in the r, θ, z directions is, respectively,

$$\begin{aligned} dE_{pnr} &= p_r r_i \frac{\partial u_i}{\partial t}\ d\theta_i\ dz_i\ dt \\ dE_{pn\theta} &= p_\theta \frac{\partial v_i}{\partial t}\ dr_i\ dz_i\ dt \\ dE_{pnz} &= p_z\ r_i \frac{\partial w_i}{\partial t}\ dr_i\ d\theta_i\ dt \end{aligned} \tag{A-9}$$

It will become evident in later considerations that it is highly desirable to choose differential forms which will permit integrations over the original configuration of the solid system. To this end, from the relations (A-2), we express the non-Lagrangian, surface coordinate differentials

$$dr_i,\ d\theta_i,\ dz_i$$

in terms of Lagrangian and time differentials as

$$dr_i = \frac{\partial r_i}{\partial \theta_o}\ d\theta_o + \frac{\partial r_i}{\partial z_o}\ dz_o + \frac{\partial r_i}{\partial t}\ dt$$

$$d\theta_i = \frac{\partial \theta_i}{\partial \theta_o} d\theta_o + \frac{\partial \theta_i}{\partial z_o} dz_o + \frac{\partial \theta_i}{\partial t} dt \qquad \text{(A-10)}$$

$$dz_i = \frac{\partial z_i}{\partial \theta_o} d\theta_o + \frac{\partial z_i}{\partial z_o} dz_o + \frac{\partial z_i}{\partial t} dt$$

But the differential areas

$$dA_r, \; dA_\theta, \; dA_z$$

of which

$$dr_i, \quad d\theta_i, \quad dz_i$$

are factorial components, are functions of the spatial coordinates

$$r_i, \; \theta_i, \; z_i$$

<u>alone</u>, so that the time differential vanishes, and the equations (A-10) reduce to

$$dr_i = \frac{\partial r_i}{\partial \theta_o} d\theta_o + \frac{\partial r_i}{\partial z_o} dz_o$$

$$d\theta_i = \frac{\partial \theta_i}{\partial \theta_o} d\theta_o + \frac{\partial \theta_i}{\partial z_o} dz_o \qquad \text{(A-11)}$$

$$dz_i = \frac{\partial z_i}{\partial \theta_o} d\theta_o + \frac{\partial z_i}{\partial z_o} dz_o$$

Combining equations (A-9) and (A-11), we obtain

$$dE_{pnr} = p_r r_i \frac{\partial u_i}{\partial t} dt \left[\frac{\partial \theta_i}{\partial \theta_o} \frac{\partial z_i}{\partial \theta_o} d\theta_o d\theta_o \right.$$

$$\left. + \left(\frac{\partial \theta_i}{\partial \theta_o} \frac{\partial z_i}{\partial z_o} + \frac{\partial \theta_i}{\partial z_o} \frac{\partial z_i}{\partial \theta_o} \right) d\theta_o dz_o + \frac{\partial \theta_i}{\partial z_o} \frac{\partial z_i}{\partial z_o} dz_o dz_o \right] \qquad \text{(A-12)}$$

$$dE_{pn\theta} = p_\theta \frac{\partial v_i}{\partial t} dt \left[\frac{\partial r_i}{\partial \theta_o} \frac{\partial z_i}{\partial \theta_o} d\theta_o d\theta_o \right.$$

$$\left. + \left(\frac{\partial r_i}{\partial \theta_o} \frac{\partial z_i}{\partial z_o} + \frac{\partial r_i}{\partial z_o} \frac{\partial z_i}{\partial \theta_o} \right) d\theta_o dz_o + \frac{\partial r_i}{\partial z_o} \frac{\partial z_i}{\partial z_o} dz_o dz_o \right] \qquad \text{(A-13)}$$

$$dE_{pnz} = p_z r_i \frac{\partial w_i}{\partial t} dt \left[\frac{\partial r_i}{\partial \theta_o} \frac{\partial \theta_i}{\partial \theta_o} d\theta_o d\theta_o \right.$$

$$\left. + \left(\frac{\partial r_i}{\partial \theta_o} \frac{\partial \theta_i}{\partial z_o} + \frac{\partial r_i}{\partial z_o} \frac{\partial \theta_i}{\partial \theta_o} \right) d\theta_o dz_o + \frac{\partial r_i}{\partial z_o} \frac{\partial \theta_i}{\partial z_o} dz_o dz_o \right] \qquad \text{(A-14)}$$

which are the components of work resulting from the differential motion of an internal differential area of the solid system subjected to dynamic loading. We define

$$dE_{pn} = dE_{pnr} + dE_{pn\theta} + dE_{pnz} \qquad \text{(A-15)}$$

from which

$$E_{pn} = \int_t \int_A (dE_{pnr} + dE_{pn\theta} + dE_{pnz}) \qquad \text{(A-16)}$$

where t and A, respectively, indicate time and original internal area limits of integration. It is necessary at this point to note that the change in variables from non-Lagrangian to Lagrangian coordinates represented in the integral (A-16) is governed by the general transformation

$$\int_{A'} f(x,y)\,dx\,dy = \int_{A} f(x,y)\,\frac{\partial(x,y)}{\partial(x_o,y_o)}\,dx_o\,dy_o\,, \qquad \begin{matrix} x = x\,(x_o,y_o) \\ y = y\,(x_o,y_o) \end{matrix}$$

Writing equation (A-16) in accord with the above, we obtain

$$E_{pn} = \int_t \int_A \left[p_r r_i \frac{\partial u_i}{\partial t}\left(\frac{\partial \theta_i}{\partial \theta_o}\frac{\partial z_i}{\partial z_o} - \frac{\partial \theta_i}{\partial z_o}\frac{\partial z_i}{\partial \theta_o} \right) + p_\theta \frac{\partial v_i}{\partial t}\left(\frac{\partial z_i}{\partial \theta_o}\frac{\partial r_i}{\partial z_o} - \frac{\partial z_i}{\partial z_o}\frac{\partial r_i}{\partial \theta_o} \right) \right.$$

$$\left. + p_z r_i \frac{\partial w_i}{\partial t}\left(\frac{\partial r_i}{\partial \theta_o}\frac{\partial \theta_i}{\partial z_o} - \frac{\partial r_i}{\partial z_o}\frac{\partial \theta_i}{\partial \theta_o} \right) \right] d\theta_o\,dz_o\,dt \qquad \text{(A-17)}$$

which is the total normal pressure-loading-force work done on the solid system.

As later consideration of the parallel pressure-loading-force work E_{pp} requires that

$$E_{pp} \equiv 0 \qquad \text{(A-18)}$$

no working analytic expression will be written for it.

A.2 Inertia-Force Energy. We next derive an expression for the inertia-force energy generated in the solid system. We

define ρ to be the uniform, constant mass density of the solid system, and the mass of the differential volume dV is

$$dm = \rho\, dV = \rho r_0\, dr_0\, d\theta_0\, dz_0$$

If

$$\begin{aligned} u &= u(r_0, \theta_0, z_0, t) \\ v &= v(r_0, \theta_0, z_0, t) \\ w &= w(r_0, \theta_0, z_0, t) \end{aligned} \tag{A-19}$$

are the radial, circumferential, and longitudinal displacements, respectively, of a solid system particle, the corresponding differential displacements through which the mass dm moves in time dt are

$$\begin{aligned} du &= \frac{\partial u}{\partial r_0} dr_0 + \frac{\partial u}{\partial \theta_0} d\theta_0 + \frac{\partial u}{\partial z_0} dz_0 + \frac{\partial u}{\partial t} dt \\ dv &= \frac{\partial v}{\partial r_0} dr_0 + \frac{\partial v}{\partial \theta_0} d\theta_0 + \frac{\partial v}{\partial z_0} dz_0 + \frac{\partial v}{\partial t} dt \\ dw &= \frac{\partial w}{\partial r_0} dr_0 + \frac{\partial w}{\partial \theta_0} d\theta_0 + \frac{\partial w}{\partial z_0} dz_0 + \frac{\partial w}{\partial t} dt \end{aligned} \tag{A-20}$$

We elect again to follow the path of a single particle in time so that the Lagrangian differentials

$$dr_0\,,\ d\theta_0\,,\ dz_0$$

vanish, and the particle differential displacements and accelerations may be written as

$$du = \frac{\partial u}{\partial t}\,dt, \qquad dv = \frac{\partial v}{\partial t}\,dt, \qquad dw = \frac{\partial w}{\partial t}\,dt \tag{A-21}$$

$$\frac{d^2u}{dt^2} = \frac{\partial^2 u}{\partial t^2}, \qquad \frac{d^2v}{dt^2} = \frac{\partial^2 v}{\partial t^2}, \qquad \frac{d^2w}{dt^2} = \frac{\partial^2 w}{\partial t^2} \tag{A-22}$$

Let

$$E_{ir}\ ,\ E_{i\theta}\ ,\ E_{iz}$$

be the translational inertia-force energies generated by linear acceleration of the solid system, respectively, in the r, θ, z directions. The corresponding differential quantities may be expressed in accord with D'Alembert's principle as

$$dE_{ir} = \frac{\partial^2 u}{\partial t^2}\ \frac{\partial u}{\partial t}\,\rho r_o\, dr_o\, d\theta_o\, dz_o\, dt$$

$$dE_{i\theta} = \frac{\partial^2 v}{\partial t^2}\ \frac{\partial v}{\partial t}\,\rho r_o\, dr_o\, d\theta_o\, dz_o\, dt \tag{A-23}$$

$$dE_{iz} = \frac{\partial^2 w}{\partial t^2}\ \frac{\partial w}{\partial t}\,\rho r_o\, dr_o\, d\theta_o\, dz_o\, dt$$

We define

$$dE_{iT} = dE_{ir} + dE_{i\theta} + dE_{iz} \tag{A-24}$$

from which

$$E_{iT} = \int_t \int_V (dE_{ir} + dE_{i\theta} + dE_{iz}) \qquad \text{(A-25)}$$

Combining equations (A-23) and (A-25) and simplifying, yields

$$E_{iT} = \rho \int_t \int_V \left(\frac{\partial^2 u}{\partial t^2} \frac{\partial u}{\partial t} + \frac{\partial^2 v}{\partial t^2} \frac{\partial v}{\partial t} + \frac{\partial^2 w}{\partial t^2} \frac{\partial w}{\partial t} \right) dV\, dt \qquad \text{(A-26)}$$

which is the total translational energy of the mass particles of the solid system or the total energy generated as a consequence of linearly accelerating the mass particles.

Let X, Y, and Z be the instantaneous principal axes about which the differential mass dm rotates and

$$I_X , I_Y , I_Z$$

be the moments of inertia of dm. If

$$\alpha = \alpha(r_o , \theta_o , z_o , t)$$

$$\beta = \beta(r_o , \theta_o , z_o , t) \qquad \text{(A-27)}$$

$$\gamma = \gamma(r_o , \theta_o , z_o , t)$$

are angular displacements about X, Y, Z, respectively, the differential angular displacements through which dm moves in time dt are

$$d\alpha = \frac{\partial \alpha}{\partial r_o} dr_o + \frac{\partial \alpha}{\partial \theta_o} d\theta_o + \frac{\partial \alpha}{\partial z_o} dz_o + \frac{\partial \alpha}{\partial t} dt$$

$$d\beta = \frac{\partial \beta}{\partial r_o} dr_o + \frac{\partial \beta}{\partial \theta_o} d\theta_o + \frac{\partial \beta}{\partial z_o} dz_o + \frac{\partial \beta}{\partial t} dt \qquad \text{(A-28)}$$

$$d\gamma = \frac{\partial \gamma}{\partial r_o} dr_o + \frac{\partial \gamma}{\partial \theta_o} d\theta_o + \frac{\partial \gamma}{\partial z_o} dz_o + \frac{\partial \gamma}{\partial t} dt$$

Consistent with the Lagrangian concept of motion, the spatial differentials vanish, and the angular displacements and accelerations are written simply as

$$d\alpha = \frac{\partial \alpha}{\partial t} dt, \; d\beta = \frac{\partial \beta}{\partial t} dt, \; d\gamma = \frac{\partial \gamma}{\partial t} dt \qquad \text{(A-29)}$$

$$\frac{d^2\alpha}{dt^2} = \frac{\partial^2 \alpha}{\partial t^2} \quad , \quad \frac{d^2\beta}{dt^2} = \frac{\partial^2 \beta}{\partial t^2} \quad , \quad \frac{d^2\gamma}{dt^2} = \frac{\partial^2 \gamma}{\partial t^2} \qquad \text{(A-30)}$$

Let

$$E_{iX} \; , E_{iY} \; , E_{iZ}$$

be the rotational inertia-force energies generated by angular acceleration of the solid system mass particles about X, Y, and Z. The corresponding differential quantities may be expressed in accord with D'Alembert's principle as

$$dE_{iX} = I_X \frac{\partial^2 \alpha}{\partial t^2} \frac{\partial \alpha}{\partial t} dt$$

$$dE_{iY} = I_Y \frac{\partial^2 \beta}{\partial t^2} \frac{\partial \beta}{\partial t} dt \qquad \text{(A-31)}$$

$$dE_{i_Z} = I_Z \frac{\partial^2 \gamma}{\partial t^2} \frac{\partial \gamma}{\partial t} dt$$

Determination of the moments of inertia appearing in equations (A-31) requires integration over the differential volume dV. To satisfy this requirement it will suffice to treat the "pie" shaped differential volume of the cylindrical coordinate system as a rectangular parallelepiped with sides

$$r_o\, d\theta_o\,,\ dr_o\,,\ dz_o$$

The moments of inertia may then be easily expressed as

$$I_X = \rho \int_{-\frac{dz_o}{2}}^{\frac{dz_o}{2}} \int_{-\frac{dr_o}{2}}^{\frac{dr_o}{2}} \int_{-\frac{r_o d\theta_o}{2}}^{\frac{r_o d\theta_o}{2}} (Y^2 + Z^2)\, dX\, dY\, dZ$$

$$I_Y = \rho \int_{-\frac{dz_o}{2}}^{\frac{dz_o}{2}} \int_{-\frac{dr_o}{2}}^{\frac{dr_o}{2}} \int_{-\frac{r_o d\theta_o}{2}}^{\frac{r_o d\theta_o}{2}} (X^2 + Z^2)\, dX\, dY\, dZ \qquad \text{(A-32)}$$

$$I_Z = \rho \int_{-\frac{dz_o}{2}}^{\frac{dz_o}{2}} \int_{-\frac{dr_o}{2}}^{\frac{dr_o}{2}} \int_{-\frac{r_o d\theta_o}{2}}^{\frac{r_o d\theta_o}{2}} (X^2 + Y^2)\, dX\, dY\, dZ$$

Performing the indicated integrations, the equations (A-32) yield

$$I_X = \frac{\rho}{12} r_o\, dr_o\, d\theta_o\, dz_o \left[(dr_o)^2 + (dz_o)^2\right]$$

$$I_Y = \frac{\rho}{12} r_o\, dr_o\, d\theta_o\, dz_o \left[(r_o\, d\theta_o)^2 + (dz_o)^2\right] \qquad \text{(A-33)}$$

$$I_Z = \frac{\rho}{12} r_o\, dr_o\, d\theta_o\, dz_o \left[(dr_o)^2 + (r_o\, d\theta_o)^2\right]$$

We define

$$dE_{iR} = dE_{iX} + dE_{iY} + dE_{iZ} \qquad \text{(A-34)}$$

from which

$$E_{iR} = \int_t \int_V (dE_{iX} + dE_{iY} + dE_{iZ}) \qquad \text{(A-35)}$$

Combining equations (A-31), (A-33), and (A-35) and simplifying, we obtain

$$E_{iR} = \frac{\rho}{12} \int_t \int_V \left\{ \frac{\partial^2 \alpha}{\partial t^2} \frac{\partial \alpha}{\partial t} \left[(dr_o)^2 + (dz_o)^2\right] \right.$$

$$+ \frac{\partial^2 \beta}{\partial t^2} \frac{\partial \beta}{\partial t} \left[(r_o\, d\theta_o)^2 + (dz_o)^2\right]$$

$$\left. + \frac{\partial^2 \gamma}{\partial t^2} \frac{\partial \gamma}{\partial t} \left[(dr_o)^2 + (r_o\, d\theta_o)^2\right] \right\} dV\, dt \equiv 0 \qquad \text{(A-36)}$$

which is the total rotational energy of the mass particles of the solid system or the total energy generated as a consequence of angularly accelerating the mass particles. The total energy generated in the solid system as a consequence of mass acceleration is

$$E_i = E_{iT} + E_{iR} = \rho \int_t \int_V \left(\frac{\partial^2 u}{\partial t^2} \frac{\partial u}{\partial t} + \frac{\partial^2 v}{\partial t^2} \frac{\partial v}{\partial t} + \frac{\partial^2 w}{\partial t^2} \frac{\partial w}{\partial t} \right) dV\, dt$$

$$+ \frac{\rho}{12} \int_t \int_V \left\{ \frac{\partial^2 \alpha}{\partial t^2} \frac{\partial \alpha}{\partial t} \left[(dr_0)^2 + (dz_0)^2 \right] + \frac{\partial^2 \beta}{\partial t^2} \frac{\partial \beta}{\partial t} \left[(r_0\, d\theta_0)^2 + (dz_0)^2 \right] \right.$$

$$\left. + \frac{\partial^2 \gamma}{\partial t^2} \frac{\partial \gamma}{\partial t} \left[(dr_0)^2 + (r_0\, d\theta_0)^2 \right] \right\} dV\, dt \qquad \text{(A-37)}$$

In equations (A-36) and (A-37) each component of rotational energy vanishes as a consequence of the first-order differentials squared

$$(dr_0)^2 \,,\ (r_0\, d\theta_0)^2 \,,\ (dz_0)^2$$

tending to zero in the limit as

$$dr_0 \to d\theta_0 \to dz_0 \to 0$$

Important physical interpretations can be imposed upon these squared differentials. It is postulated that

(a) if the inertia energy generated in the solid system is determined by analytic integration, as in equation (A-26), all of the energy will appear in the form of translational energy, the rotational energy being identically zero.

(b) if the inertia energy generated in the solid system is determined by numerical integration, the squared differentials do not tend to zero but must be assigned some constant, incremental, non-zero value. The ratio of rotational inertia-force energy to translational inertia-force energy manifested will be a function of the dimensions assigned to the elemental volume

$$\Delta V = r_o \; \Delta r_o \; \Delta \theta_o \; \Delta z_o$$

As

$$\Delta r_o \rightarrow \Delta \theta_o \rightarrow \Delta z_o \rightarrow 0$$

it is clear that

$$\frac{E_R}{E_T} \rightarrow 0$$

A-3 Potential Energy of Position. The total change in the potential energy of position of the solid system is

$$E_{po} = \rho g \int_t \int_V \frac{\partial w}{\partial t} \, dV \, dt \qquad \text{(A-38)}$$

A-4 Work Done on Atmosphere. To complete our accounting of the energy terms appearing in equation (A-1) we must reflect upon the work E_a required to compress and accelerate the atmosphere external to the solid system. We first recognize for the subject experiments that, during gross motion of the

simulant, pressure acting on the internal wall will always considerably exceed the opposing atmospheric pressure. We also recognize that the density of the simulant greatly exceeds that of the atmosphere. From elementary gas dynamics, then, we can deduce, with no appreciable loss in generality for the subject work, that E_a is a negligibly small quantity. We shall, however, retain the quantity for a later and more appropriate disposition.

A-5 Exact General Equation. Equation (A-1) may be written as

$$E_s = E_p - E_i - E_{po} - E_a = E_{pp} + E_{pn} - E_{iT} - E_{iR} - E_{po} - E_a \qquad \text{(A-39)}$$

which states that the strain energy absorbed by the solid system can be expressed as functions of the dynamic pressure bearing upon the internal and external walls of the system, the mass motion of the system, and the mass motion of the atmosphere external to the system. Combining equations (A-17), (A-37), (A-38), and (A-39), we obtain

$$E_s = E_{pp} + \int_t \int_A \left[p_r r_i \frac{\partial u_i}{\partial t} \left(\frac{\partial \theta_i}{\partial \theta_o} \frac{\partial z_i}{\partial z_o} - \frac{\partial \theta_i}{\partial z_o} \frac{\partial z_i}{\partial \theta_o} \right) + p_\theta \frac{\partial v_i}{\partial t} \left(\frac{\partial z_i}{\partial \theta_o} \frac{\partial r_i}{\partial z_o} - \frac{\partial z_i}{\partial z_o} \frac{\partial r_i}{\partial \theta_o} \right) \right.$$

$$\left. + p_z r_i \frac{\partial w_i}{\partial t} \left(\frac{\partial r_i}{\partial \theta_o} \frac{\partial \theta_i}{\partial z_o} - \frac{\partial r_i}{\partial z_o} \frac{\partial \theta_i}{\partial \theta_o} \right) \right] d\theta_o dz_o dt - \rho \int_t \int_V \left(\frac{\partial^2 u}{\partial t^2} \frac{\partial u}{\partial t} + \frac{\partial^2 v}{\partial t^2} \frac{\partial v}{\partial t} + \frac{\partial^2 w}{\partial t^2} \frac{\partial w}{\partial t} \right) dV dt$$

$$- E_a - \frac{\rho}{12} \int_t \int_V \left\{ \frac{\partial^2 \alpha}{\partial t^2} \frac{\partial \alpha}{\partial t} \left[(dr_o)^2 + (dz_o)^2 \right] + \frac{\partial^2 \beta}{\partial t^2} \frac{\partial \beta}{\partial t} \left[(r_o d\theta_o)^2 + (dz_o)^2 \right] \right.$$

$$\left. + \frac{\partial^2 \gamma}{\partial t^2} \frac{\partial \gamma}{\partial t} \left[(dr_o)^2 + (r_o d\theta_o)^2 \right] \right\} dV dt - \rho g \int_t \int_V \frac{\partial w}{\partial t} dV dt \qquad \text{(A-40)}$$

Equation (A-40) is the general strain energy equation of dynamic equilibrium for a vessel subjected to internal dynamic loading.

It seems in order at this time to make a further statement as to the relation between the general strain energy equation and correlative experimental work. The mathematical and physical formulation of the strain energy equation is not a theory designed for experimental confirmation; but rather the principal analytic tool through which experimental work can be utilized in assessing the effectiveness of strain-energy absorption as a means for increasing the containment potential of reactor vessels. This assessment can be expressed as the partition of mechanical (strain energy) and non-mechanical energy resulting from excursion-type energy releases in simulated reactor vessels. With the total energy input known, the general strain energy equation provides the means for obtaining the desired partition without further knowledge as to the disposition of non-mechanical energy.

A-6 Simplified Working Equations. The general equation (A-40) is greatly simplified for the case of the homogeneous and isotropic, right-circular cylinder closed with rigid, radial constraints at the ends. The conditions of circularity, cylindricality, and rightness of the vessel provide that the spatial limits of integration be constant. If the loading is rotationally symmetric, the structural response of the homogeneous, isotropic, solid system will be rotationally symmetric with the result that

$$v = p_\theta = E_{pp} = \frac{\partial r_i}{\partial \theta_o} = \frac{\partial \theta_i}{\partial z_o} = \frac{\partial z_i}{\partial \theta_o} = \frac{\partial \beta}{\partial t} = \frac{\partial \gamma}{\partial t} = 0 \qquad \text{(A-41)}$$

and

$$\frac{\partial \theta_i}{\partial \theta_o} = 1 \qquad \text{(A-42)}$$

It may also be shown, for the subject work, that the change in the energy of position of the solid system is negligibly small relative to the accompanying generation of pressure-force and inertia-force energies. With respect to the total energy absorbed at any time t, we can impose the condition

$$\rho g \int_t \int_V \frac{\partial w}{\partial t} \, dV \, dt = 0 \qquad \text{(A-43)}$$

with a loss in accuracy of less than one-thousandth of one per cent. We also elect at this time to take

$$E_a = 0 \qquad \text{(A-44)}$$

which elementary considerations indicate will likewise result in a loss in accuracy not greater than one-thousandth of one per cent.

Imposing conditions (A-41), (A-42), (A-43), and (A-44) on the general equation (A-40), we obtain

$$E_s = \int_t \int_A \left(p_r r_i \frac{\partial u_i}{\partial t} \frac{\partial z_i}{\partial z_o} + p_z r_i \frac{\partial w_i}{\partial t} \frac{\partial r_i}{\partial z_o} \right) d\theta_o \, dz_o \, dt$$

$$-\rho \int_t \int_V \left(\frac{\partial^2 u}{\partial t^2} \frac{\partial u}{\partial t} + \frac{\partial^2 w}{\partial t^2} \frac{\partial w}{\partial t} \right) r_o \, dr_o \, d\theta_o \, dz_o \, dt$$

$$-\frac{\rho}{12} \int_t \int_V \frac{\partial^2 \alpha}{\partial t^2} \frac{\partial \alpha}{\partial t} \left[(dr_o)^2 + (dz_o)^2 \right] r_o \, dr_o \, d\theta_o \, dz_o \, dt \qquad \text{(A-45)}$$

which is the strain energy absorbed by a right-circular, homogeneous, isotropic cylinder subjected to internal, rotationally symmetric, dynamic loading. To express explicitly the integration limits of equation (A-45), it is necessary to write distinct integrations over the primary and secondary systems. We are particularly interested in the case for which the secondary system consists of right discs fitted concentrically with the primary system. If the closures are not stressed beyond the elastic limit during loading of the cylinder unit, we can, with a negligible loss in accuracy, assume that the dimensions of the discs remain constant during the loading phenomenon. Imposing upon equation (A-45) the conditions that the internal face of the lower closure be constrained to lie in the r, θ, z = 0 plane and that the dimensions of both closures remain constant, we obtain

$$E_s = \int_{t_o}^{t_1} \int_0^{H_o} \int_0^{2\pi} \left(p_r r_i \frac{\partial u_i}{\partial t} \frac{\partial z_i}{\partial z_o} + p_z r_i \frac{\partial w_i}{\partial t} \frac{\partial r_i}{\partial z_o} \right) d\theta_o \, dz_o \, dt$$

$$-\rho \int_{t_o}^{t_1} \int_0^{H_o} \int_0^{2\pi} \int_{r_{io}}^{r_{eo}} \left(\frac{\partial^2 u}{\partial t^2} \frac{\partial u}{\partial t} + \frac{\partial^2 w}{\partial t^2} \frac{\partial w}{\partial t} \right) r_o \, dr_o \, d\theta_o \, dz_o \, dt$$

$$-\frac{\rho}{12}\int_{t_o}^{t_1}\int_{0}^{H_o}\int_{0}^{2\pi}\int_{r_{io}}^{r_{eo}}\frac{\partial^2\alpha}{\partial t^2}\,\frac{\partial\alpha}{\partial t}\left[(dr_o)^2+(dz_o)^2\right]r_o\,dr_o\,d\theta_o\,dz_o\,dt$$

$$+\int_{t_o}^{t_1}\int_{0}^{2\pi}\int_{0}^{r_{io}}p_z r_o\,\frac{\partial w_i}{\partial t}\,dr_o\,d\theta_o\,dt-\rho V_2\int_{0}^{t_1}\frac{\partial^2 w}{\partial t^2}\,\frac{\partial w}{\partial t}\,dt \qquad \text{(A-46)}$$

where

H_o .... is original length of primary system between closures, inches

r_{io} ... is original internal radius of primary system, inches

r_{eo} ... is original external radius of primary system, inches

t_o .... is time at $t = t_o = 0$

t_1 .... is time subsequent to $t = t_o$, milliseconds

V_2 .... is volume of upper closure of secondary system, cubic inches

If both of the closures, which constitute the secondary system, are rigidly constrained, their pressure and inertia-force energies vanish, we take

$$\frac{\partial z_i}{\partial z_o}=1 \qquad \text{(A-47)}$$

and equation (A-46) reduces to

$$E_s=\int_{t_o}^{t_1}\int_{0}^{H_o}\int_{0}^{2\pi}\left(p_r r_i\,\frac{\partial u_i}{\partial t}+p_z r_i\,\frac{\partial w_i}{\partial t}\,\frac{\partial r_i}{\partial z_o}\right)d\theta_o\;dz_o\,dt$$

$$-\rho \int_{t_o}^{t_1} \int_0^{H_o} \int_0^{2\pi} \int_{r_{io}}^{r_{eo}} \left(\frac{\partial^2 u}{\partial t^2} \frac{\partial u}{\partial t} + \frac{\partial^2 w}{\partial t^2} \frac{\partial w}{\partial t} \right) r_o \, dr_o \, d\theta_o \, dz_o \, dt$$

$$-\frac{\rho}{12} \int_{t_o}^{t_1} \int_0^{H_o} \int_0^{2\pi} \int_{r_{io}}^{r_{eo}} \frac{\partial^2 \alpha}{\partial t^2} \frac{\partial \alpha}{\partial t} \left[(dr_o)^2 + (dz_o)^2 \right] r_o \, dr_o \, d\theta_o \, dz_o \, dt \qquad \text{(A-48)}$$

If equation (A-40) is integrated over the entire range

$$t_o \text{ to } t_a = (t_1)_{\text{velocity}=0}$$

i.e., the time required to accelerate and decelerate all particles of the solid system from and to a state of rest, then the total work done upon the system in accelerating it must be precisely equivalent to the kinetic energy relinquished by the system during deceleration. The structural response significance of this statement is that the inertia forces oppose the pressure forces and decrease the internal stresses in the system during acceleration and, conversely, assist the pressure forces and increase the internal stresses during deceleration. The net effect of this phenomenon is such that with respect to equation (A-40), the inertia terms E_i vanish. It follows that we can conveniently reduce equations (A-46) and (A-48), respectively, to

$$E_{sa} = \int_{t_o}^{t_a} \int_0^{H_o} \int_0^{2\pi} \left(p_r r_i \frac{\partial u_i}{\partial t} \frac{\partial z_i}{\partial z_o} + p_z r_i \frac{\partial w_i}{\partial t} \frac{\partial r_i}{\partial z_o} \right) d\theta_o \, dz_o \, dt$$

$$+ \int_{t_o}^{t_a} \int_0^{2\pi} \int_0^{r_{io}} p_z r_o \frac{\partial w_i}{\partial t} \, dr_o \, d\theta_o \, dt \qquad \text{(A-4}$$

for the case of constraining the lower closure and

$$E_{sa}=\int_{t_o}^{t_a}\int_{0}^{H_o}\int_{0}^{2\pi}\left(p_r r_i \frac{\partial u_i}{\partial t} + p_z r_i \frac{\partial w_i}{\partial t}\frac{\partial r_i}{\partial z_o}\right) d\theta_o\, dz_o\, dt \qquad \text{(A-50)}$$

for the case of constraining both closures.

With respect to the general energy equation, a single important simplifying assumption remains to be considered. Let the loading generator be a circular cylinder with length equal to and longitudinal axis common to the primary system. Let this generator be capable of delivering the desired energy flux to its immediate external environment in a rotationally symmetric pattern. If the annular space between the external wall of the generator and the internal walls of the primary system is filled with a liquid, it is assumed for the range

$$\frac{1}{10}\ \text{millisecond} \le t_a \le 100\ \text{milliseconds}$$

that the loading is delivered normal to the walls of the solid system and that

$$p_r = p_\theta = p_z = p = p(r_i, z_i, t) \qquad \text{(A-51)}$$

The magnitude of the error incurred by this assumption has not been evaluated, but it is believed to be small. Imposing the condition (A-51) on equations (A-49) and (A-50), respectively, we obtain

$$E_{so} = \int_{t_o}^{t_a} \int_{0}^{H_o} \int_{0}^{2\pi} p r_i \left(\frac{\partial u_i}{\partial t} \frac{\partial z_i}{\partial z_o} + \frac{\partial w_i}{\partial t} \frac{\partial r_i}{\partial z_o} \right) d\theta_o \, dz_o \, dt$$

$$+ \int_{t_o}^{t_a} \int_{0}^{2\pi} \int_{0}^{r_{io}} p r_o \frac{\partial w_i}{\partial t} \, dr_o \, d\theta_o \, dt \qquad \text{(A-52)}$$

for the case of completely constraining the lower closure, and

$$E_{so} = \int_{t_o}^{t_a} \int_{0}^{H_a} \int_{0}^{2\pi} p r_i \left(\frac{\partial u_i}{\partial t} + \frac{\partial w_i}{\partial t} \frac{\partial r_i}{\partial z_o} \right) d\theta_o \, dz_o \, dt \qquad \text{(A-53)}$$

for the case of completely constraining both closures. Equation (A-52) constitutes the basic analytic working expression. It may be seen from an examination of this equation that its solution requires experimental determination of

(a) the pressure bearing upon every internal differential area of the solid system at time t, i.e.,

$$p = p(r_i , z_i , t), \qquad t_o \le t \le t_o \qquad \text{(A-54)}$$

(b) the radial and longitudinal coordinates of every internal differential area of the solid system at time t, i.e.,

$$r_i = r_i(z_o , t)$$

$$z_i = z_i(z_o , t) \qquad , t_o \le t \le t_a \qquad \text{(A-55)}$$

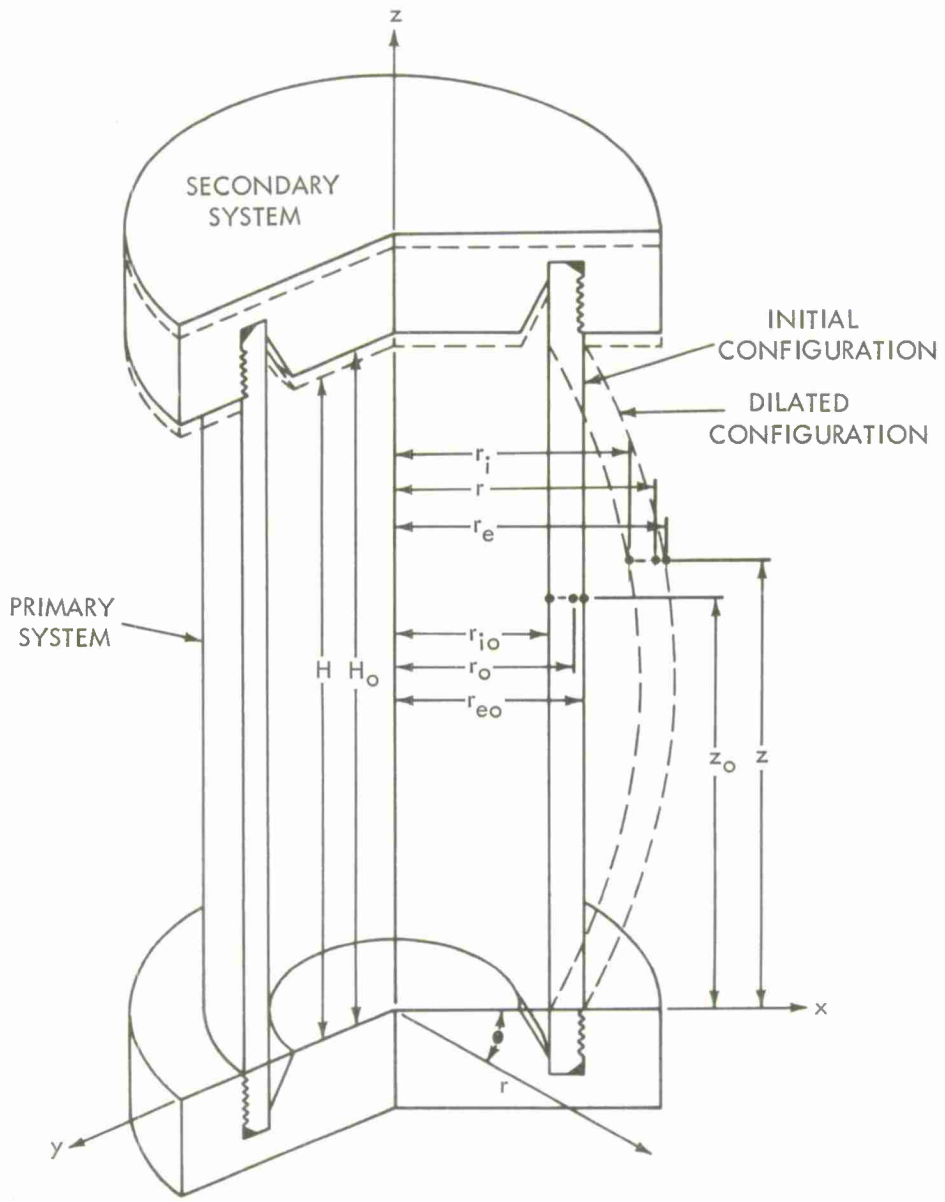

FIG. A-1 SECTIONAL VIEW OF TYPICAL REACTOR SIMULANT DEFINING COORDINATES OF ORIGINAL AND DILATED CONFIGURATIONS

APPENDIX B

STRAIN PATTERNS AROUND AN APERTURE AND NOZZLE

This appendix presents strain data that provide insight into the design of nozzle junctions. The deformed vessels shown in Figure 7.6 were accurately measured to determine the internal radii and wall thicknesses in the regions of discontinuity. Figures B-1 and B-2 give these data in the form of graphical profiles.

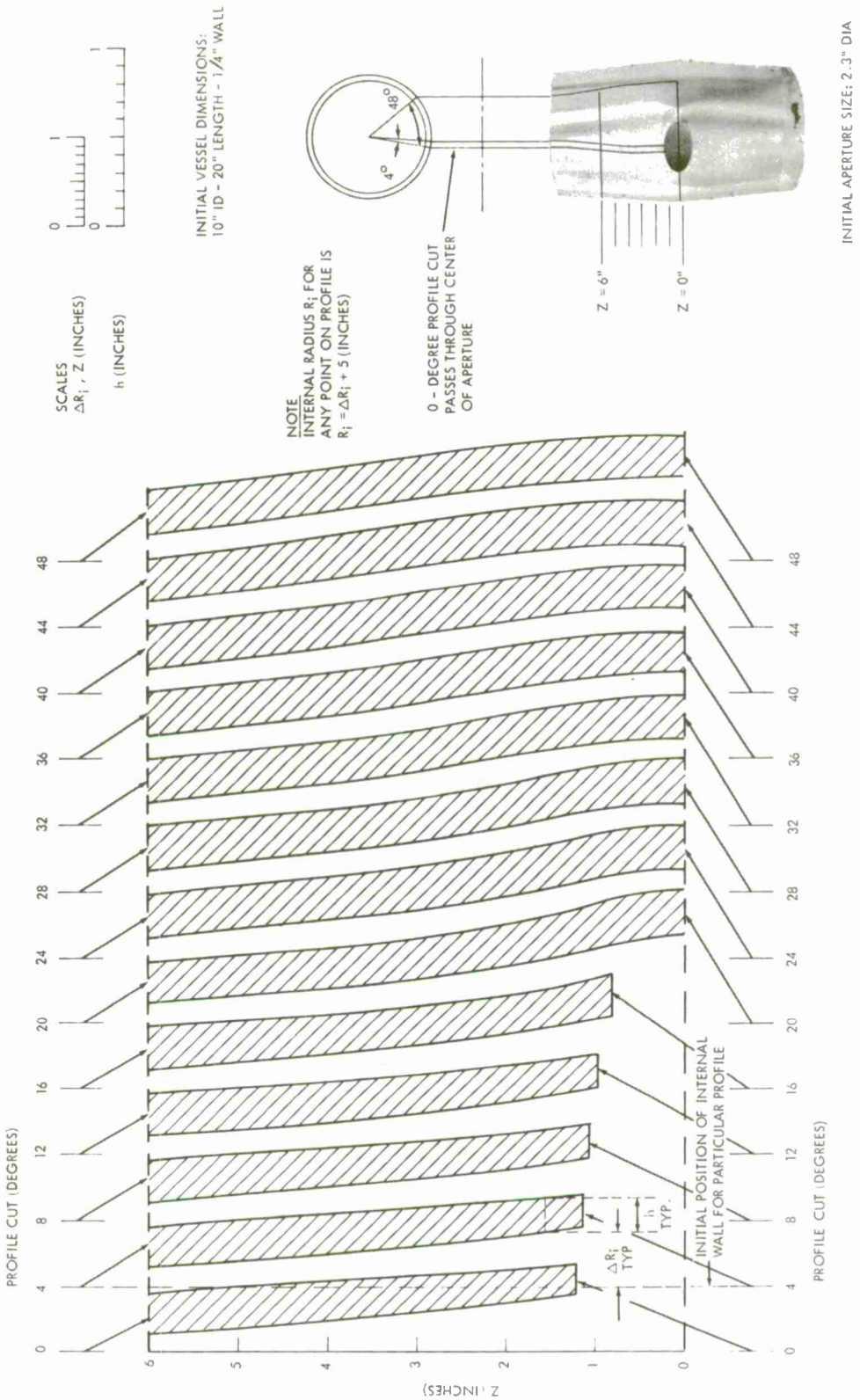

FIG. B - 1 WALL PROFILES OF EXPLOSIVELY DILATED VESSEL WITH UNCONSTRAINED APERTURE

SCALES
ΔR_i , Z (INCHES)

h (INCHES)

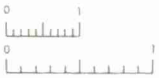

INITIAL VESSEL DIMENSIONS:
10" ID - 20" LENGTH - 1/4" WALL

NOTE
INTERNAL RADIUS R_i FOR ANY POINT ON PROFILE IS
$R_i = \Delta R_i + 5$ (INCHES)

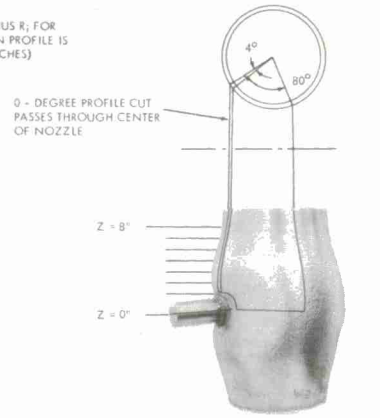

INITIAL NOZZLE DIAMETER: 2.3"

FIG. B - 2 WALL PROFILES OF EXPLOSIVELY DILATED VESSEL WITH SINGLE NOZZLE

NOLTR 63-140

APPENDIX C

CALCULATION OF EMBRYONIC FUNCTIONS, Ψ_1 AND Ψ_2

Table C-1 presents calculations for Ψ_1 and Ψ_2 for all experiments given in Table 7.1 for which containment occurred. Nomenclature and units are compatible with equation (8.1), and tests have been grouped according to material. Average mechanical and physical properties were determined for each material based on certified standard tensile tests (see section 7.1); the form in which they were used in equation (8.1) is presented below.

Type Material	Stress σ_t (psi)	Weight Density (lb/ft3)
304 stainless steel (welded plate)	43,000 + 151,700ϵ	490
304 stainless steel (centrifugally cast)	30,000 + 123,700ϵ	490
410 stainless steel annealed (centrifugally cast)	66,000 + 203,200ϵ	490
410 stainless steel hardened (centrifugally cast)	151,500 + 778,500ϵ	490
212 flange steel (welded plate)	46,500 + 186,000ϵ	490
1020 mild steel (welded plate)	42,000 + 150,000ϵ	490
6061 - T6 Aluminum (extruded)	40,000 + 78,000ϵ	170

Table C-2 presents calculations for ξ, equation (8.5).

TABLE C-1

CALCULATIONS FOR Ψ_1 AND Ψ_2 FROM EQUATION (8.1)

TEST * NO.	ID (in)	WALL THICK. (in)	CHARGE WEIGHT (gm)	TERMINAL RADIAL STRAIN (in/in)	$\Psi_1\ \Psi_2 \times 10^5$ EQ. (8.1)	R_i/h_o (ft/ft)	$\Psi_2 \times 10^5$ EQ. (8.2)	Ψ_1 ($\Psi_1\ \Psi_2/\ \Psi_2$)	STRAIN RATE EQ. (8.7) (in/in/sec)	DEVIATION ** OF CHARGE WEIGHT (%)	REMARKS ****
					304 STAINLESS STEEL, WELDED-PLATE CYLINDERS						
1	5	0.060	8.0	0.289	8.39	41.7	8.29	1.012	2110	- 0.7	
5	5	0.118	12.0	0.195	6.50	21.2	5.89	1.104	1860	- 8.3	1
6	5	0.118	18.0	0.271	6.87	21.2	5.89	1.166	2420	- 9.3	1
7	5	0.118	22.0	0.331	6.64	21.2	5.89	1.127	2780	- 5.7	1
8	5	0.118	22.0	0.349	6.12	21.2	5.89	1.039	2780	+ 0.3	
9	5	0.118	23.0	0.357	6.27	21.2	5.89	1.065	2840	- 1.1	
12	5	0.253	50.1	0.295	4.90	9.9	4.57	1.072	2680	- 2.3	
13	5	0.253	56.1	0.338	4.63	9.9	4.57	1.013	2890	+ 3.9	
16	10	0.118	80.2	0.366	8.18	42.4	8.37	0.977	1230	- 4.1	
17	10	0.118	100.8	0.434	8.47	42.4	8.37	1.012	1440	- 4.8	
18	10	0.118	120.1	0.506	8.33	42.4	8.37	0.995	1610	- 2.4	
19	10	0.118	140.0	0.568	8.44	42.4	8.37	1.008	1790	- 2.2	
20	10	0.253	160.0	0.280	6.55	19.8	5.73	1.143	1240	-14.7	1
21	10	0.253	180.0	0.315	6.41	19.8	5.73	1.119	1340	-12.4	1
22	10	0.253	200.0	0.348	6.33	19.8	5.73	1.105	1440	-10.9	1
23	10	0.253	210.2	0.383	5.83	19.8	5.73	1.017	1490	- 4.9	
24	10	0.253	229.3	0.425	5.54	19.8	5.73	0.967	1580	- 0.8	
25	10	0.253	275.5	0.487	5.68	19.8	5.73	0.991	1780	- 0.9	
29	10	0.515	669.3	0.512	3.92	9.7	4.54	0.863	1870	+10.5	
32	20	0.253	280.8	0.180	6.71	39.5	8.03	0.836	340	- 6.6	
36	20	0.515	1702.6	0.412	5.09	19.4	5.68	0.896	750	- 3.1	
37	20	0.515	2103.1	0.523	4.58	19.4	5.68	0.806	860	+ 6.6	
39	20	0.515	2248.5	0.529	4.92	19.4	5.68	0.866	900	+ 1.2	
41	20	1.030	1000.0	0.110	3.94	9.7	4.54	0.868	300	-10.7	
42	20	1.030	2501.0	0.265	3.99	9.7	4.54	0.879	560	- 5.1	
					304 STAINLESS STEEL, CENTRIFUGALLY-CAST CYLINDERS						
46	5	0.125 ***	16.0	0.295	6.07	20.0	5.75	1.056	2170	- 3.6	
47	5	0.125 ***	18.0	0.352	5.39	20.0	5.75	0.937	2330	+ 6.3	
50	5	0.250 ***	50.1	0.375	4.54	10.0	4.58	0.991	2720	+ 3.9	
51	5	0.250 ***	50.5	0.354	5.03	10.0	4.58	1.098	2730	- 3.8	
53	5	0.250	58.1	0.425	4.51	10.0	4.58	0.985	3000	+ 5.4	
54	5	0.250	70.2	0.461	5.09	10.0	4.58	1.111	3400	- 2.2	
55	5	0.250	75.3	0.497	4.92	10.0	4.58	1.074	3560	+ 0.6	
58	5	0.125 ***	19.0	0.370	5.33	20.0	5.75	0.927	2410	+ 7.7	4
59	10	0.250	189.8	0.463	4.99	20.0	5.75	0.868	1400	+ 6.5	
63	10	0.500	461.0	0.421	4.54	10.0	4.58	0.991	1490	- 3.0	
64	10	0.500	481.2	0.447	4.36	10.0	4.58	0.952	1540	+ 0.5	

TABLE C-1 (cont'd)

410 STAINLESS STEEL, CENTRIFUGALLY-CAST CYLINDERS

ANNEALED											
67	5	0.250	25.3	0.118	4.93	10.0	4.58	1.076	1720	- 7.3	
68	5	0.250	28.0	0.131	4.94	10.0	4.58	1.079	1840	- 6.8	
69	5	0.250	28.0	0.132	4.89	10.0	4.58	1.068	1840	- 6.0	
70	5	0.250	28.0	0.141	4.49	10.0	4.58	0.980	1840	+ 0.2	
73	10	0.250	110.2	0.173	5.58	20.0	5.75	0.970	980	- 6.0	
74	10	0.250	130.1	0.220	5.01	20.0	5.75	0.871	1090	+ 3.0	
75	10	0.250	160.6	0.258	5.29	20.0	5.75	0.920	1260	+ 0.7	
76	10	0.250	180.4	0.292	5.17	20.0	5.75	0.899	1360	+ 3.2	2
77	10	0.250	199.6	0.341	4.67	20.0	5.75	0.812	1450	+12.3	2
78	10	0.250	220.5	0.364	4.83	20.0	5.75	0.840	1550	+10.2	2
80	10	0.500	210.0	0.125	4.81	10.0	4.58	1.050	880	-12.4	
81	10	0.500	230.4	0.147	4.41	10.0	4.58	0.963	940	- 6.0	
HARDENED											
84	5	0.250	22.0	0.045	5.17	10.0	4.58	1.129	1570	-11.4	
212 FLANGE STEEL, WELDED-PLATE CYLINDERS											
86	10	0.515	200.0	0.154	4.19	9.7	4.54	0.923	830	- 4.3	
87	10	0.515	229.3	0.183	3.94	9.7	4.54	0.868	910	+ 1.3	
90	20	0.515	902.7	0.242	4.28	19.4	5.68	0.754	490	+ 5.0	
91	20	0.515	1103.0	0.300	4.04	19.4	5.68	0.711	560	+11.3	2
92	20	0.515	1200.3	0.328	3.93	19.4	5.68	0.692	590	+14.3	2
95	20	1.030	2251.0	0.230	3.72	9.7	4.54	0.819	520	- 0.8	
MILD STEEL, WELDED-PLATE CYLINDERS											
98	10	0.253	140.0	0.271	5.85	19.8	5.73	1.021	1140	- 7.8	1,3
6061 - T6 ALUMINUM, EXTRUDED CYLINDERS											
101	15	0.500	60.0	0.0553	5.55	15.0	5.18	1.071	450	-20.0	1
102	15	0.500	85.2	0.0855	5.42	15.0	5.18	1.046	570	-16.4	1

NOTES

* Order of presentation in this table is same as Table 7.1, but only tests resulting in containment are listed here.

** This colum gives deviations of predicted charge weight (equation (9.1)) from experimental results. Positive deviations indicate predicted charge weights greater than experimental values; conversely for negative deviations.

*** Experiments were conducted in vessels with rigid end closures.

**** The following code is used for remarks.

1 ---- no certified mechanical properties available for this vessel

2 ---- strains exceeded sfatic maximum strains of tensile specimens

3 ---- explosion resulted in marginal rupture

4 ---- vessel was 8 R_i in length (20 inches)

TABLE C-2

CALCULATIONS FOR ξ FROM EQUATION (8.5)

TEST* NO.	ID (in)	WALL THICK. (in)	CHARGE WEIGHT (gm)	INITIAL STRAIN RATE (in/in/sec)	ξ EQ. (8.5)	R_i / h_o (ft/ft)	DEVIATION ** OF STRAIN RATE (%)
			304 STAINLESS STEEL, WELDED-PLATE CYLINDERS				
2	5	0.060	9.0	2070	3.34	41.7	+10.2
9	5	0.118	23.0	2850	2.27	21.2	+ 0.4
13	5	0.253	56.1	2900	1.84	9.9	+ 0.0
18	10	0.118	120.1	1570	3.14	42.4	+ 3.0
22	10	0.253	200.0	1300	2.45	19.8	+10.9
25	10	0.253	275.5	1570	2.51	19.8	+13.6
26	10	0.253	325.4	1870	2.36	19.8	+ 6.8
28	10	0.253	359.8	1940	2.43	19.8	+10.0
29	10	0.515	669.3	1640	2.08	9.7	+13.7
31	10	0.515	775.5	1970	1.91	9.7	+ 4.4
33	20	0.253	477.8	568	2.53	39.5	-14.0
34	20	0.253	960.0	790	2.90	39.5	- 1.4
35	20	0.253	960.8	805	2.85	39.5	- 3.1
			304 STAINLESS STEEL, CENTRIFUGALLY-CAST CYLINDERS				
59	10	0.250	189.8	1450	2.15	20.0	- 3.2
60	10	0.250	189.9	1490	2.09	20.0	- 5.9
64	10	0.500	481.2	1810	1.56	10.0	-15.2
			410 STAINLESS STEEL, CENTRIFUGALLY-CAST CYLINDERS				
			ANNEALED				
69	5	0.250	28.0	1860	1.82	10.0	- 1.1
75	10	0.250	160.6	1310	2.13	20.0	- 4.1
81	10	0.500	230.4	950	1.82	10.0	- 1.1
			212 FLANGE STEEL, WELDED PLATE CYLINDERS				
87	10	0.515	229.3	867	1.92	9.7	+ 4.9
92	20	0.515	1200.3	670	1.93	19.4	-11.9
93	20	0.515	1351.5	650	2.15	19.4	- 1.8
			MILD STEEL, WELDED PLATE CYLINDERS				
98	10	0.253	140.0	1010	2.48	19.8	+12.2

NOTES

* Order of presentation in this table is same as Table 7.1.

** This column gives deviations of predicted strain rates (equation (8.7)) from experimental results (column 5). Positive deviations indicate predicted strain rates greater than experimental values; conversely for negative deviations.

APPENDIX D

HEAT-SINK RATIONALE

In Appendix G of reference (1), equations were developed for a hypothetical model that prescribes the magnitude of the peak internal blast pressure resulting from a TNT explosion. This pressure, as defined earlier in the text, is the quasi-static equilibrium pressure that exists in a closed chamber after decay of the shock wave. The reference (1) analysis is reproduced here, and its relation to slower release rates is discussed.

D-1 Hypothetical Model. Since a simple quantitative analysis of an explosion in a closed vessel with extensive liquid and/or metal heat sinks is not feasible, the following hypothetical model is entertained.

(a) A closed vessel contains a charge, heat sinks, and nitrogen gas with the following initial conditions.

Charge:	volume V_c and temperature $T_c = 25^oC$
Heat sinks:	temperature T_o
Nitrogen:	pressure $P_o = 14.7$ psia, volume V_o, and temperature T_o

(b) The charge is detonated in a manner such that the product gases are contained within the solid charge volume V_c, the total heat of detonation is absorbed and stored for later distribution, and the temperature of the product gases becomes $T_c = 25^oC$. The total heat of detonation or explosion energy E_T momentarily stored is

$$E_T = Wh \qquad (D-1)$$

where

W . . . . is charge weight, gm

h . . . . is heat of detonation, cal/gm

Conditions of the products at this point are pressure P_c, volume V_c, temperature T_c, and they are related by the perfect gas law

$$P_c V_c = n_c R T_c$$

where

n_c . . . . is moles of gas released by explosive

R . . . . is universal gas constant

(c) Now, part of the explosion energy E_T is given back to the product gases to raise their temperature to that of the surroundings T_o, or

$$E_1 = n_c c_v (T_o - T_c) \qquad \text{(D-2)}$$

where

E_1 . . . . is energy required to raise product gas temperature to T_o

c_v . . . . is specific heat at constant volume of charge products

(d) The charge products and the initial nitrogen gas are mixed in an isothermal process for which the mixed-gas pressure P_1 is

$$P_1 = P_o \left(\frac{n_1}{n_N} \right) \left(\frac{V_o}{V_1} \right)$$

where

n_1 . . . . is sum of moles of initial N_2 and charge product gas

n_N . . . . is moles of initial N_2

V_1 . . . . is sum of initial N_2 volumes and charge volume

(e) A portion of the explosion energy, in the amount E_2, is now released as a shock wave which deforms the reactor vessel wall. This deformation provides an additional volume V_2 into which the mixed gases can expand, so that the final volume V_F becomes

$$V_F = V_o + V_c + V_2$$

the pressure becomes

$$P_2 = P_1 \left(\frac{V_1}{V_F} \right) = P_o \left(\frac{n_1}{n_N} \right) \left(\frac{V_o}{V_F} \right) \qquad \text{(D-3)}$$

and the temperature is still T_o.

(f) Energy is now given to the various heat sinks in the amount E_3. Here the assumption is made that the heat sinks are sufficiently large to absorb the energy E_3 without a significant rise in temperature. Thus the mixed gas temperature still remains essentially at T_o.

(g) The unused explosion energy E_R at this point is

$$E_R = E_T - E_1 - E_2 - E_3 \qquad \text{(D-4)}$$

This remaining energy is given to the mixed gases to raise the gas pressure to a new value P_p (peak internal blast pressure). If the compressibility of the heat sinks is neglected, then

$$P_p = \frac{E_R\ (k - 1)}{V_F} + P_2$$

where k is the ratio of specific heat at constant pressure to the specific heat at constant volume. Substitution of equations (D-1), (D-2), (D-3), and (D-4) into this expression yields

$$P_p = P_o \left(\frac{n_1}{n_N} \right) \left(\frac{V_o}{V_F} \right) - \frac{n_c R}{V_F} \ (T_o - T_c)$$

$$+ \frac{(k - 1)}{V_F} \ (Wh - E_2 - E_3) \qquad \text{(D-5)}$$

Equation (D-5) prescribes the peak internal blast pressure for the hypothetical model.

D-2 Special Cases. If it is assumed that the liquid and/or metal heat sinks are sufficiently large to absorb all of the energy released by the explosive, then

$$\frac{(k - 1)}{V_F} \ (Wh - E_2 - E_3) - \frac{n_c R}{V_F} \ (T_o - T_c) = 0$$

and (D-5) reduces to

$$P_p = P_o \left(\frac{n_1}{n_N} \right) \left(\frac{V_o}{V_F} \right) \qquad \text{(D-6)}$$

Experimental results with the water, molten sodium, and/or metal heat sink models presented in reference (1) exhibit good agreement with equation (D-6).

For marginal containment in reactor vessels, the charge volume V_c is usually very small compared with the sum of the initial gas volume V_o and the deformation volume V_2; for this case

$$V_F \approx V_o + V_2$$

Conversely, the gas released by the charge n_c is usually very large compared with the amount of initial gas n_N; this yields

$$n_1 \approx n_c$$

In view of the above simplifications, equation (D-6) can be approximated by

$$P_p = P_o \left(\frac{n_c}{n_N} \right) \left(\frac{V_o}{V_o + V_2} \right) \qquad \text{(D-7)}$$

Since n_c is proportional to the explosive charge weight W, and since the perfect gas law gives

$$\frac{P_o V_o}{n_N} = R T_o$$

equation (D-7), for a given vessel, can be expressed as

$$P_p \propto T_o W \qquad \text{(D-8)}$$

D-3 Slower Release Rates. The above analysis was based on a TNT explosion. Entertain now a release rate slower than that of TNT. The assumptions are that the non-explosive charge weight W would be sufficient to produce marginal containment, that the heat sinks would be sufficiently large to absorb energy without a significant rise in temperature, and that

$$V_c << V_o + V_2$$

Although most reactors possess the extensive metal and coolant heat sinks in the region of the core necessary to satisfy the above assumption on energy absorption, it is shown in reference (1) that liquid coolant or metal heat sinks separately may not be sufficient.

For marginal containment, the vessel deformation pattern of slow releases would be similar to that produced by TNT in a liquid filled vessel; the deformation volumes V_2 would be equivalent. The slower release would have to be accompanied by energy in the amount E_2 to produce this deformation. The event time would be longer for the slower rate and would allow more time for heat transfer. Since in the short event time of the TNT release all of the remaining energy is transferred to the heat sinks, certainly no less could be expected for the slower release.

From an examination of the above conditions in light of the preceding analysis, it is hypothesized that equation (D-8) adequately prescribes the equilibrium pressure in a reactor vessel with extensive heat sinks irrespective of the energy release rate.

DISTRIBUTION

	Copies
Aerojet-General Corporation P. O. Box 296 Azusa, California (Attn: Myra T. Grenier, Librarian)	1
Aerojet-General Nucleonics P. O. Box 78 San Ramon, California 94583 (Attn: Barbara Probert)	1
Aeronautical Systems Division Wright-Patterson Air Force Base, Ohio 45433 (Attn: Augustus Daniels, SEPRR)	2
Commander School of Aerospace Medicine Aerospace Medical Division Brooks Air Force Base, Texas 78235 (Attn: Chief, Bionucleonics Dept)	1
Detachment 4, Directorate of Armament Development Research and Technology Division (AFSC) United States Air Force Eglin Air Force Base, Florida 32542 (Attn: R. Lenton Hill, ATWR)	1
Air Force Cambridge Research Laboratories Laurence G. Hanscom Field Bedford, Massachusetts 01731 (Attn: CRMXLR, Res. Library, Stop 29)	1
Air Force Institute of Technology Detachment No. 5 Malmstrom Air Force Base, Montana (Attn: Library)	1
Air Force Institute of Technology Library Air University, USAF Wright-Patterson Air Force Base, Ohio 45433 (Attn: AFIT-LIB)	1
Lowry Technical Training Center Lowry Air Force Base, Colorado 80230 (Attn: Department of Weapons Training)	1
Headquarters U. S. Air Force (AFMSPA) Special Weapons Defense Officer Washington, D. C. 20333	1

DISTRIBUTION

	Copies
Air Force Weapons Laboratory Kirtland Air Force Base, New Mexico (Attn: M. F. Canova, WLL)	2
(Attn: Capt. O. W. Lyle, Jr. WLRPE)	1
Allied Chemical and Dye Corp. General Chemical Division 40 Rector Street New York 6, New York (Attn: Mr. K.R. Osborn,Manager Industrial Development)	1
Allis-Chalmers Manufacturing Company Atomic Energy Division, Greendale Labs 5400 South 60th Street Greendale, Wisconsin 53129 (Attn: R. Medard)	1
Allis-Chalmers Manufacturing Company Atomic Energy Division 6936 Arlington Road Bethesda, Maryland 20014 (Attn: Library)	1
Allison Division - GMC Plant 8, Library P. O. Box 894 Indianapolis, Indiana 46206 (Attn: W. H. Richardson)	1
Argonne National Laboratory 9700 S. Case Avenue Argonne, Illinois 60440 (Attn: Report Section)	10
(Attn: Dr. R. C. Vogel)	2
Armed Forces Radiobiology Research Institute National Naval Medical Center Bethesda, Maryland 20014 (Attn: Library)	1
Armed Services Explosive Safety Board Rm 333, Nassif Bldg. 5616 Columbia Pike Arlington, Virginia (Attn: Col. L. S. McCants, USAF)	1

DISTRIBUTION

	Copies
Commanding General Aberdeen Proving Ground, Maryland 21005 (Attn: Technical Library, Bldg. 313)	4
Commanding Officer U. S. Chemical Research & Development Laboratories Edgewood Arsenal, Maryland 21010 (Attn: Librarian)	2
Commanding General U. S. Army Edgewood Arsenal Edgewood Arsenal, Maryland 21010 (Attn: Robert Dean, Ch. Toxie and Radiological Br.)	1
Commanding Officer U. S. Army Electronics Research & Development Laboratory Fort Monmouth, New Jersey 07703 (Attn: SELRA/XS, Dr. W. J. Ramm)	1
Department of the Army Chief of Engineers Washington, D. C. 20315 (Attn: ENGAS-L)	1
Commanding Officer U. S. Army Engineer Research & Development Lab. Fort Belvoir, Virginia 22060 (Attn: Technical Documents Center)	1
Headquarters U. S. Army Environmental Hygiene Agency Edgewood Arsenal, Maryland 21010 (Attn: Chief, Library Branch)	1
Office of Inspector General Department of the Army Washington, D. C. 20315 (Attn: Nuclear Reactor Branch)	1
Commanding Officer U. S. Army Materials Research Agency Watertown Arsenal Watertown, Massachusetts 02172	1

DISTRIBUTION

	Copies
Redstone Scientific Information Center U. S. Army Missile Command Redstone Arsenal, Alabama 35809 (Attn: Chief, Document Section)	1
Commanding Officer U. S. Army Munitions Command Frankford Arsenal Philadelphia, Pennsylvania 19137 (Attn: 0270 - Library)	1
U. S. Army Research Office - Durham Box CM, Duke Station Durham, North Carolina 27706 (Attn: CRD-AA-IP)	1
Commanding General U. S. Army Tank - Automotive Center Detroit Arsenal Warren, Michigan 48090 (Attn: Ch. Nucleonics Section, SMOTA-RCS.1)	1
Arthur D. Little, Inc. Cambridge 40, Massachusetts (Attn: P. C. Johnson)	1
Advisory Committee on Reactor Safeguards Atomic Energy Commission Washington, D. C. 20545 (Attn: Mr. R. F. Fraley)	17
U. S. Atomic Energy Commission Albuquerque Operations Office P. O. Box 5400 Albuquerque, New Mexico 87115 (Attn: K. F. Hertford)	1
Ames Laboratory U. S. Atomic Energy Commission Iowa State University P. O. Box 1129, ISU Station Ames, Iowa 50012	2
Atomic Energy Commission Army Reactors Division of Reactor Development Washington, D. C. 20545	1

DISTRIBUTION

	Copies
U. S. Atomic Energy Commission Bethesda Technical Library 4915 St. Elmo Avenue Bethesda, Maryland 20545	2
Canoga Park Area Office P. O. Box 591 Canoga Park, California 91305 (Attn: Mr. C. W. Richards)	1
U. S. Atomic Energy Commission Chicago Operations Office 9800 South Cass Avenue Argonne, Illinois (Attn: George H. Lee)	1
U. S. Atomic Energy Commission Chicago Operations Office Health and Safety Division P. O. Box 59 Lemont, Illinois (Attn: Mr. Donald M. Gardiner)	1
Atomic Energy Commission Civilian Reactors Division of Reactor Development Washington, D. C. 20545 (Attn: Mr. A. Giambusso)	1
Atomic Energy Commission Division of Compliance Washington, D. C. 20545 (Attn:Mr. L. Kornblith, Jr.)	1
Atomic Energy Commission Division of Compliance, Region IV P. O. Box 15266 Denver 15, Colorado 80215 (Attn: Mr. John W. Flora)	1
U. S. Atomic Energy Commission Headquarters Library, Reports Section Mail Station G-017 Washington, D. C. 20545	5
Idaho Operations Office Atomic Energy Commission P. O. Box 2108 Idaho Falls, Idaho 83401 (Attn: Mr. I. Peltier) (Attn: Mr. D. Williams)	1 1

DISTRIBUTION

	Copies
Atomic Energy Commission Division of Licensing and Regulation Washington, D. C. 20545	
(Attn: Mr. Edson G. Case)	4
(Attn: Mr. Joseph J. DiNunno)	3
Atomic Energy Commission Maritime Reactors Branch Division of Reactor Development Washington, D. C. 20545	1
Atomic Energy Commission Naval Reactors Branch Division of Reactor Development Washington, D. C. 20545	
(Attn: Mr. T. Rockwell)	1
(Attn: Mr. R. S. Brodsky)	1
U. S. Atomic Energy Commission New York Operations Office 376 Hudson Street New York, New York 10014	
(Attn: Reports Librarian)	1
(Attn: Mr. James E. McLaughlin)	1
U. S. Atomic Energy Commission Office of Assistant General Counsel for Patents Washington 25, D. C.	
(Attn: Roland A. Anderson)	1
Atomic Energy Commission Research and Development Branch Division of Reactor Development Washington, D. C. 20545	
(Attn: Mr. S. A. Szawlewicz)	5
U. S. Atomic Energy Commission Director, Division of Research Washington 25, D. C.	1
Richland Operations Office P. O. Box 550 Richland, Washington 99352	
(Attn: Mr. C. L. Robinson)	1
U. S. Atomic Energy Commission San Francisco Operations Office 2111 Bancroft Way Berkeley, California 94704	
(Attn: Technical Services Division)	1
(Attn: Lt.Col. John B. Radcliffe)	1

DISTRIBUTION

	Copies
U. S. Atomic Energy Commission Division of Technical Information Extension P. O. Box 62 Oak Ridge, Tennessee 37831	325
Atomic Power Development Associates, Inc. Nuclear and Analytic Division 1911 First Street Detroit 26, Michigan (Attn: Mr. Walter J. McCarthy, Jr.)	1
(Attn: Dr. Alton Klickman)	1
Atomics International P. O. Box 309 Canoga Park, California 91304 (Attn: Library)	4
(Attn: Mr. A. A. Jarrett)	2
Avco Corporation Research and Advanced Development Division 201 Lowell Street Wilmington, Massachusetts 01887 (Attn: Chief Librarian)	1
The Babcock and Wilcox Company Atomic Energy Division P. O. Box 1260 Lynchburg, Virginia (Attn: Information Services)	4
Ballistic Research Laboratories Aberdeen Proving Ground, Maryland (Attn: Mr. Orlando T. Johnson)	1
Battelle Memorial Institute 505 King Avenue Columbus, Ohio 43201 (Attn: Dr. H. W. Russell)	2
Bechtel Corporation 220 Bush Street San Francisco 4, California) (Attn: J. D. Plawchan)	1
U. S. Atomic Energy Commission Schenectady Naval Reactors Office P. O. Box 1069 Schenectady, New York 12301 (Attn: Document Custodian)	1

DISTRIBUTION

	Copies
The Beryllium Corporation P. O. Box 1462 Reading, Pennsylvania 19603 (Attn: W. H. Santschi)	1
Brookhaven National Laboratory Technical Information Division Upton, Long Island, New York 11973 (Attn: Research Library) (Attn: Mr. A. W. Castleman)	4 1
Carnegie Institute of Technology Schenley Park Pittsburgh 19, Pennsylvania (Attn: Dr. Emerson M. Pugh)	1
Columbia University Engineering Research Laboratories 632 West 125th Street New York, New York 10027	1
Combustion Engineering, Inc. Prospect Hill Road Windsor, Connecticut 06095 (Attn: Document Custodian Naval Reactors Div) (Attn: Document Custodian Nuclear Division)	1 1
Corning Glass Works Electronics Research Laboratory 3900 Electronics Drive Raleigh, North Carolina (Attn: Mr. Larry Langley)	1
Director Defense Atomic Support Agency P. O. Box 2610 Washington, D. C. 20301 (Attn: Document Library Branch)	2
Defense Documentation Center Cameron Station Alexandria, Virginia	20

DISTRIBUTION

	Copies
Director of Defense Research and Engineering The Pentagon Washington 25, D. C.	1
Denver Research Institute P. O. Box 8786 University Park Sub-Station Denver, Colorado 80210 (Attn: Dr. William M. Mueller)	1
Detroit Edison Company Chemistry Research Department Detroit, Michigan (Attn: Mr. Edward Hines)	1
The Dow Chemical Company Rocky Flats Division P. O. Box 938 Golden, Colorado 80402 (Attn: Library)	1
Duke University College of Engineering Durham, North Carolina (Attn: Library) (Attn: Van L. Kenyon, Jr.) (Attn: Ernest Elsevier)	1 1 1
E. I. duPont deNemours and Company Savannah River Laboratory Technical Information Service - 773A Aiken, South Carolina	4
E. I. duPont deNemours and Company Explosives Department Atomic Energy Division Wilmington, Delaware 19898 (Attn: Document Custodian)	1
Edgerton, Germeshausen and Grier, Inc. P. O. Box 1912 Las Vegas, Nevada 89101 (Attn: Librarian)	1
Franklin Institute of Pennsylvania Laboratory for Research and Development Philadelphia 3, Pennsylvania (Attn: F. L. Jackson, Technical Director)	1

DISTRIBUTION

	Copies
Fundamental Methods Association 31 Union Square West New York, New York (Attn: Dr. Carl N. Klahr)	1
General Atomic Division General Dynamics Corporation P. O. Box 608 San Diego, California 92112 (Attn: Library)	2
General Dynamics/Fort Worth P. O. Box 748 Fort Worth, Texas (Attn: Keith G. Brown)	2
General Electric Company Post Office Box 100 Richland, Washington 99352 (Attn: Technical Information Operation)	6
General Electric Company 2151 South First Street San Jose, California (Attn: Mr. C. H. Robbins) (Attn: Mr. E. R. Kilsby)	1 1
General Electric Company Atomic Power Equipment Department P. O. Box 1131 San Jose, California 95108 (Attn: Alleen Thompson)	4
General Electric Company Hanford Atomic Products Operation Richland, Washington 99352 (Attn: Mr. E. Irish)	2
General Electric Company Nuclear Materials and Propulsion Operation P. O. Box 15132 Cincinnati, Ohio 45215 (Attn: J. W. Stephenson)	3
General Electric Company Vallecitos Atomic Laboratory P. O. Box 846 Pleasanton, California (Attn: Librarian)	1

DISTRIBUTION

	Copies
General Nuclear Engineering Corporation P. O. Box 10 Dunedin, Florida 33528 (Attn: William P. Bigler)	1
Goodyear Atomic Corporation P. O. Box 628 Piketon, Ohio (Attn: Department 423)	1
Harvard University Cambridge, Massachusetts (Attn: Dr. Harvey Brooks, Dean of Engineering and Applied Physics)	1
Hercules Powder Company Research Department Wilmington, Delaware (Attn: Dr. Willard P. Conner, Manager Physical Chemical Division)	1
Hughes Aircraft Company P. O. Box 3310 Fullerton, California (Attn: Dr. A. M. Liebschutz)	1
IIT Research Institute 10 West 35th Street Chicago, Illinois 60616 (Attn: Central Document Control, for TAS (Attn: Dr. T. A. Zaker)	1 1
Ingersoll-Rand Company Research and Development Laboratory Electro-Mechanical Development Bedminster, New Jersey (Attn: Dr. W. R. Wise, Jr., Director) (Attn: L. P. Walker)	25 2
Jet Propulsion Laboratory California Institute of Technology 4800 Oak Grove Drive Pasadena, California 91103 (Attn: N. E. Devereux, Library Supv.)	2
Johns Hopkins University Operations Research Office 7100 Connecticut Avenue Washington 15, D. C. (Attn: Document Control Office)	1

DISTRIBUTION

	Copies
Knolls Atomic Power Laboratory P. O. Box 1072 Schenectady, New York 12301 (Attn: Document Librarian)	2
Ling Temco Vought, Inc. P. O. Box 5907 Dallas, Texas 75222 (Attn: J. E. Standefer)	1
Lockheed-Georgia Company Division of Lockheed Aircraft Corporation Marietta, Georgia (Attn: Charles K. Bauer, Manager, Scientific and Technical Information Department)	1
Lockheed Missiles and Space Company Division of Lockheed Aircraft Corporation Sunnyvale, California (Attn: Harold F. Plank)	1
Los Alamos Scientific Laboratory P. O. Box 1663 Los Alamos, New Mexico 87544 (Attn: Report Librarian)	4
Mallinckrodt Chemical Works Uranium Division P. O. Box 472 St. Charles, Missouri 63302 (Attn: Document Control Group)	1
The Maritime Administration U. S. Department of Commerce New GAO Building Washington 25, D. C.	1
Martin Company Nuclear Division P. O. Box 5042 Middle River, Maryland 21203 (Attn: AEC Document Custodian)	1
Massachusetts Institute of Technology Division of Sponsored Research Room 5-105 Cambridge, Massachusetts 02139 (Attn: Dr. N. Sage)	1

DISTRIBUTION

	Copies
Monsanto Research Corporation Boston Laboratories Everett, Massachusetts 02149 (Attn: Research Library)	1
Monsanto Research Corporation Mound Laboratory P. O. Box 32 Miamisburg, Ohio 45342 (Attn: Library)	1
National Aeronautics & Space Administration Ames Research Center Moffett Field, California (Attn: William R. Johnson, Librarian)	1
National Aeronautics and Space Administration Goddard Space Flight Center Glenn Dale Road Greenbelt, Maryland (Attn: Librarian) (Attn: Mr. L. J. Veillatte)	1 1
National Aeronautics & Space Administration Lewis Research Center 21000 Brookpark Road Cleveland, Ohio 44135 (Attn: George Mandel)	1
National Aeronautics & Space Administration Manned Spacecraft Center Houston, Texas 77001 (Attn: Chief, Technical Information Division)	1
National Aeronautics & Space Administration Plum Brook Station Sandusky, Ohio 44871 (Attn: Library)	1
Scientific & Technical Information Facility P. O. Box 5700 Bethesda, Maryland 20014 (Attn: NASA Representative, S-AK/DL)	2
National Aeronautics & Space Administration Western Operations Office 150 Pico Boulevard Santa Monica, California (Attn: M. C. Romano)	1

DISTRIBUTION

	Copies
National Bureau of Standards U. S. Department of Commerce Coordinator of Atomic Energy Projects Washington 25, D. C. (Attn: L. S. Taylor, Room 306 West)	1
National Bureau of Standards Room 301, Building 7 Connecticut and Van Ness St., N. W. Washington, D. C. 20234 (Attn: Library)	1
National Bureau of Standards Washington 25, D. C. (Attn: Dr. C. Muehlhause)	1
National Lead Company of Ohio P. O. Box 39158 Cincinnati, Ohio 45239 (Attn: Reports Library)	1
Commanding Officer and Director David Taylor Model Basin Washington 7, D. C.	1
Naval Medical Research Institute National Naval Medical Center Bethesda 14, Maryland (Attn: Mrs. Mabel D. Clark, Tech. Reference Library)	1
Office of the Chief of Naval Operations Atomic Energy Division Washington, D. C. 20350 (Attn: Director, Atomic Energy Division)	1
U. S. Naval Postgraduate School Monterey, California 93940 (Attn: George R. Luckett, Director of Libraries)	1
Commanding Officer and Director U. S. Naval Radiological Defense Laboratory San Francisco, California 94135 (Attn: T. J. Mathews)	1
Department of the Navy Office of Naval Research Washington, D. C. 20360 (Attn: Code 418) (Attn: Code 422)	2 1

DISTRIBUTION

	Copies
Commanding Officer Office of Naval Research Box 39, Navy 100 F. P. O. New York, New York 09599	10
U. S. Naval Research Laboratory Washington, D. C. 20390	
(Attn: Code 2027)	3
(Attn: Dr. G. R. Irwin, Supt., Mechanics Div)	1
(Attn: Dr. J. M. Kraft, Mechanics Div)	1
(Attn: Mr. W. S. Pellini, Metallurgy Div)	1
Department of the Navy Bureau of Ships, Code 1500 Washington, D. C. 20360 (Attn: E. Patricia Norris)	1
Chief, Bureau of Naval Weapons Department of the Navy Washington, D. C. 20360	
(Attn: RRNU)	1
(Attn: RRRE-5, W. T. August)	1
(Attn: RMMO-13, E. M. Fisher)	1
(Attn: Library, DLI-3)	4
Commanding Officer U. S. Naval Weapons Evaluation Facility Kirtland AFB, Albuquerque, New Mexico	1
Commander Naval Weapons Laboratory Dahlgren, Virginia	1
Bureau of Yards and Docks Department of the Navy Washington, D. C. 20390 (Attn: Code 42.330)	1
New York University AEC Computing and Applied Mathematics Center 4 Washington Place New York, New York 10003 (Attn: Director)	1
Nuclear Materials and Equipment Corpration 609 North Warren Avenue Apollo, Pennsylvania (Attn: Mary Barber, Document Custodian)	1

DISTRIBUTION

	Copies
Nuclear Metals, Inc. P. O. Box 125 West Concord, Massachusetts (Attn: AEC Document Custodian)	1
Nuclear Technology Corporation 55 Church Street White Plains, New York (Attn: J. E. DeFelice)	1
Nuclear Utility Services, Inc. 1730 M Street, N. W. Washington, D. C. 20036 (Attn: Library)	1
Oak Ridge National Laboratory Oak Ridge, Tennessee 37831 (Attn: Nuclear Safety Information Center) (Attn: Mr. William B. Cottrell) (Attn: Mr. Frank Bruce) (Attn: Dr. William Ergen) (Attn: Mr. R. E. Schappel)	1 3 1 1 1
Pacific Missile Range Code 4113 P. O. Box 10 Point Mugu, California (Attn: Mr. Harry B. Benefiel)	1
U. S. Patent Office Scientific Library Washington 25, D. C.	1
Pennsylvania State University Nuclear Physics, Accelerator Bldg. University Park, Pennsylvania 16802	1
Phillips Petroleum Company Idaho Falls, Idaho 83401 (Attn: NRTS Technical Library) (Attn: Mr. Glenn O. Bright) (Attn: Mr. Warren E. Nyer) (Attn: Mr. Frank Schroeder) (Attn: Mr. T. R. Wilson)	6 2 2 2 2
Physics International, Inc. 2229 Fourth Street Berkeley, California	1

DISTRIBUTION

	Copies
Picatinny Arsenal Feltman Research Laboratories Dover, New Jersey	
(Attn: Technical Information Library)	1
(Attn: Mr. A. Mackenzie)	1
U. S. Pipe and Foundry Company Steel and Tubes Division Burlington, New Jersey	
(Attn: Dr. A. E. Schuh)	1
Power Reactor Development Company 1911 First Street Detroit 26, Michigan	
(Attn: Ada J. Maclean, Document Librarian, AT(11-1)-476)	1
Pratt and Whitney Aircraft Division Connecticut Operations - CANEL P. O. Box 611 Middletown, Connecticut 06458	
(Attn: Library)	3
Pressure Science Incorporated 11642 Old Baltimore Pike Beltsville, Maryland	
(Attn: Dudley D. Taylor)	1
(Attn: John F. Daugherty)	1
Deputy Chief, Division of Radiological Health U. S. Public Health Service 4th and C Streets, S. W. Washington, D. C. 20201	
(Attn: James G. Terrill, Jr.)	2
U. S. Public Health Service Robert A. Taft Sanitary Engineering Center 4676 Columbia Parkway Cincinnati 26, Ohio	
(Attn: Clarence L. Code)	1
Puerto Rico Water Resources Authority P. O. Box 4267 San Juan, Puerto Rico	
(Attn: S. L. Descartes, Executive Director)	1
Purdue University Department of Nuclear Engineering Lafayette, Indiana 47907	
(Attn: Prof. Alexander Sesonshe)	1

DISTRIBUTION

	Copies
Radioptics, Inc. 121 Old Country Road Carle Place Long Island, New York (Attn: Dr. Kalman Held)	1
Director, USAF Project RAND Via: Air Force Liaison Office The RAND Corporation 1700 Main Street Santa Monica, California 90406 (Attn: Library)	1
Rensselaer Polytechnic Institute Troy, New York 12181 (Attn: Reference Librarian)	1
Republic Aviation Corporation Farmingdale, New York 11735 (Attn: Engineering Library)	1
Research Triangle Institute P. O. Box 490 Durham, North Carolina 27701 (Attn: Dr. Hugh W. Hunter)	1
Mr. James R. Crockett, Project General Manager Reynolds Electrical & Engineering Company, Inc. P. O. Box 1360 Las Vegas, Nevada 89101 (Attn: Radiological Safety Library)	1
Headquarters Rocky Mountain Arsenal Denver, Colorado 80240 (Attn: Radiological Safety Officer)	1
Sandia Corporation P. O. Box 5800 Albu querque, New Mexico 87115 (Attn: Technical Library)	1
Mr. Leonard Solon 28 Pilgrim Avenue Yonkers, New York 10710	1

DISTRIBUTION

	Copies
Space Technology Laboratories, Inc. P. O. Box 95001 Los Angeles 45, California (Attn: Margaret N. Sloane, Chief Librarian)	1
Space Technology Laboratories, Inc. One Space Park Redondo Beach, California (Attn: Dr. D. B. Langmuir) (Attn: Mr. S. M. Zivi)	 1 1
Stanford Research Institute Poulter Laboratories Menlo Park, California (Attn: Mr. G. R. Fowles)	 1
U. S. Department of Commerce U. S. Clearing House for Scientific & Tech. Info. Sills Building, 5285 Port Royal Road Springfield, Virginia 22151	 100
Tennessee Valley Authority Chattanooga, Tennessee (Attn: William E. Dean, Jr., Assistant Director of Power Supply)	 1
Todd Shipyards Corporation Nuclear Division P. O. Box 1750 Galveston, Texas 77551 (Attn: Central File)	 1
Union Carbide Corporation Nuclear Division Oak Ridge. Tennessee 37831 (Attn: CRGDP Records Dept) (Attn: X-10 Laboratory Records Dept) (Attn: Y-12 Technical Library)	 2 8 1

DISTRIBUTION

	Copies
United Nuclear Corporation 5 New Street White Plains, New York 10601	
(Attn: Records Management)	1
(Attn: Dr. C. Graves, Development Div)	1
University of California Institute of Engineering Research Berkeley 4, California	
(Attn: Prof. H. A. Johnson)	1
(Attn: Dr. V. E. Schrock)	1
University of California Lawrence Radiation Laboratory Technical Information Division Berkeley, California 94720	
(Attn: Dr. R. K. Wakerling)	1
University of California Lawrence Radiation Laboratory Technical Information Division P. O. Box 808 Livermore, California 94551	
(Attn: Clovis G. Craig)	2
University of Maryland College Park, Maryland	
(Attn: Prof. C. A. Shreeve, Jr., Chairman Mechanical Engineering Department)	1
(Attn: Dr. Donald T. Bonney Chemical Engineering Department)	1
University of Minnesota Department of Chemical Engineering Minneapolis, Minnesota	
(Attn: Prof. H. Isbin)	1
Westinghouse Electric Corporation Astronuclear Laboratory P. O. Box 10864 Pittsburgh, Pennsylvania 15236	
(Attn: Florence M. McKenna)	1
Commanding General White Sands Missile Range New Mexico 88002	
(Attn: Technical Library)	1

DISTRIBUTION

	Copies
University of Puerto Rico Puerto Rico Nuclear Center College Station Mayaguez, Puerto Rico	1
University of Rochester Atomic Energy Project P. O. Box 287, Station 3 Rochester 20, New York (Attn: Technical Report Control Unit)	1
University of Rochester Department of Physics and Astronomy Rochester, New York 14627 (Attn: Dr. R. E. Marshak)	2
Vitro Engineering Division Technical Reports Section 225 Fourth Avenue New York 3, New York	1
Division of Nuclear Medicine Walter Reed Army Institute of Research Walter Reed Army Medical Center Washington, D. C. 20012	1
Commanding Officer Watertown Arsenal Watertown 72, Masachusetts (Attn: Technical Information Section)	1
Westinghouse Electric Corporation Bettis Atomic Power Laboratory P. O. Box 1468 Pittsburgh, Pennsylvania 15230 (Attn: Mrs. Virginia Sternberg)	4
Westinghouse Electric Corporation Atomic Power Division P. O. Box 355 Pittsburgh, Pennsylvania 15230 (Attn: Document Custodian)	2
Westinghouse Electric Corporation Westinghouse Research Laboratories Physics Department Pittsburgh, Pennsylvania 15235 (Attn: Dr. Russell Fox)	1

DISTRIBUTION

	Copies
Allegheny Ballistics Laboratory Hercules Powder Company Cumberland, Maryland (Attn: Mr. E. T. Hanley)	1
University of Missouri Mechanics Department Rolla, Missouri (Attn: Dr. R. L. Davis)	1
Space Technology Laboratory 7001 North Atlantic Ave. Cape Canaveral, Florida (Attn: Mr. George Byrant)	1
Defense Atomic Support Agency Blast and Shock Division Naval Effects Branch The Pentagon Washington, D. C. (Attn: Mr. J. F. Moulton, Jr., Chief)	1

UNCLASSIFIED
Security Classification

DOCUMENT CONTROL DATA - R&D

(Security classification of title, body of abstract and indexing annotation must be entered when the overall report is classified)

1. ORIGINATING ACTIVITY *(Corporate author)*
U. S. Naval Ordnance Laboratory
White Oak, Silver Spring, Maryland

2a. REPORT SECURITY CLASSIFICATION
Unclassified

2b GROUP

3. REPORT TITLE
Explosion Containment Laws for Nuclear Reactor Vessels

4. DESCRIPTIVE NOTES *(Type of report and inclusive dates)*
Final

5. AUTHOR(S) *(Last name, first name, initial)*
Wise, Walter R., Jr., and Proctor, James F.

6. REPORT DATE	7a. TOTAL NO. OF PAGES	7b. NO. OF REFS
16 August 1965	152	24

8a. CONTRACT OR GRANT NO.	9a. ORIGINATOR'S REPORT NUMBER(S)
b. PROJECT NO. Task NOL-285	NOLTR 63-140
c.	9b. OTHER REPORT NO(S) *(Any other numbers that may be assigned this report)*
d.	

10. AVAILABILITY/LIMITATION NOTICES
(1) Qualified requestors may obtain copies of this report from DDC

11. SUPPLEMENTARY NOTES	12. SPONSORING MILITARY ACTIVITY
	Division of Reactor Development U. S. Atomic Energy Commission Washington, D.C.

13. ABSTRACT

The location of power reactors in urban areas increases the need for containment of the maximum credible nuclear accident. Such an accident could possibly involve a large and rapid energy release in the core region due to a nuclear excursion. To contain the energy release (and any subsequent release of fission products), the integrity of the reactor primary vessel is very important. To investigate this integrity, extensive theoretical and experimental analyses were performed, and basic explosion containment laws for water-filled right-circular cylinders were formulated and verified for a wide range of vessel materials and sizes. These laws express explosive charge weight as a function of vessel geometry and conventional material properties. The basic containment laws were amplified to characterize the response of reactor primary vessels to a large spectrum of postulated nuclear accidents. Included in the study are experimental data on the effects upon containment of weldments, nozzles, and end constraints.

DD FORM 1 JAN 64 1473

UNCLASSIFIED
Security Classification

UNCLASSIFIED
Security Classification

14. KEY WORDS	LINK A		LINK B		LINK C	
	ROLE	WT	ROLE	WT	ROLE	WT
1. Reactors - Safety 2. Reactors - Containment 3. Response - Dynamic 4. Cylinders - Internal Dynamic Loading 5. Explosions - Containment 6. Structural Behavior						

INSTRUCTIONS

1. ORIGINATING ACTIVITY: Enter the name and address of the contractor, subcontractor, grantee, Department of Defense activity or other organization *(corporate author)* issuing the report.

2a. REPORT SECURITY CLASSIFICATION: Enter the overall security classification of the report. Indicate whether "Restricted Data" is included. Marking is to be in accordance with appropriate security regulations.

2b. GROUP: Automatic downgrading is specified in DoD Directive 5200.10 and Armed Forces Industrial Manual. Enter the group number. Also, when applicable, show that optional markings have been used for Group 3 and Group 4 as authorized.

3. REPORT TITLE: Enter the complete report title in all capital letters. Titles in all cases should be unclassified. If a meaningful title cannot be selected without classification, show title classification in all capitals in parenthesis immediately following the title.

4. DESCRIPTIVE NOTES: If appropriate, enter the type of report, e.g., interim, progress, summary, annual, or final. Give the inclusive dates when a specific reporting period is covered.

5. AUTHOR(S): Enter the name(s) of author(s) as shown on or in the report. Enter last name, first name, middle initial. If military, show rank and branch of service. The name of the principal author is an absolute minimum requirement.

6. REPORT DATE: Enter the date of the report as day, month, year; or month, year. If more than one date appears on the report, use date of publication.

7a. TOTAL NUMBER OF PAGES: The total page count should follow normal pagination procedures, i.e., enter the number of pages containing information.

7b. NUMBER OF REFERENCES: Enter the total number of references cited in the report.

8a. CONTRACT OR GRANT NUMBER: If appropriate, enter the applicable number of the contract or grant under which the report was written.

8b, 8c, & 8d. PROJECT NUMBER: Enter the appropriate military department identification, such as project number, subproject number, system numbers, task number, etc.

9a. ORIGINATOR'S REPORT NUMBER(S): Enter the official report number by which the document will be identified and controlled by the originating activity. This number must be unique to this report.

9b. OTHER REPORT NUMBER(S): If the report has been assigned any other report numbers *(either by the originator or by the sponsor)*, also enter this number(s).

10. AVAILABILITY/LIMITATION NOTICES: Enter any limitations on further dissemination of the report, other than those imposed by security classification, using standard statements such as:

(1) "Qualified requesters may obtain copies of this report from DDC."

(2) "Foreign announcement and dissemination of this report by DDC is not authorized."

(3) "U. S. Government agencies may obtain copies of this report directly from DDC. Other qualified DDC users shall request through

_____."

(4) "U. S. military agencies may obtain copies of this report directly from DDC. Other qualified users shall request through

_____."

(5) "All distribution of this report is controlled. Qualified DDC users shall request through

_____"

If the report has been furnished to the Office of Technical Services, Department of Commerce, for sale to the public, indicate this fact and enter the price, if known.

11. SUPPLEMENTARY NOTES: Use for additional explanatory notes.

12. SPONSORING MILITARY ACTIVITY: Enter the name of the departmental project office or laboratory sponsoring *(paying for)* the research and development. Include address.

13. ABSTRACT: Enter an abstract giving a brief and factual summary of the document indicative of the report, even though it may also appear elsewhere in the body of the technical report. If additional space is required, a continuation sheet shall be attached.

It is highly desirable that the abstract of classified reports be unclassified. Each paragraph of the abstract shall end with an indication of the military security classification of the information in the paragraph, represented as *(TS), (S), (C), or (U)*.

There is no limitation on the length of the abstract. However, the suggested length is from 150 to 225 words.

14. KEY WORDS: Key words are technically meaningful terms or short phrases that characterize a report and may be used as index entries for cataloging the report. Key words must be selected so that no security classification is required. Identifiers, such as equipment model designation, trade name, military project code name, geographic location, may be used as key words but will be followed by an indication of technical context. The assignment of links, roles, and weights is optional.

UNCLASSIFIED
Security Classification

Naval Ordnance Laboratory, White Oak, Md.
(NOL technical report 63-140)
EXPLOSION CONTAINMENT LAWS FOR NUCLEAR REACTOR VESSELS, by W. R. Wise, jr. and J. F. Proctor. 16 Aug. 1965. v.p. illus., charts, tables. NOL task 285.

UNCLASSIFIED

Basic explosion containment laws for water-filled right-circular cylinders were formulated and verified for a wide range of vessel materials and sizes. These laws express explosive charge weight as a function of vessel geometry and conventional material properties. The basic containment laws were amplified to characterize the response of reactor primary vessels to a large spectrum of postulated nuclear accidents.

1. Reactors - Safety
2. Reactors - Containment
I. Title
II. Wise, Walter R.,jr.
III. Proctor, James F., jt. author
IV. Project

Abstract card is unclassified.

Naval Ordnance Laboratory, White Oak, Md.
(NOL technical report 63-140)
EXPLOSION CONTAINMENT LAWS FOR NUCLEAR REACTOR VESSELS, by W. R. Wise, jr. and J. F. Proctor. 16 Aug. 1965. v.p. illus., charts, tables. NOL task 285.

UNCLASSIFIED

Basic explosion containment laws for water-filled right-circular cylinders were formulated and verified for a wide range of vessel materials and sizes. These laws express explosive charge weight as a function of vessel geometry and conventional material properties. The basic containment laws were amplified to characterize the response of reactor primary vessels to a large spectrum of postulated nuclear accidents.

1. Reactors - Safety
2. Reactors - Containment
I. Title
II. Wise, Walter R.,jr.
III. Proctor, James F., jt. author
IV. Project

Abstract card is unclassified.

Naval Ordnance Laboratory, White Oak, Md.
(NOL technical report 63-140)
EXPLOSION CONTAINMENT LAWS FOR NUCLEAR REACTOR VESSELS, by W. R. Wise, jr. and J. F. Proctor. 16 Aug. 1965. v.p. illus., charts, tables. NOL task 285.

UNCLASSIFIED

Basic explosion containment laws for water-filled right-circular cylinders were formulated and verified for a wide range of vessel materials and sizes. These laws express explosive charge weight as a function of vessel geometry and conventional material properties. The basic containment laws were amplified to characterize the response of reactor primary vessels to a large spectrum of postulated nuclear accidents.

1. Reactors - Safety
2. Reactors - Containment
I. Title
II. Wise, Walter R.,jr.
III. Proctor, James F., jt. author
IV. Project

Abstract card is unclassified.

Naval Ordnance Laboratory, White Oak, Md.
(NOL technical report 63-140)
EXPLOSION CONTAINMENT LAWS FOR NUCLEAR REACTOR VESSELS, by W. R. Wise, jr. and J. F. Proctor. 16 Aug. 1965. v.p. illus., charts, tables. NOL task 285.

UNCLASSIFIED

Basic explosion containment laws for water-filled right-circular cylinders were formulated and verified for a wide range of vessel materials and sizes. These laws express explosive charge weight as a function of vessel geometry and conventional material properties. The basic containment laws were amplified to characterize the response of reactor primary vessels to a large spectrum of postulated nuclear accidents.

1. Reactors - Safety
2. Reactors - Containment
I. Title
II. Wise, Walter R.,jr.
III. Proctor, James F., jt. author
IV. Project

Abstract card is unclassified.